Carol: New File "RIV"

GENERAL ELECTRIC

INSULATOR DEPARTMENT
2525 Insulator Drive
Baltimore, Md. 21230

DIAL COMM
8*272-9

COPIES: ES Wheeler
R. Weller
J. Kaminski

file - BEK

February 3, 1967

Mr. J. J. LaForest
PITTSFIELD

As I discussed with you about ten days ago, we are interested in determining whether or not our standard suspension insulator, as per the attached drawing U-1840, can be designed to be more corona-free than is now the case.

Let me digress for just a moment to give you a little background on the overall problem. As you know, our scope of business covers all types of line hardware, such as clamps, yoke plates, and fittings, as well as insulators. In fact, we are concerned with the entire assembly which supports the power conductor to the tower. Sometimes a customer specication will demand that the assembly, when subjected to a given voltage, will have less than a specified amount of RIV. At other times the specification will demand that there be no corona at the specified test voltage. The third possibility is that both a specified RIV level and no visual corona will be required at the test voltage level.

Generally speaking, it is quite feasible to design an assembly to meet the RIV levels specified, and the hardware parts can also be designed to meet the visual corona requirements. But, it becomes quite impossible to design to eliminate visual corona from the insulators, even when using quite elaborate shielding (grading rings). The amounts of visual corona on the insulators do not usually cause very much noise (RIV), at least in comparison with the noise caused by a brush discharge on a piece of hardware.

See the attached curve sheet which shows a generalized plot of RIV versus Test Voltage. The lower section of the curve will be created solely by insulator noise, and the upper part by corona on hardware parts. Usually, the RIV, as caused by the insulators, is about as shown, increasing linearly with test voltage.

As far as I am concerned, where there is RIV there must be corona (at least 10-15 microvolts). Then, the question arises, can we correlate the visual corona levels on the insulators with the RIV curves? The answer is no. The visual corona levels obtained on the insulators depend upon a variety of things such as how dark the laboratory is, how good the observers vision is, and how long the observer has waited to allow his eyes to adjust to the darkness. This situation has created some major problems for us in that, depending upon how zealous we are in observing corona, we can "look" ourselves right out of specification.

I mentioned that the noise resulting from hardware is generally manifested by brush corona, however, the type of corona on suspension insulators is mostly what we define as "glow" corona (i.e. There is no brush discharge, only a glow or haze of bluish light). This glow can persist and persist as the test voltage is lowered until, depending upon room darkness and observer care, it just disappears from sight (But it must still be there because we have an appreciable RIV level, perhaps only 30-50 microvolts, which is certainly of little consequence on a 500 KV transmission line).

The tabulation below illustrates, in a qualitative way, the change in performance we experience in testing an insulator assembly under two extremes of humidity. For purposes of illustration, assume a constant applied test voltage and the two extremes of humidity are defined as being approximately 0.200 and 0.600 inches of mercury, vapor pressure.

	Low Humidity	High Humidity
RIV Level	High	Low
Visual Corona		
insulator pin-hole	slight glow	glow plus spitting over the first porcelain petticoat
insulator cap	glow to spitting	no corona

The best performance from an RIV standpoint is generally with high humidity which might perhaps be because we can see no corona in the air gap between the bottom of the cap and the top porcelain surface. The corona which is visible in the pin-hole of the insulator at low humidity is a ring of low glow at the cement-porcelain interface, and at high humidity is much the same except that the streamers extend from the glow area outward and "play" over the first petticoat (sometimes to the second petticoat depending upon the voltage level).

Jim, I guess what we want to know is this:

(1) Can you tell us what changes to make in design?
(2) Can you tell us why the above things occur?

Also attached are two characteristic sheets which give the details regarding characteristics of the porcelains. No 1520 is the one which should be primarily used. No. 1521 represents our high strength body, with slightly different characteristics. However, when we test our insulator made of the latter, we get essentially the same results as with the former regarding corona.

Please let me know what you can do, when you can do it, and how much it will cost.

Very truly yours,

B. E. Kingsbury, Manager
Product Engineering

clk

Attachments (4)

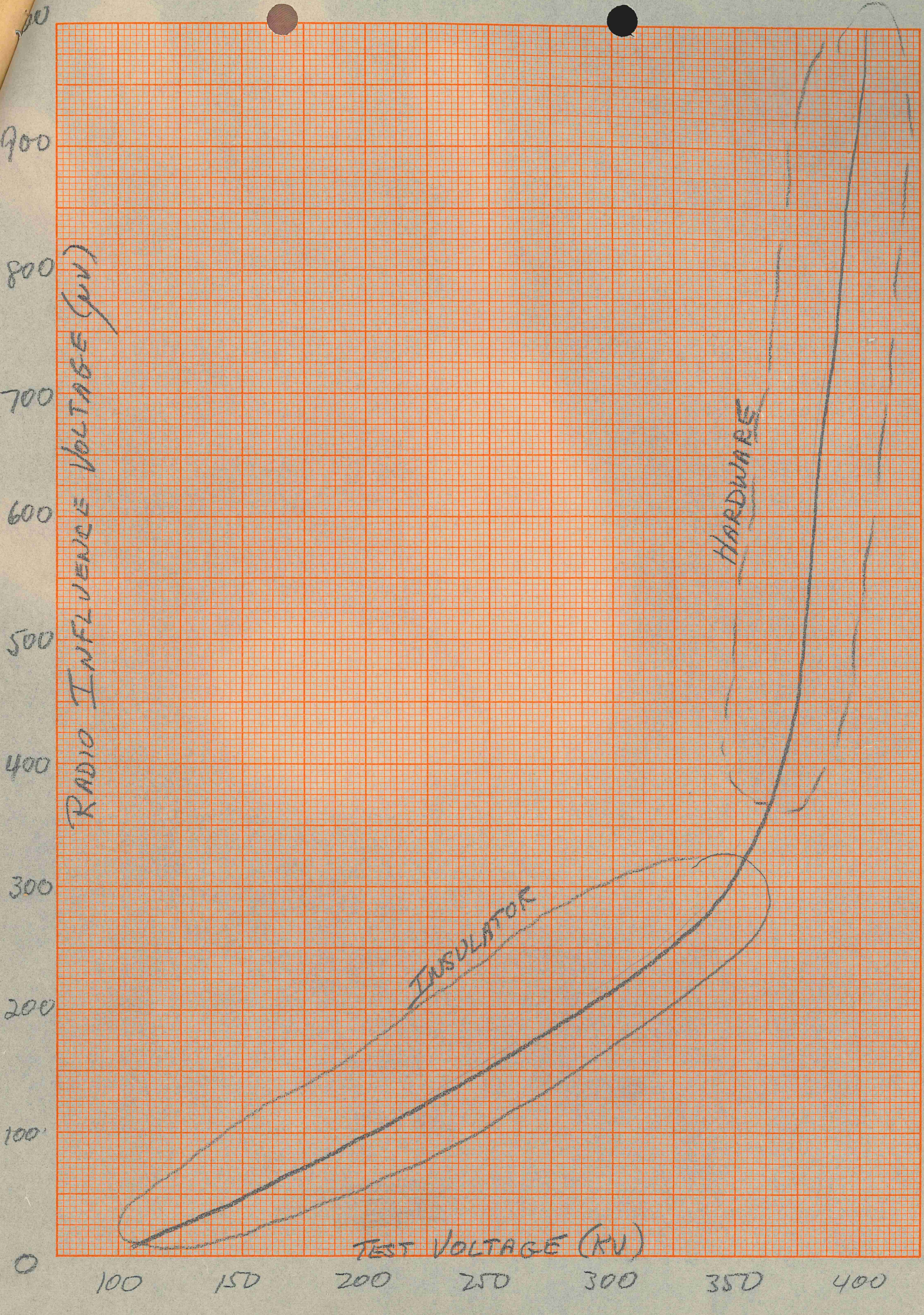

K+E 10 X 10 TO ½ INCH 46 1327
7 X 10 IN. • ALBANENE® MADE IN U.S.A.
KEUFFEL & ESSER CO.

INSULATOR DEPARTMENT
GENERAL ELECTRIC COMPANY

April 3, 1964

RADIO INTERFERENCE FROM E. H. V. TRANSMISSION LINES AND SUBSTATIONS

ML-9, Tabs L and N

As most of you are by now already aware, the subject of radio noise generated by conductors and insulator assemblies on E. H. V. transmission lines has been one which has been very controversial for some two or three years and there has undoubtedly been a tendency to go way overboard by many utility and consulting engineering organizations in the specification of very severe corona and radio influence voltage requirements on insulator assemblies of all kinds.

This undoubtedly has arisen from the fear that E. H. V. lines may produce tremendous amount of radio interference and thus be a cause of poor public relations between the utility and people living in areas adjacent to or near E. H. V. transmission lines.

The relationship between radio influence voltage on insulator components measured in the laboratory on a directly coupled basis to the radio field intensity which these devices would produce on the line has not been well understood in the past and it now appears that radio noise suppression on insulator assemblies and components has in most cases been greatly overemphasized far beyond the actual needs.

At the inception of E. H. V. work in the early years after World War II, with the almost complete lack of knowledge and understanding about these things, the concept was that insulator assemblies should never show any visible or audible corona at a voltage at least 10% above line to neutral voltage and that the R. I. V. on the components as measured in the laboratory should be held at 50 to 100 microvolts or lower when the assembly was energized at 110% of line to ground voltage. This has resulted in a lot of costly designs with all components made with either large and bulky radii at the edges or else has involved rather complete and thorough shielding.

More recently, these R. I. V. specifications for insulator assemblies for E. H. V. projects have been somewhat liberalized where specifications have permitted the R. I. V. levels to go to 350 to 500 microvolts at voltages applied equal to 110% of the maximum line to ground operating voltage.

It now becomes apparent that these liberalized specifications are requiring much better performance radio interference wise than is actually needed, which is causing the cost of insulator assemblies to be higher than is necessary for the actual performance of the line.

In the final analysis, the utility building an E. H. V. circuit is concerned with what the radio interference field is at the edge of the transmission line right-of-way, usually 100 to 150 ft. from the centerline of the transmission circuit.

The main generator of radio interference on a transmission line, under the best of conditions is the conductor which extends continuously throughout every foot of the transmission line. As a practical matter, it is virtually impossible to get this conductor into place with no mars or scratches on its surface and even if they did, insects, air borne particles, dirt, etc., will give rise to radio interference almost continuously along the transmission circuit.

Insulator assemblies are dispersed along the line at perhaps one assembly per phase every 1,000 to 1,200 ft. and these become discrete noise sources infrequently interposed on top of the noise sources which the conductors themselves produce.

The ultimate result of this is that within reason it matters very little what the magnitude of the noise is arising from the insulator assemblies, their effect will generally be swamped by the hundreds of thousands of noise generators arising in connection with the conductor. Work done on project E. H. V. and other experimental high voltage projects, as well as experience with actual operating E. H. V. transmission lines is now beginning to show that a great deal of undue emphasis has been put in the past on the question of radio noise generation of insulator assemblies and components.

In many discussions over the past two or three years with utilities, I have tried to reflect this type of attitude and have been suggesting to the utility engineers not to set their R. I. requirements for insulator assemblies too low, suggesting that by doing so, they are increasing the cost of these assemblies without obtaining any improvement in overall performance in their lines in this respect. For lack of any authoritative backing in this, this urging has to a large extent gone unheeded.

For the past several years, the Transmission and Distribution Committee of I. E. E. E. has had a Radio Noise Sub-Committee which has been investigating and discussing this subject. This Sub-Committee has been broken up into several working groups and Working Group No. 4, headed by Mr. T. W. Liao, of the General Electric Company, has been studying the problem of radio noise generation from line and station components.

As of March 10, 1964, Mr. Liao's Working Group on this subject has issued a tentative report which is, I think, very illuminating, and which comments on many phases of the whole situation. The work of this group has reviewed the results of many experimental transmission line investigations as well as the performance of various E. H. V. lines now in service and their findings certainly confirm the recommendations which we have been making, only in general, they would go considerably further than anything we had ventured to propose so far. For your information, I am attaching a copy of this tentative Working Group's report. Please bear in mind that this report is not yet official; it has not been adopted by the Radio Noise Sub-Committee, nor by the I. E. E. E. Transmission and Distribution Committee. However, it does reflect the thinking of the group of individuals in the industry who are most conversant to the whole situation and shows the trend of thinking among the experts on this subject. I commend this report highly for your thorough study and hope that you will grasp its full importance.

There is no reason why this document cannot be shown to utility customers who are interested in this subject provided that they thoroughly understand that it is a tentative report of the Working Group reflecting their best thoughts on the subject in view of their intimate knowledge of it. It should be borne in mind that this report may not be accepted in its entirety by either the Radio Noise Sub-Committee or the Transmission and Distribution Committee after these bodies have had a chance to thoroughly digest it. However, it is quite likely that it will not be greatly modified.

To summarize the situation, for lack of knowledge and understanding on this subject, most of the E. H. V. transmission lines which have been built so far, have undoubtedly gone to unnecessary lengths in the suppression of corona and radio influence voltage on insulator assemblies. Research work in the field which has been done on experimental transmission lines such as the Penelec 500 kv Project, the E. H. V. Project, the Apple Grove Project, the Public Service of Colorado High Altitude Project, etc., is now beginning to turn in results to show the way toward sensible specification for R. I. V. performance of insulator assemblies and components.

The chart shown in Figure 2 of this report gives quite definite recommendations for the specification of R. I. V. performance for insulator and hardware assemblies for transmission lines of all voltages and you notice, for instance, that at 500 kv they have recommended a limitation of 2,000 microvolts R. I. V. as measured in the laboratory at 110% of the normal line to ground maximum operating voltage. Liberalization of specifications for insulator assemblies to this degree could result in a marked reduction in the cost of such assemblies.

RL McCoy

R. L. McCoy

lr

att.

Pittsfield, January 24, 1964

RECEIVED
FEB 11 1964
H. A. FREY

cc: EM Hunter - 2-616 - SCHENECTADY
NR Schultz - SCHENECTADY
JG Anderson
LO Barthold - 2-612 - SCHENECTADY
HH Brustle - 9-314
HA Frey - Insulator Dept.-BALTIMORE
JJ LaForest
F Olsen

"CONTRIBUTION TO THE STUDY OF RADIO NOISE GENERATED BY MEDIUM VOLTAGE LINES"

By
MM. C. Gary and M. Moreau

Article from "Revue Générale de L'Électricité", October 1963, pages 503 to 518 Inclusive

Translation by D. D. MacCarthy

Giving account of work showing the possibility of evaluating the radio noise fields created by high frequency currents which are generated by insulators on medium voltage lines. In the first part, the authors analyze the process of forming these currents both in rigid insulators and then in suspension insulators; they show that the spectrum of the disturbing current is characterized by the line geometry and by the capacitance between the two metal parts of the insulator. An equivalent circuit of the insulator and line proves that they behave as a current generator injecting high frequency current in the two halves of the line on each side of the insulator. This current, determined by a series of laboratory tests, is the principal characteristic of insulator noise.

In the second part of the article, the authors reveal the possibility of obtaining correlation between the disturbance field measured under the medium tension line and the disturbance current injected in the line and determined from laboratory tests. A formula is established allowing the prediction of attenuation of the disturbance field in a direction perpendicular to the line as well as the absolute value of the disturbance field.

PART I: STUDY OF INSULATORS

Radio noise disturbances observed under lines of medium voltage cannot be attributed to the conductors, as is the case for high voltage lines, because the gradient to which they are subjected, of the order of 3 to 6 kv/cm, is much too low to generate, except during rain, leakage currents caused by corona. In the present work, we propose to demonstrate the possibility of evaluating the disturbance field of a medium voltage line due to the insulators, basing it on the laboratory measurements of the high frequency currents generated by the latter.

I. THEORETICAL STUDY OF INSULATORS.

Experience shows that the disturbance field of a medium voltage line does not vary in the same way, depending on whether the line is equipped with rigid [pin?] or suspension insulators: in the first case the disturbance field decreases markedly in fog or rain, whereas the opposite occurs beneath lines with suspension insulators. It seems then that insulators are, according to their type, the seat of different phenomena, phenomena that we are going to attempt to explain in what follows:

A. Rigid Insulators [pin type?]: - In the case of rigid insulators, the conductor is simply supported at the insulator neck by a lashing-like attachment, so that, if some portions of the conductor are in intimate contact with the insulator body, others must be separated by small air gaps. Because the insulation resistance is very high, it is justifiable to represent by independent capacitors the lines of force bordering on the zones of intimate contact and the lines of force bordering upon the air spaces. The same representation is valuable in the case of a defective insulator, where air gaps are caused by cracks in the insulator body or in the cement of the metal support.

The equivalent circuit is the following (fig. 1). When the voltage applied between A and B varies sinusoidally, practically all of it is carried by the air-gap terminals 1-2, 3-4. It produces then small sparks which charge C_1---C_2, in an extremely short time, and which are the origin of the disturbance. During fog or rain, it is conceeded that the small air gaps existing at the insulator surface must be short-circuited by water drops: then sparks do not occur, causing the disturbance to disappear. On the other hand, the discharges produced in the cracks continue; as they have, in addition, large amplitudes, it is possible to detect defective insulators by all methods sensitive to an effect external to the phenomena.

Granting that the short circuit of these gaps starts instantaneously, each of them may be represented analytically by applying to the terminals of the gaps, at the instant 0, a voltage step equal in value and opposite to the steady-state voltage at this instant. As one is only interested in the transient operation generated by the start of sparking between 1 and 2 for example, it is necessary to disregard all steady-state currents and voltages and this results in, according to figure 2, Z representing the characteristic impedance of each half line which goes away from the insulator.

$$i = \frac{1}{2}\,\frac{VC_1}{(C_0 + C_1)Z/2}\exp\left[-\frac{t}{(C_0 + C_1)Z/2}\right].$$

where $C_1 \ll C_0$, this may be written

$$i = \frac{VC_1}{ZC_0}\exp\left[-\frac{t}{ZC_0/2}\right].$$

B. Suspension Insulators (Cap and pin, isoblocks, etc.). - Experience has shown, in this case, the disturbance field increases with rain or fog, it is attempted to explain the disturbance phenomenon by the same process which occurs on high voltage lines: at points of very high gradient, plumes are produced corresponding physically to instantaneous emission into adjoining space of positive or negative electric charges (ions or electrons). The deposit of water drops on the insulator fittings under voltage again re-enforces these local gradients and multiply the points where they appear, which increases the number and amplitude of the discharges.

The equivalent circuit of an insulator and line, always from the transient-state view point, is then represented as follows (fig. 3): at the start, supposed to be instantaneous, of a charge q corresponding to the instantaneous appearance of a voltage q/C_0 at the terminals of the insulator capacity. Applying Thévenin's theorem, it is deduced that it acts as though the insulator were a voltage generator, with an internal impedance defined by C_0 and supplying a step voltage of q/C_0; the expression for the current injected in each half of the lines is

$$i = \frac{1}{2}\,\frac{q}{C_0 Z/2}\exp\left[-\frac{t}{C_0 Z/2}\right]$$

or

$$i = \frac{q}{C_0 Z}\exp\left[-\frac{t}{C_0 Z/2}\right].$$

C. Discussion. Value of the spectral components.

The comparison of the expressions obtained for the two insulator cases makes evident a remarkable fact that, whatever the hypothesis considered, the current injected in the line has rigorously the same behavior represented by an exponential function with a time constant $\frac{C_0 Z}{2}$. Physically this exponential behavior corresponds to equalization of the charge emitted by the insulator capacitance C_0 across the impedance Z/2 resulting from the two half lines. The difference lies in the fact that the charge lost by the suspension insulator designated by q is absorbed by ambient space, while the charge lost by the capacitance C_0 of the rigid insulator is absorbed by the small capacitance C_1 and has a value VC_1 (granting $C_1 \ll C_0$).

Thus, these phenomena, which are of fundamentally different physical nature, should in analysis appear as being mathematically identical. The equations which define the behavior of the insulator with respect to the line are the same in the two cases, whence the result that the disturbance field of a line on one hand, and the conditions of laboratory measurement on the other hand, obey the same rules which are the type of insulator or the hypothesis of generation of the disturbance considered. Consequently, from the strict viewpoint of mathematical analysis of the phenomena, there will be no consequent need to take account of their physical nature.

Now evaluating the spectral density of the current pulse injected in the line by application of Fourier's transform

$$g(\omega) = \int_{-\infty}^{+\infty} i(t) e^{-j\omega t} dt,$$

that is

$$g(\omega) = \frac{q}{C_0 Z} \int_0^{\infty} \exp - t \left[\frac{2}{C_0 Z} + j\omega \right] dt$$

(it is sufficient to integrate from $t = 0$ to $t = \infty$, since by definition the pulse is zero for $t < 0$).

Then

$$g(\omega) = \frac{q}{2} \frac{1}{1 + j\omega \frac{C_0 Z}{2}}.$$

In reality the insulator does not produce a unique pulse, but series of pulses of variable amplitudes, and groups in "bursts" which generally repeat twice in each period T of the supply voltage, with a certain dispension around the average repetition time.

We classify these pulses in categories corresponding to discharges of average amplitude $q_1, q_2, \ldots q_i \ldots q_n$ and assuming for each category an amplitude coefficient $\lambda_i < 1$ corresponding to the maximum discharge q. Designating, on the other hand by σ^2 the square of the average deviation in time corresponding to the repetition period T_i. This gives

$$G^2(\omega) = \left[1 - \exp(-\sigma^2\omega^2) + \exp(-\sigma^2\omega^2)\,\frac{2\pi}{T}\delta\left(\omega - \frac{2m\pi}{T}\right)\right] \mathrm{X}\ \frac{[g(\omega)]^2}{T}\sum_0^N \lambda^2{}_i$$

where δ is Dirac's function which makes the second term in the bracket zero except for harmonics of $\frac{2\pi}{T}$.

The spectrum is analyzed into a line spectrum with the amplitudes decreasing very fast with frequency, and into a continuous spectrum.

At radio frequencies (broadcast and television) the term $e^{-\sigma^2\omega^2}$ becomes negligible, there is no line spectrum and most simply

$$G^2(\omega) = \frac{1}{T}\,\frac{q^2}{4}\left[\frac{1}{1 + j\omega\frac{ZC_0}{2}}\right]^2 \sum_0^N \lambda^2{}_i.$$

All radio receivers of the type used for our studies are characterized by a band width $B = \Delta\omega$, which are sensitive only to a fraction of the energy spectrum centered on the frequency ω_0; in other words, they respond only to the energy in the band between $\omega_o - \frac{B}{2}$ and $\omega_o + \frac{B}{2}$. Parseval's theorem shows us that this energy is proportional to the band width; the quadratic value of the current "seen" by the receiver from the frequency ω_0 is

$$i^2(\omega_o) = BG^2(\omega_o),$$

since B is sufficiently narrow to consider that $G(\omega)$ is constant in the frequency interval.

The measurements of fields and currents conform to CISPR standard and give a reading proportional to current crest; for a given band width and type of signal in question assuming they have a corresponding constant k relating the crest and effective values, the measuring equipment indicates a current

$$i(\omega_o) = \left[k\frac{q}{2}\sqrt{\frac{B}{T}\sum_0^N \lambda^2{}_i}\right]\frac{1}{1 + j\omega_o\frac{C_oZ}{2}}$$

Designating by i_o the term in brackets, which represents a current amplitude independent of frequency, we finally measure a current

$$i(\omega_o) = \frac{i_o}{1 + j\omega_o\,\frac{C_oZ}{2}}$$

It is this current $i(\omega_o)$ which, in all the following of this study, we designate as "insulator disturbance current at frequency $\frac{\omega_o}{2\pi}$".

From this last expression, we are able to make some observations that are extremely important in interpreting the experimental results.

1. Everything occurs as though the current of the amplitude found, independent of the frequency, were injected at a point P of the combination of the line impedance and the insulator capacity. This concept is fruitful, because it allows the behavior of the line to be accounted for by the external injection of a known artificial current (fig. 4).

2. The current injected in the line is practically constant, as a function of frequency, up to a frequency as large as

$$\frac{\omega C_0 Z}{2} = 1$$

or

$$f = \frac{1}{\pi C_0 Z}$$

Beyond this frequency "of cut-off" the amplitude of the measured current decreases at a rate of 6 db per octave. The spectrum which is recorded is not a characteristic spectrum of the insulator or the discharge, but is determined by the association of its capacitance with the impedance of injection in the line. This discovery is fundamental for comparing spectra obtained from laboratory measurements and from direct measurements of the disturbance fields beneath lines.

3. Television frequencies are far beyond the highest cut-off frequency defined. At these frequencies, the current injected in the line by an insulator, is reduced considerably in comparison to the value i_o for low frequencies. This is one of the fundamental reasons (but not the only one, we will see others later) why television disturbances created by an insulator have an entirely local effect, and will not be transmitted by the line.

A numeric example will define the order of magnitude

Let $C_0 = 100$ pF and $\frac{Z}{2} = 300$ ohms. The cut-off frequency has a value $F_0 = 5$ mc; at 100 mc the attenuation has become 26 db (1/20).

II. EXPERIMENTAL PROOF OF THE THEORY. -

Related to checking at what point the theoretical considerations which were developed are valid, we have had certain experiences which we are going to describe. They bear on the following points:

A. Experimental curves of spectra;

B. Displays of current pulses and photographs of discharges;

C. Artificial reproduction of the disturbance phenomena.

For these measurements we have adopted the circuit shown in fig. 5b which moreover corresponds, with some variations, to the circuit recommended by CISPR.

The insulator tested (rigid or suspended type) is fastened to a metal support aligned to the body, representing the pole, and supports a bar, placed under voltage which represents the conductor. The bar, 10 mm in diameter, is smooth and terminated by a small sphere to avoid corona.

The circuit, which is the so-called measuring circuit, from the viewpoint of high-frequency transients is equivalent to the theoretical circuit, the only difference is due to the presence of the capacitor C_m which blocks the 50-cycle supply voltage from the branch to ground. When it is connected in the circuit, it modifies the amplitude of the disturbing current at the cut-off frequency, in accordance with the new expression

$$i_m(\omega) = \frac{i_o}{1 + \frac{C_o}{C_m} + j\omega RC_o} ;$$

It is possible to take into account the presence of this capacitor if its capacitance is very small compared to C_o, but it suffices that it equals 5 C_o for then it may be neglected: it is necessary to specify that C_o is not made up only of the insulator but equals the capacitance of the connections (bar under voltage and sphere) and by the parasitic capacitance of the mass of the capacitor C_m itself; these elements entering the computation of the cut-off frequency of the spectrum.

On the other hand, it is important to note that the decoupling capacitor must have an inherent inductance as small as possible, at the expense of not providing the correct spectral analysis of the pulses up to high frequencies: in effect an ordinary capacitor of oil-impregnated paper gives a frequency of the order of megacycles which is the limit of its usefulness. Hence we have used a special capacitor of 1000 pF made of an assembly of dielectric ceramic in oil, which reduces its inductance to that of the leads. The resonant frequency of the high frequency circuit has then become 15 or 20 mc, as is shown by curves of capacitance vs. frequency obtained with a Q-meter (fig. 6).

The resistor B is of the order of 20 k ohms, which has the purpose of decoupling the measuring and 50-cycle supply circuits; its advantage in the rejector circuit recommended by CISPR is to provide uniform decoupling at all frequencies without needing adjustment.

Finally, the measuring apparatus used in the Siemens 3800 meter, meeting CISPR specifications, will measure the high frequency current injected across the resistor R.

A. Study of spectra. - We have plotted, for a rigid insulator type HT 30 and for a suspension insulator type CT 175, a series of spectra of this current $i = f(\omega)$ with respect to many values of resistance R (fig. 7 and 8). It is found that the general form of the spectra remarkably agree with that predicted by theory: first a region where the current is independent of frequency, then after a bend joining the cut-off frequency, a decrease of field of 6 db per octave. The displacement of the cut-off frequencies toward the left, at increasing resistances, as well as the parallelism of the right-hand slopes, appears in a particularly clear manner.

Comparing the cut-off frequencies obtained experimentally with those which calculation gives, take into account the values of charging resistance and apparent capacitance of the circuit (measured with a Q-meter) (fig. 8), one obtains Table I.

TABLE I

Comparison of the calculated and measured
values of cut-off frequencies

Resistance R (ohms)	CT 175 $F_o$mc		HT 30 $F_o$mc	
	Calculated	Measured	Calculated	Measured
15,300	0.10	0.10	0.13	0.15
6,200	0.26	0.30	0.32	0.30
2,250	0.70	0.60	0.90	0.80
600	2.7	2.0	3.3	2.5
210	~ 5.0	~ 4	7.5	~ 6

For high resistances, a very good agreement is found between the experimental and calculated cut-off frequencies.

At about 600 ohms, the measured cut-off frequencies appear systematically smaller, a phenomenon for which we have not found a satisfactory explanation; perhaps other damping elements exist in the circuit (proximity of iron pieces, skin effect...) having the effect of increasing the total value of circuit resistance.

In relation to resistances less than 200 ohms, the theoretical cut-off frequency reaches the normal resonant frequency of the circuit, and its calculation does not make sense; we have studied the evaluation taking account of the apparent increase of the capacitance, values are found agreeing well with measurement, but the spectrum does not have the theoretical shape, and in particular, the inclined zone falls at a slope greater than 6 db per octave, which occurs at resonance.

B. Visualization of the pulses. - Photographs of discharges. - We have seen in the preceding section, that the spectrum, which is recorded when the insulator subjected to voltage generates disturbances, results from the superposition of a great number of pulses of identical individual shape, but variable amplitudes, and whose position is distributed about the average repetition frequency according to a law of stationary risk. Equally we have seen that the total spectrum must have the same behavior as the spectrum of a single pulse. The verification of the pulse shape constitutes another confirmation of our hypothesis because of the relation known to exist between the spectrum and pulse shape, in addition the latter has been established by calculation.

To this effect, we have used a special oscillograph, with vertical amplifier presenting a band width of the order of 50 mc; this permits reproduction without distortion of fronts that have a "rise time" of 6×10^{-9} seconds.

The lead of this oscillograph should be connected to terminals on a portion of the resistance R, in a manner to assure its correct use; thanks to a delay cable it will be possible to adjust the triggering and duration of the sweep so that the entire pulses will be visible on the screen. Thus it is easily possible to perfectly observe the shapes whatever may be the amplitudes of the successive pulses.

In regulating the sensitivity of triggering so that only the largest pulses are recorded on the screen, it has been possible to note their form precisely as is shown by the oscillograms of fig. 9.

The cut-off frequencies f_o of the spectra and the time constant of the pulse tails T_o are related by the theoretical relation $2\pi f_o T_o = 1$ although crossover between values recorded from spectra and the pulse shapes may not be rigorous, it is again found to be between compatible orders of magnitude. On the other hand, the wave front rise time of the order of 20 ns explains the begining of the very steep slope of the spectra starting at about 20 mc. Regarding the pulses showing a superposed slightly damped oscillation, at a frequency of the order of 20 mc, which are shown by spectra around this frequency: this has been shown to correspond to a resonance in the high frequency circuit, preceding the steeper fall off of the spectrum.

In parallel with these measurements, we photographed the insulators under voltage in darkness to reveal the location of the discharges.

In this concern the pin insulators (type HT 30) have been usually observed to produce small sparks at the neck where the conductor is attached, the number increasing in proportion to the increase of voltage.

In figure 10 which has been taken at a voltage well above normal to better show the nature of the phenomenon, these sparks form a luminescent ring. On the contrary the phenomenon totally disappears in rain (fig. 10b), also at very high voltages, at the limit of the insulator contour.

In this concern the suspension insulator (glass insulators CT 175), it seems that the disturbance starts by the formation of corona beneath the skirt (fig. 10C), short circuiting the cement between the pin and the glass: the phenomenon then appears to be of the same nature as for the rigid insulators, that is charge of small capacitances through air which is energized. At increased voltage, the corona appears equal beneath the skirt and at the level of the cap (fig. 10C). With rain the upper corona disappears, the lower corona increases markedly; it is certain to come from water drops (fig. 10d).

Finally plumes from the conductor are not observed.

C. Artificial reproduction of the disturbance phenomenon. - To allow direct work on the parameters controlling the shape of the disturbing pulses, we made the following setup (fig. 11), which synthesises the high frequency transient behavior, without the necessity of applying high voltage: the insulator must always be in the setup described, the excitation of the air gap has been replaced by periodic closing of a vibrating electromechanical relay ("Clare" having wetted contacts, to prevent chatter) charging a capacitor C_1 of exactly 5 pF. A dc source of 100 v represents the quasi-steady state voltage applied to the insulator: the 50 mega-ohm resistance r is to discharge C_1 between successive closures of the relay to assure consistency.

For these new conditions we have made oscillographic observations of the wave form over a wide range obtained at the terminals of resistance R: we observed the very same wave shapes as with high voltage: in particular to again find the pulse front of 20 nS, the charge on C_1 must be damped by a resistance of the order of 5,000 ohms. This must be explained by the fact that the elementary capacitance in the actual phenomenon is made up of flux lines that terminate on the very highly insulating surface greater than the impact point of the spark; the charges which dissipate relatively slowly, because of the surface resistance, which damps the front (fig. 12).

Under the same conditions, we have traced spectra for many values of resistance R; the appearance of these spectra is seen to coincide remarkably well with those of the actual disturbances (fig. 13).

The following results were obtained:

Resistance (ohms)	$T_o = \frac{1}{2\pi f_o}$ obtained from spectra (ns)	T_o from oscillograms (ns)
210	30	30
600	80	100
2,200	270	300
6,000	800	800
15,300	~2,000	2,500

III. SYSTEMATIC MEASUREMENT OF INSULATOR DISTURBANCE LEVELS. -

A. Circuit used. Mode of operation. - For this series of measurements we have again used the general circuit and material which we have described. The arrangement of the insulators is the same; we must respect the actual distribution of the electric fields by choosing supports of suitable dimensions.

The measuring resistor of 300 ohms conforms to the CISPR standards, all values have been taken at a frequency of 1 mc. It is seen from the spectra we have taken that, at this frequency taking the capacity of the test piece into account, the disturbance level corresponds to the horizontal part of the spectrum; i.e. is independent of frequency.

In accordance with practice, the levels are expressed by the disturbance voltage on the 300-ohm resistor (we will see later that this value is not of much significance, but that the value which enters the calculation of the field under a line is the disturbance current injected by the insulator). In this connection it is noted that the readings must be made of complete cycles of increasing and decreasing voltage, and, for each measurement the disturbance field stabilizes after waiting for ten minutes: only under these conditions a proper superposition of increasing and decreasing current is observed; it is well known that this is caused by burning off contaminants by corona which in fact corresponds to an "aging" of the disturbing element.

B. Test results. - The tests have been made for the operating conditions of a new line: insulators in good condition with correct ties.

The material studied consists of (fig. 14):

three chains of suspension insulators CT 175 (glass);

a chain of suspension insulators CT 175 (porcelain);

rigid insulators HT 30 with re-enforced crossties, or with ties in an arch;

porcelain monoblock insulators:

a) with four skirts and ball-and-socket attachment;

b) with three skirts and shackle or ball-and-socket;

c) a spiralex insulator;
a cable only, and with a broken strand (7-strand almélec).
<7-strand electrical grade aluminum>

Measurements were made under the following climactic conditions:

"warm: : temperature 32°C hygrometric degrees 30 for 100 per cent;
<perhaps 30 per cent relative humidity>

"dry" : temperature 18°C hygrometric degrees 50 for 100;

fog : temperature 14°C hygrometric degrees 100 for 100;
normal rain: temperature 20°C hygrometric degrees 100 for 100.

Different arrangements of the same type (cap and pin monoblock, monoblock rigid) are shown to behave in a practically identical manner, with a small variation in practice which makes it practically useless to give the results.

In Table II we have for clarity simply shown the most significant average values obtained for voltages of $15/\sqrt{3}$ kv and $20/\sqrt{3}$ kv corresponding to network voltages of 15 kv and 20 kv.

TABLE II. - Average values obtained

(*) Test condition	Equipment							
	String of 3 insulators CT 175 µv		Isoblock insulators µv		HT 30 insulators µv		Cable almélec	
	15 kv	20 kv	15 kv	20 kv	15 kv	20 kv	15 kv	20 kv
warm					500	900		
dry	1	1	1	2	400	700	Not measurable	
fog	1	2	4	5	2	2		
rain	6	20	10	10	8	20		

*Values less than 10 µv, below the threshold, have been extrapolated.

The curves (figures 15 to 19) show how the disturbance field varies for several types of material as a function of voltage and for several climactic conditions.

The following curves result from this series of measurements.

The rigid insulators < pin insulator > under normal conditions and voltage have an appreciable ionization level in a dry condition. Under rain and fog the field decreases below the threshold of measurement (<10 µ v). At 15 to 20 kv the disturbance field approximately doubles.

In this concern the suspension insulators (cap and pin or isoblock), the level found in the laboratory is always less than or of the order of the measurement threshold except with some exceptions under rain.

The conclusions made up to the present and the hypotheses from which they were deduced have on the whole been well confirmed, namely:

a) the disturbance field of the rigid insulators which is relatively important "dry" decreases to a negligible value with rain or fog;

b) the disturbance field of the suspension insulators is higher with rain than dry, but is generally less than that of the rigid insulators;

c) in each case, plumes which determine the disturbance level of the medium tension line do not form on the conductors: their only role is to propagate the disturbance currents.

Although the laboratory tests described account well for the behavior most frequently observed under the lines, it seems that the actual levels are a little higher than those which will be predicted; on the other hand, several important differences are apparent which can probably be explained by more extended laboratory tests taking into account the particular circumstances under which these differences have been observed and we will only cite that of intense sunlight. These several points will be explained in the second part of this article.

PART II: DISTURBANCE FIELD OF MEDIUM VOLTAGE LINES

I. PHYSICAL REPRESENTATION OF THE PHENOMENA AT WORK

We have now seen that the transient phenomena of which the insulators are the seat are manifested by two current waves injected in the conductors and propagating themselves in opposite directions on each side of each insulator. We have equally seen that these current waves, at a very steep front at their origin, may be analyzed in a Fourier spectrum; now the components of this spectrum behave in very different fashions, according to their frequency band, and this behavior has a direct influence on the way receivers are disturbed in the vicinity of the line. In general, the phenomena may be represented as follows.

So long as the wave length of the spectral compared is large because of the transverse dimensions of the line, that is to say to the extent of the transverse propagation of voltages, one can consider that at this component of current there are associated two orthogonal fields, one electric the other magnetic, which propagate together along the line, they form a plane (guided) wave, whose energy vector is parallel to the line. The attenuation, which increases as a function of frequency, is sufficiently small for the disturbance to thus transmit only for distances of several kilometers.

When the wave length becomes of the same order of magnitude as the transverse dimensions of the line, that is to say, when it is necessary to introduce the concept of retarded potential, bringing into play an altogether different process: part of the energy is radiated directly by the line, acting as an antenna, in the form of an electromagnetic wave, at the same time which with frequency increases the conductor lengths participating in this radiation around the point of generation being reduced more and more.

At television frequencies (above 50 mc) it is not a practiacl wave guide, but only electromagnetic radiation of a more or less very local sphere of action.

Thus the high frequency energy generated by an insulator propagates in two entirely different manners. It must flow out along the line, by which it is guided, called "channel disturbance" (this is the case for long and medium waves), being radiated from the insulator as a space wave, referred to as direct radiation (this is the case of ultra short waves). The short waves participate in the two types of propagation simultaneously.

From the preceding analysis it results that for the long and medium waves, the dominant part of the disturbance field is caused by the superposition of the effects of all insulators distributed along several tens of kilometers on each side of the point of measurement, and not on the direct effect of nearby insulators.

To the contrary for very short waves (television), the disturbance is not propagated by the line, and has only a local action. As we have seen on the other hand that a sound insulator generates very high frequency current (200 mc) very feebly, a sound line does not normally disturb television. Only a defective element (cracked insulator, bad contact, steady arc) can generate a disturbance which has a local effect for a radius of 200 to 500 meters.

Thus, television disturbances constitute a special case, and it is useless to search for the theoretical value of their level; on the contrary, it is possible to acknowledge that all insulators of a long line present on the average an identical disturbance field, to try to calculate the exact disturbance field for long and medium waves, that is to say for frequencies less than about 5 mc ($\lambda = 60$ m).

II. GENERAL METHOD OF CALCULATING THE GUIDED DISTURBANCE FIELD. -

It was noted earlier that it is easier to reason if the disturbance were a current generator, as we have shown in the first part, it is independent of the loading impedance of the high frequency circuit as long as the spectral frequency studied is less than the cut-off frequency of the pulse spectrum; this is the case for the long and medium waves, taking into account the capacitances of the insulators and the characteristic impedances of the usual three-phase lines.

The current injected in the conductor on both sides of each insulator, induces currents in the nearby conductors whose values depend on the capacities between conductors and in relation to ground. Thus, proceeding from each insulator one obtaines a system of three currents whose propagation must now be studied.

For such a system of any currents, one discovers that a simple law of attenuation of propagation does not exist, the currents and voltages relative to each conductor do not depend on the same relation, and the system undergoes a deformation which is a function of the distance of propagation. But, it is shown that there are particular systems of currents and voltages, called "symmetrical modes" which propagate without deformation and which have a well-defined attenuation constant, thus with the same impedance characteristic common to all conductors. Their value is obtained starting with the potential coefficients of the line considered, resulting in as many modes of propagation for each line as there are conductors. For a three-phase line, the calculation results in three modes of propagation, which we designate

"homopolar mode" - identical polarity on the three conductors symbolized by + + +,

"bipolar mode" - symbolized by + 0 -, and

"interphase mode" - symbolized by + - +

if the line has a flat configuration.

Attenuation of propagation is caused by losses in the earth and in the conductors. It is possible to evaluate the attenuation coefficients relative to each mode, for a given line, it brings in the superficial resistivity of the terrain traversed by the line, the resistivity of the conductors, as well as the geometric structure of the electromagnetic guided field (which is supposed to be a plane wave) associated with the mode considered.

The following formula is used

$$\alpha = \frac{\sqrt{\varepsilon_o}\,\omega}{2\sqrt{2}}\left[\sqrt{\rho_o}\int_{Sol}\left(\frac{d\phi}{dn}\right)^2 dS + \sqrt{\rho_c}\int_{cond.}\left(\frac{d\phi}{dn}\right)^2 dS\right]$$

where ρ_o and ρ_c are the resistivities of the earth and the conductors, ϕ is a potential function dependent on the mode considered, and ω is the angular velocity corresponding to the frequency.

When one wants to study the propagation of any system of currents such as we are interested in here, it is necessary to analyze it into symmetrical modes (which have linear properties and consequently can be superposed to constitute the given system) to study separately the propagation of each of them, then recombine at each point of the line the modes which have been obtained after they have independently undergone their own natural attenuation. But in reality, at any point of the line (supposedly infinite) the noise current of each mode considered, is made up by superposing the modal currents due to all insulators on a conductor. On the other hand, it is shown that, because of the random generation of these currents, it is convenient to evaluate the total current by a quadratic summation.

Then α being the attenuation for propagation of the mode considered and i_m being the modal current injected by an insulator, at a distance ℓ from the point of generation, the square of this element of current has a value of

$$dI^2_m = i^2_m \, e^{-2\alpha\ell} . d\ell$$

The total modal current obtained is

$$I^2_m = 2i^2_m \int_0^{\infty} \left[e^{-2\alpha\ell} \right] \frac{d\ell}{D} ,$$

where D is the span between adjacent insulators

and $$I^2_m = \frac{i^2_m}{\alpha D} .$$

Beginning with this total current, and knowing the characteristic impedance of the mode, it is necessary to determine the magnetic and electric components of the field of the ground mode.

The same calculation is repeated for each of the other two modes, and the total disturbance field is finally computed from the quadratic superposition of the three modal fields.

This operation has been made by assuming that each of the insulators on one conductor simultaneously generates disturbance; this is certainly true, since each conductor of a three-phase system reaches its voltage in turn. It is therefore necessary to repeat the calculations separately for each conductor and to compare the ground fields which are obtained in each case, if they are practically equal, the repetition frequency of the noise is multiplied by three, which represents an increase of about 3 db in the CISPR level; if the three fields are not equal, one takes the strongest, increased by a quantity which must be evaluated, but which will always be less then 3 db.

III. SIMPLIFIED FORMULA FOR A MEDIUM VOLTAGE LINE. - PREDETERMINATION OF THE LEVEL. -

When the detailed calculations are made, one verifies that, recognizing the dimensions of a medium voltage line, and because of the supplementary attenuation important owing to the conductors, the disburbance field is practically that of the homopolar mode, the other modes enter little in forming the field at the ground.

This property found only for lines of medium voltage (and which results from the small spacing between the conductors in relation to their distance to earth) contributes a considerable simplification to practical calculation; everything happens as though the line were unipolar and the three currents of the homopolar mode were concentrated in one conductor only. For the usual line dimensions, this equivalent single current has a value in the neighborhood of half the current injected in the half line, being a fourth of the total current injected by the insulator (this holds because the current injected in one of the conductors induces a current of the opposite sign in the other two). The sum of these three currents is then less than the current injected.

The noise current I_p at a point on the line is then given by the simplified expression

$$I_p = \frac{I_{insul}}{4\sqrt{\alpha D}}.$$

The magnetic component of the disturbance field at the ground is obtained (this component is horizontal) by applying Laplace's law and the theory of images (fig. 20);

$$\mathcal{H} = \frac{I_p}{\pi} \frac{h}{h^2 + d^2}$$

where h is the average height of the conductor above ground, and d the distance computed from the axis of the line.

The equivalent electric field in volts per meter obtained from the magnetic field by introducing the concept of the characteristic impedance of space, being $E(V/m) = 120\pi \times H$ (Amp Turns/m) and finds

$$E(V/m) = I_{insul} \frac{30\,h}{(h^2 + d^2)\sqrt{\alpha D}}$$

The reading in decibels (CISPR), calculated taking into account the repitition frequency, then gives

$$N(db) = 3 + 20 \log_{10} E(\mu V/M),$$

if I_{insul} is in microamperes.

The preceding formula may be altered to

$$N(db) = 33 + 20 \log_{10} \frac{h}{h^2 + d^2} - 10 \log_{10}\alpha D + 20 \log I_{insul} ,$$

which permits the influences entering the formation of the real field at the ground to be separated (the first term being a constant, depending on the system of units); the second term accounting for the attenuation perpendicular to the line and determining the form of the transverse profile; the third term accounting for the cumulative effect of various sources of disturbance distributed along the line; finally the fourth term characterizes the intensity of an individual source of disturbance.

These formulas, in a practical way, allow prediction of the disturbance field from the insulators on a line starting with the laboratory measurement of the noise current from an individual device.

IV. APPLICATIONS TO AN ACTUAL LINE. - COMPARISON WITH MEASUREMENTS UNDER THE LINE. -

Characteristics of the line

Service voltage: 15 kv

Average height of conductors above ground: $h = 8$ m

Distance between poles: $D = 64$ m

Homopolar attenuation: $\alpha = 2$ db/km being 2×10^{-4} nepers per meter

Pin insulators type HT 30, triangular arrangement.

Calculation of the profile of this line; the field varying as a function of d follows:

d (in meters)	0	1	2	5	10	15	20	50	100
$20 \log_{10} \frac{h}{h^2 + d^2}$	-18	-18	-18.5	-21	-26.2	-31.2	-35.3	-50	-62
ΔN	0	0	-0.5	-3	-8.2	-13.2	-17.3	-32	-44

The slope of the asymptote is -12 db by doubling the distance. On the other hand, the cumulative effect of the sources contributes

$$10 \log_{10}\alpha D = 10 \log_{10} 64 \times 2 \times 10^{-4} = -19.$$

The field under the line will then be given in final calculation by the expression

$$N(db) = 34 - \Delta N + 20 \log_{10} I_{insul}$$

If the profile thus calculated is adjusted with the real profile recorded under the line, in the first place, the disturbance current of each insulator is deduced from it.

Thus, at the time of measuring beneath the line (the meteorological conditions being: dry weather, 18^oC temperature, sky lightly covered) the field beneath the center of the line being 44 db at 1 mc (fig. 21). Then one has:

$$44 = N_o = 20 \log_{10} I_{insul} + 34$$

or $20 \log_{10} I_{insul} = 10$ db, which level corresponds at this moment to a disturbing current of 3 μA. This value is in reasonable agreement with those found in the laboratory on the same type of insulators.

In the second place, the comparison of calculated and actual profiles shows an excellent agreement up to about 20 meters, fig. 22. For greater distances from the line, between 20 and 80 m, the slope is only of the order of 9 db for double the distance (which corresponds to a decrease of $1/d^{1.5}$ instead of $1/d^2$. This can be explained by the fact that, rigorously, the other modes are not wholly negligible at these distances, besides the earth is not a perfect conductor, the image of the conductor does not have as clean an effect as in the theoretical calculation; at still greater distances, measurement becomes practically impossible because the natural level of the line is drowned in the background of natural radio noise.

V. VARIOUS OBSERVATIONS AT THE TIME OF MEASURING DIRECTLY UNDER LINES. -

Numerous measurements made beneath other medium voltage lines have shown that, generally, the levels calculated from laboratory tests are weaker than the actual levels.

In this concern, lines with rigid insulators (for example type HT 30), the variation between the calculated level and the measured level ranges between 3 and 10 db; this relatively small variation may easily be interpreted by recognizing that the ties on actual lines loosen because of wind and bad weather, cause more interference than a new tie, well tightened, studied indoors.

In this concern, for lines having suspension insulators (for example type CT 175), some extremely different levels have been noted: when beneath certain lines the agreement with calculation was satisfactory, beneath others variations of 50 db have been discovered. Perhaps these variations are attributable to the effect of insulator polution, corrosion of attachments, oxidation at the position of the ties, which introduce unfavorable conditions are not represented in laboratory tests. To check these points, we now propose laboratory measurement of the disturbance current of ties and insulators taken from lines after a certain time of operation, and for which the disturbance level disagrees with our theory.

Other anomalies have been discovered. In particular, at high temperatures and intense sunshine, an excessive increase in the disturbance level have been observed accompanied by a change in the behavior of the spectrum; intense sunlight seems to favor the generation of high spectral frequencies, without another hypothesis it is not actually possible to explain this phenomenon.

VI. SUMMARY AND CONCLUSION. -

In the first part of this work, we have tried to explain the phenomena of insulator disturbance in mathematical form, finally to analyze the behavior of the assembly constituted by the insulator and the line. To the first approximation, the analytical expression for the disturbance current generated does not depend upon the physical phenomena which is the cause of the disturbance, but nevertheless in a range of frequencies less than some megacycles, is characterized only by the geometry of the line and by the capacity between the two fittings of the insulator.

The experimental studies in the laboratory of the disturbance spectrums have well confirmed this theory. A group of laboratory tests allows determination of the characteristic magnitude of the disturbance effect of the insulator, this magnitude being an intensity of high frequency current injected in the line, without which it would be necessary to make complementary hypotheses on the physical nature of the disturbance.

In the second part we have shown that it is becoming possible to obtain a correlation between the disturbance field measured under the line and disturbing currents injected in the line by the insulators, to take account of the propagation times of these currents and of the cumulative effect of sources of disturbance repeated along the line. The complete calculation is long, but by means of some simplifications justified for lines of medium voltage, one can establish a practical formula for prediction, very simple to use. This formula allows prediction of the attenuation of the field normal to the line (transverse profile) as well as the absolute level of the disturbance field.

Comparison between the predicted fields and those taken under lines show remarkable coincidence of the two profiles. But, in this concern the prediction of the absolute level, measurements beneath a certain number of lines equipped with rigid or suspension [insulators] show the fields derived from laboratory tests are generally weaker than actual fields. This variation can be explained by the fact that insulators on lines are responding to climactic conditions much more severe than insulators tested in the laboratory, some subsequent tests are foreseen to prove this point.

We do not pretend to have explained all of the problems. Many phenomena remain unknown and their interpretation will demand more work and tests.

But in spite of the restrictions which we state, we hope to have contributed to the problem of predicting the disturbance field of medium voltage lines, principally by a better understanding of the mechanisms of injection and propagation of high-frequency currents generated by insulators. It is hoped also that this improved knowledge of the generation of disturbances constitutes only a first step in research on their elimination, the ideal aim to which we must devote our efforts.

DDM:ed

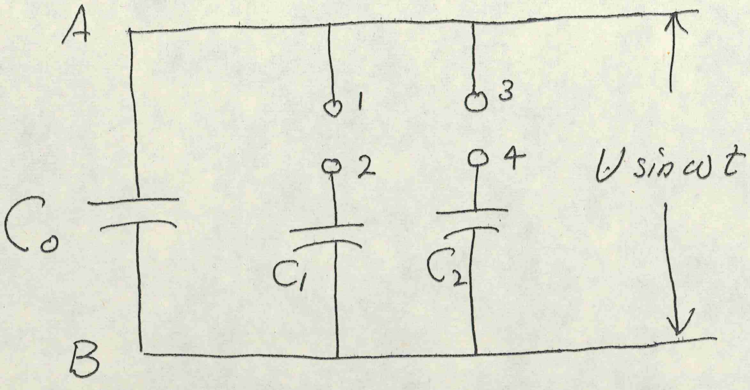
A
1
3
2
4
$U \sin \omega t$
C_0
C_1
C_2
B

Fig. 1. Equivalent diagram of rigid insulator: 1-2, 3, 4, represent spark gaps between conductor and glass, between cement and pin, or internal cracks.

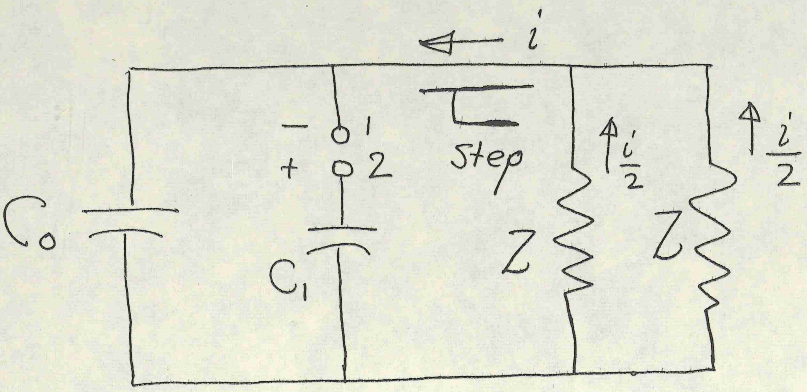
i
−
1
+
2
Step
$\frac{i}{2}$
$\frac{i}{2}$
C_0
C_1
Z
Z

Fig. 2. Representation for transient state caused by sparking of air gap.

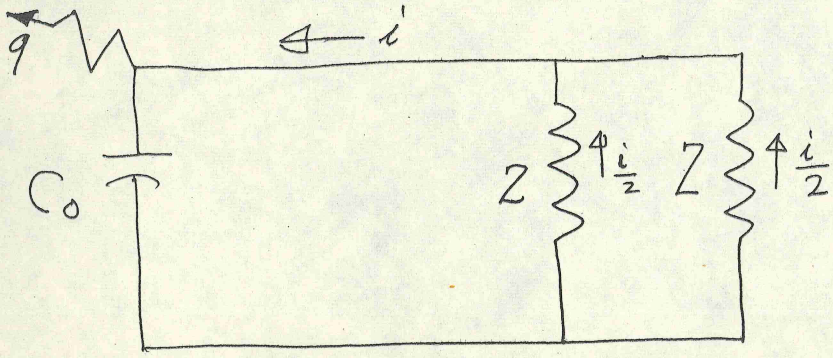
q
i
C_0
Z
$\frac{i}{2}$
Z
$\frac{i}{2}$

Fig. 3. Equivalent circuit of an insulator which causes disturbance by emitting charge to nearby space.

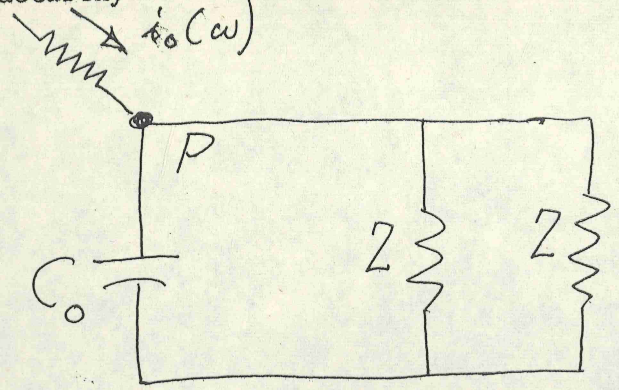

Fig. 4. The instantaneous emission of charge by an insulator is mathematically equivalent to the injection at point P of a current of constant spectral density independent of the frequency.

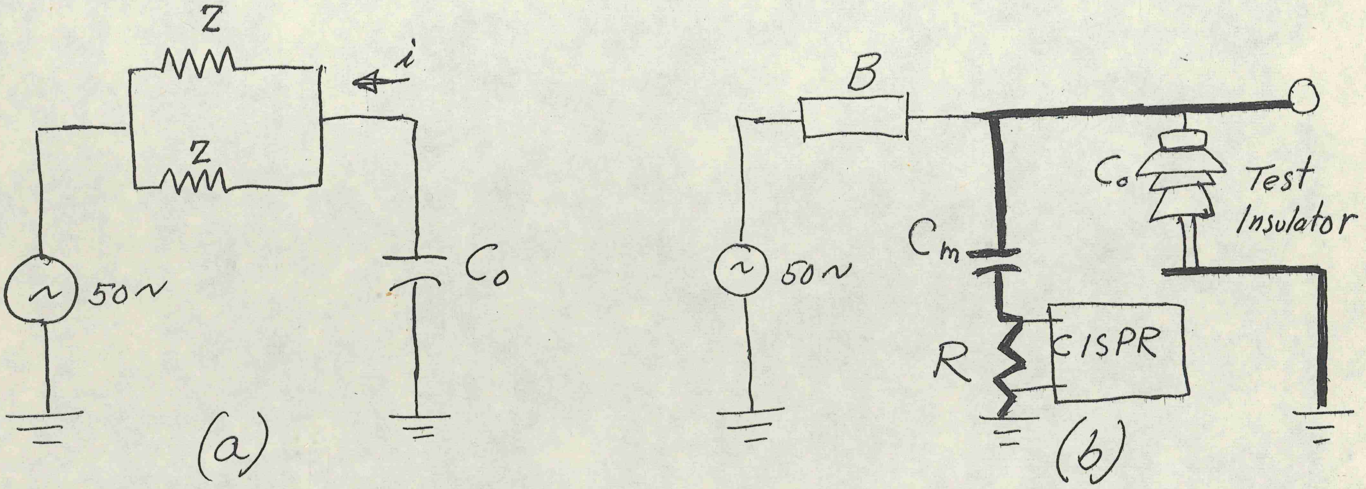

Fig. 5. (a) Equivalent circuit of an actual line subjected to voltage, from the point of view of the production of disturbance currents.
(b) Equivalent circuit of setup used to test insulators: the circuit in heavy lines is for high frequencies equivalent to circuit (a).

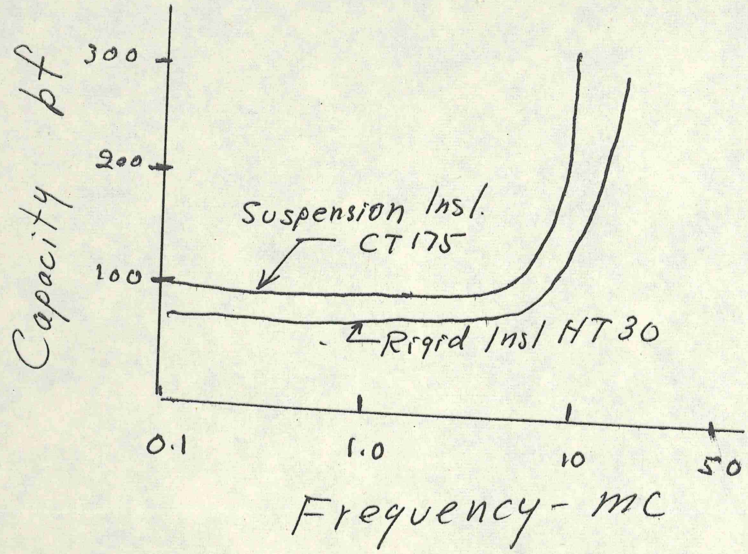

Fig. 6. Curves as function of frequency, for the apparent capacitance of an insulator with its system of attachments and a 1 m portion of the conductor, from the viewpoint of the decoupling capacitor C_m (measured with a Q-meter).

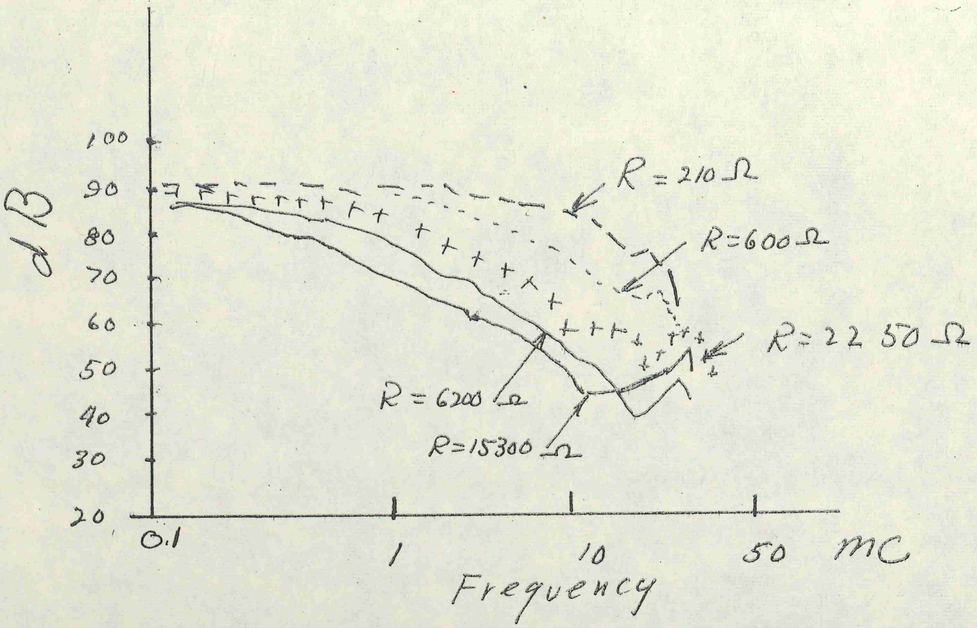

Fig. 7. Spectra of disturbance current for various values of resistor R for a rigid insulator HT 30.

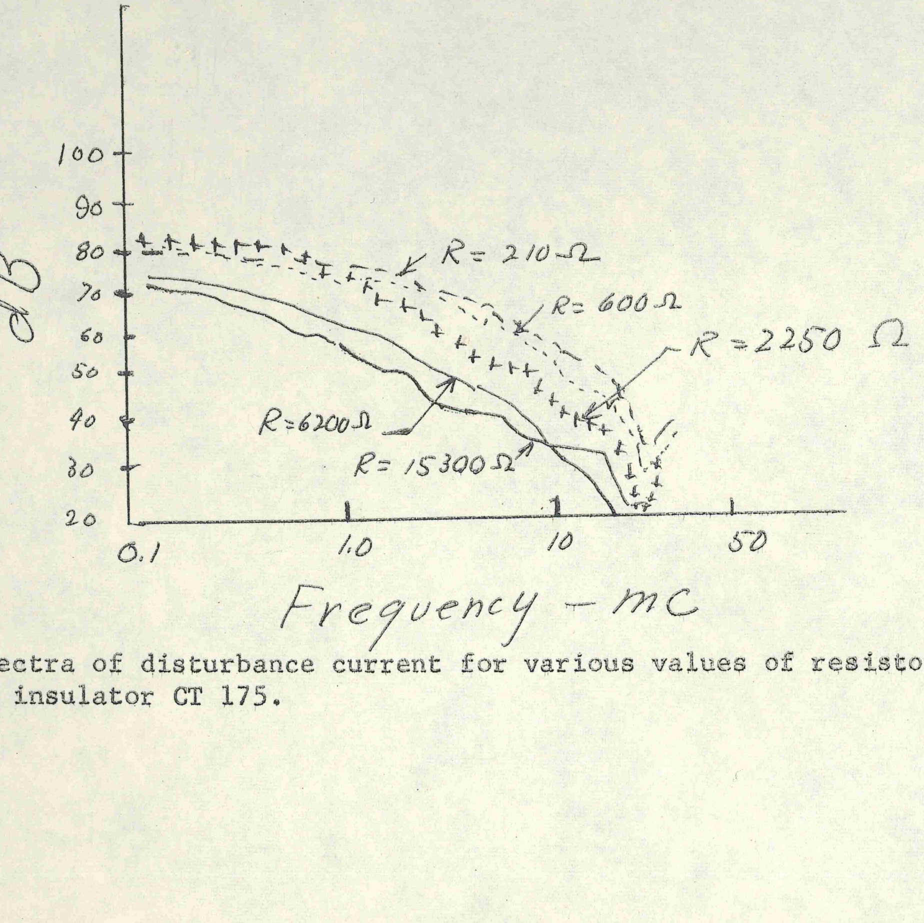

Fig. 8. Spectra of disturbance current for various values of resistor R for a suspense on insulator CT 175.

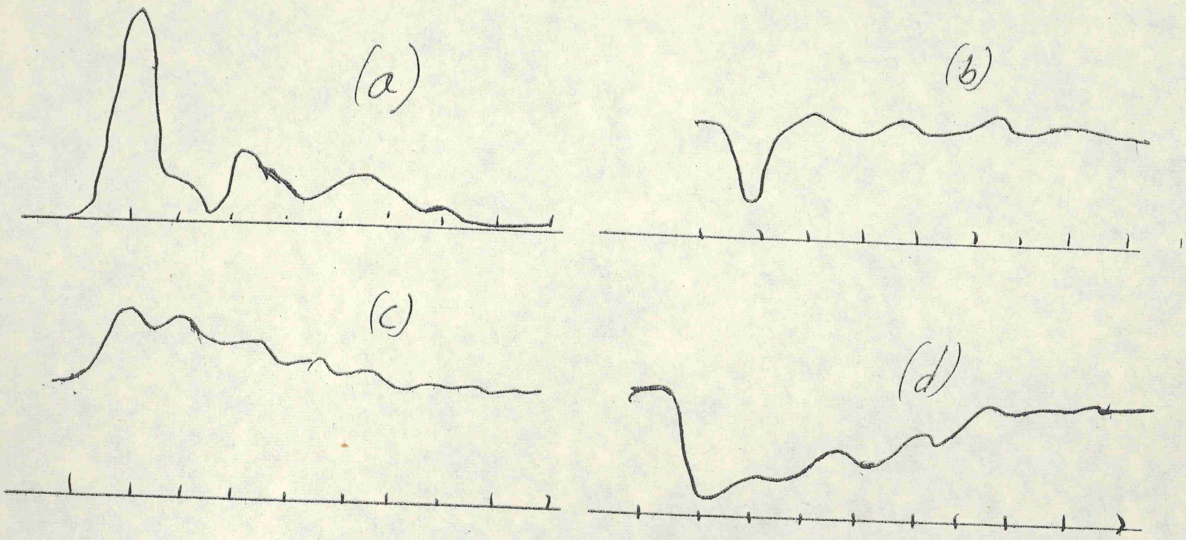

Fig. 9. Oscillograms for disturbance pulses generated by insulators. Suspension insulator CT 175:
a) R = 125 ohms, c) R = 600 ohms; Rigid insulator HT 30: b) R = 125 ohms, d) R = 600 ohms. (R = discharge resistor.) (Sweep: 50 ns/cm).

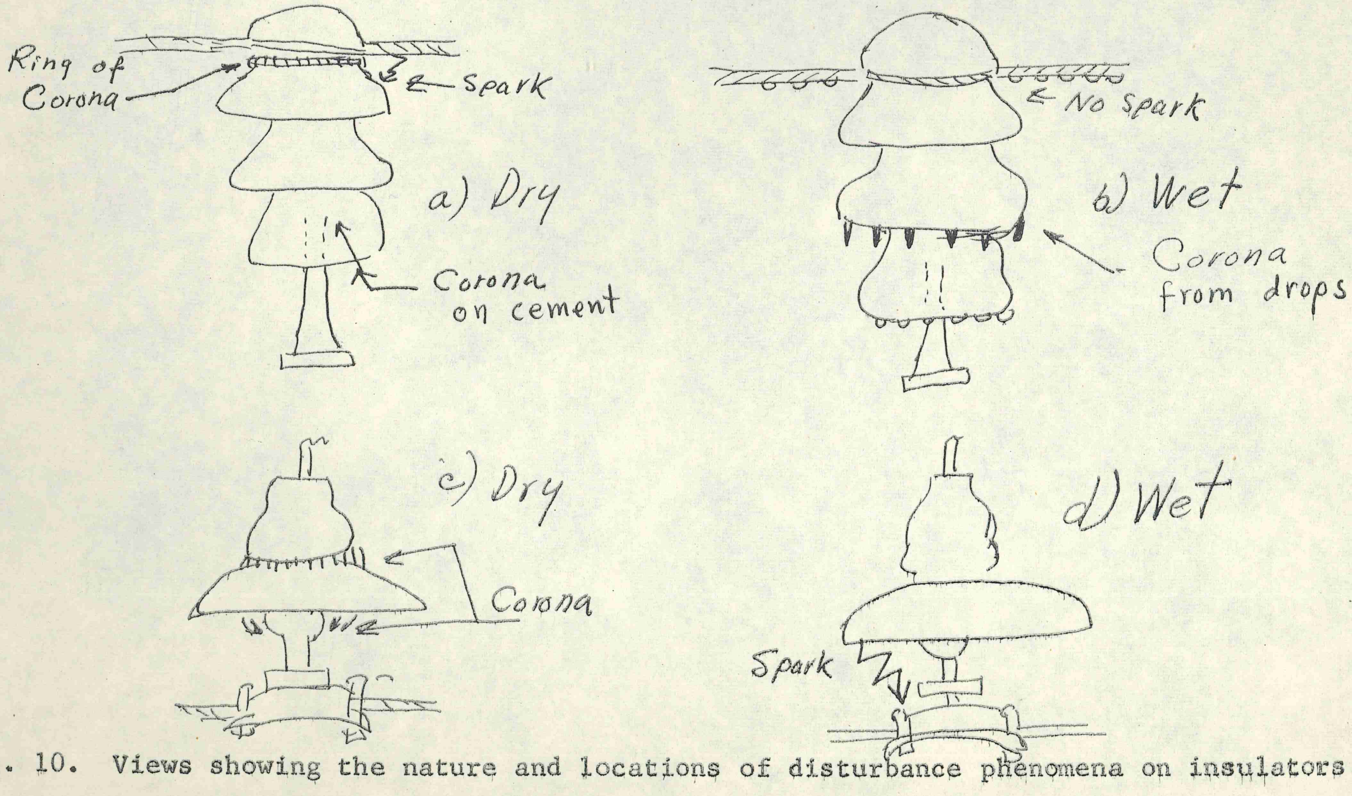
Ring of Corona
Spark
a) Dry
Corona on cement
No Spark
b) Wet
Corona from drops
c) Dry
Corona
d) Wet
Spark

Fig. 10. Views showing the nature and locations of disturbance phenomena on insulators.

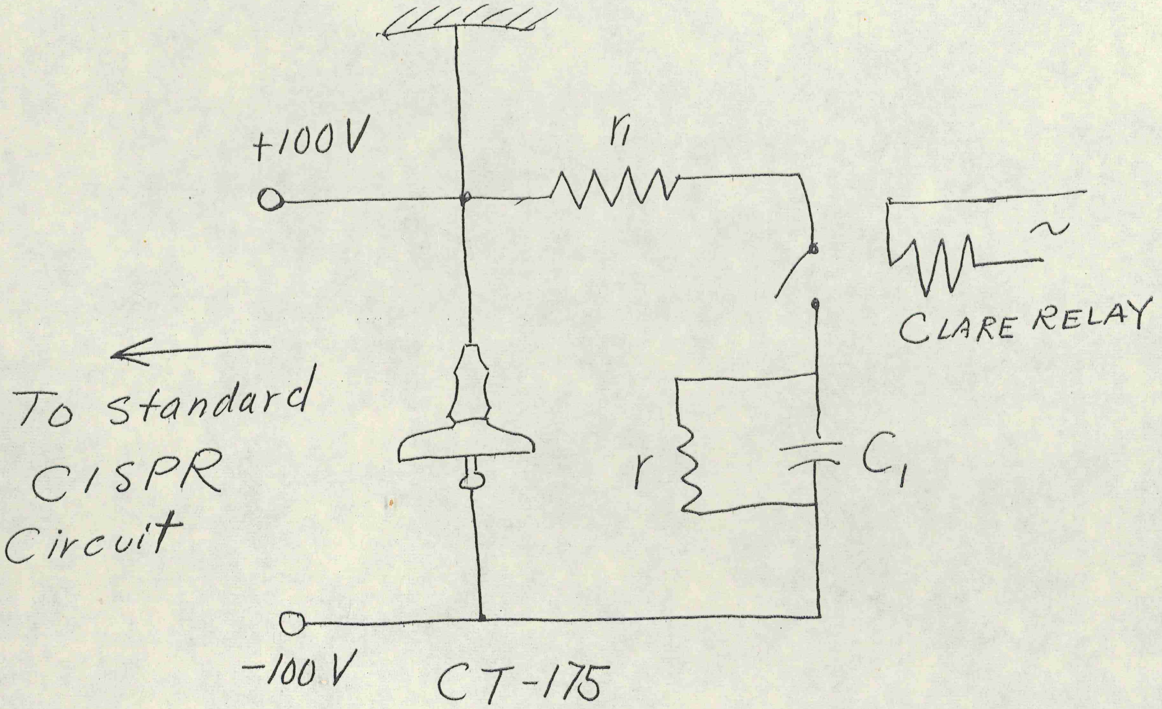
+100V
r_1
CLARE RELAY
To standard CISPR Circuit
r
C_1
-100V
CT-175

Fig. 11. Setup for the artificial production of disturbance pulses.

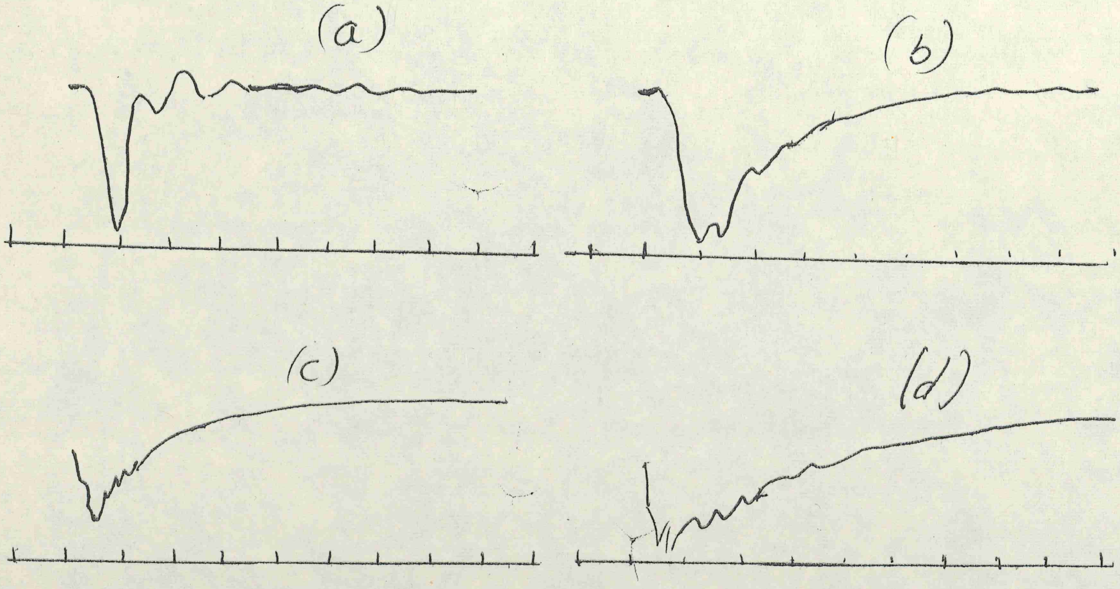

Fig. 12. Oscillograms of artificial disturbance pulses for comparison with natural pulses of figure 9. Suspension insulator CT 175: a) R = 210 ohms: Sweep 30 ns/cm; b) R = 600 ohms Sweep: 50 ns/cm; c) R = 2100 ohms: Sweep 200 ns/cm; d) R = 6000 ohms, Sweep: 200 ns/cm. (R = discharge resistor.)

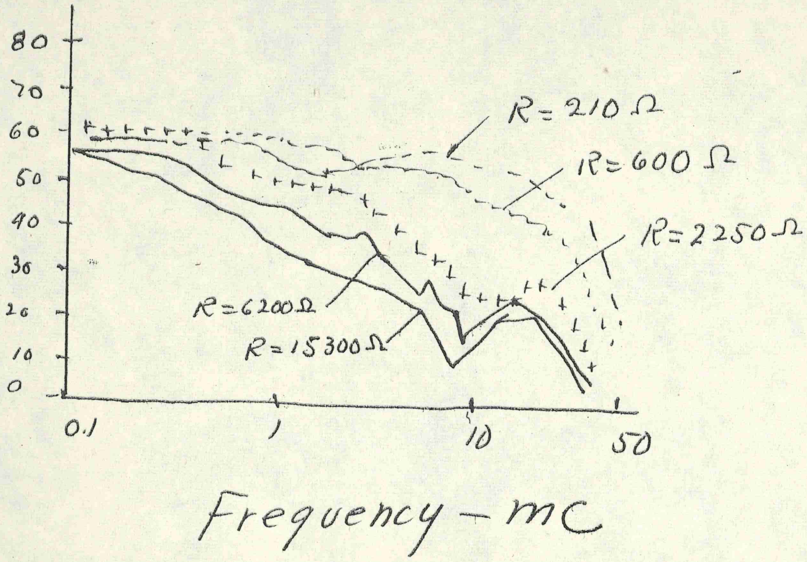

Fig. 13. Spectra of the current for various values of resistor R, generated by artificial pulses repeated at rate of 100 per second, applying to a CT 175 insulator.

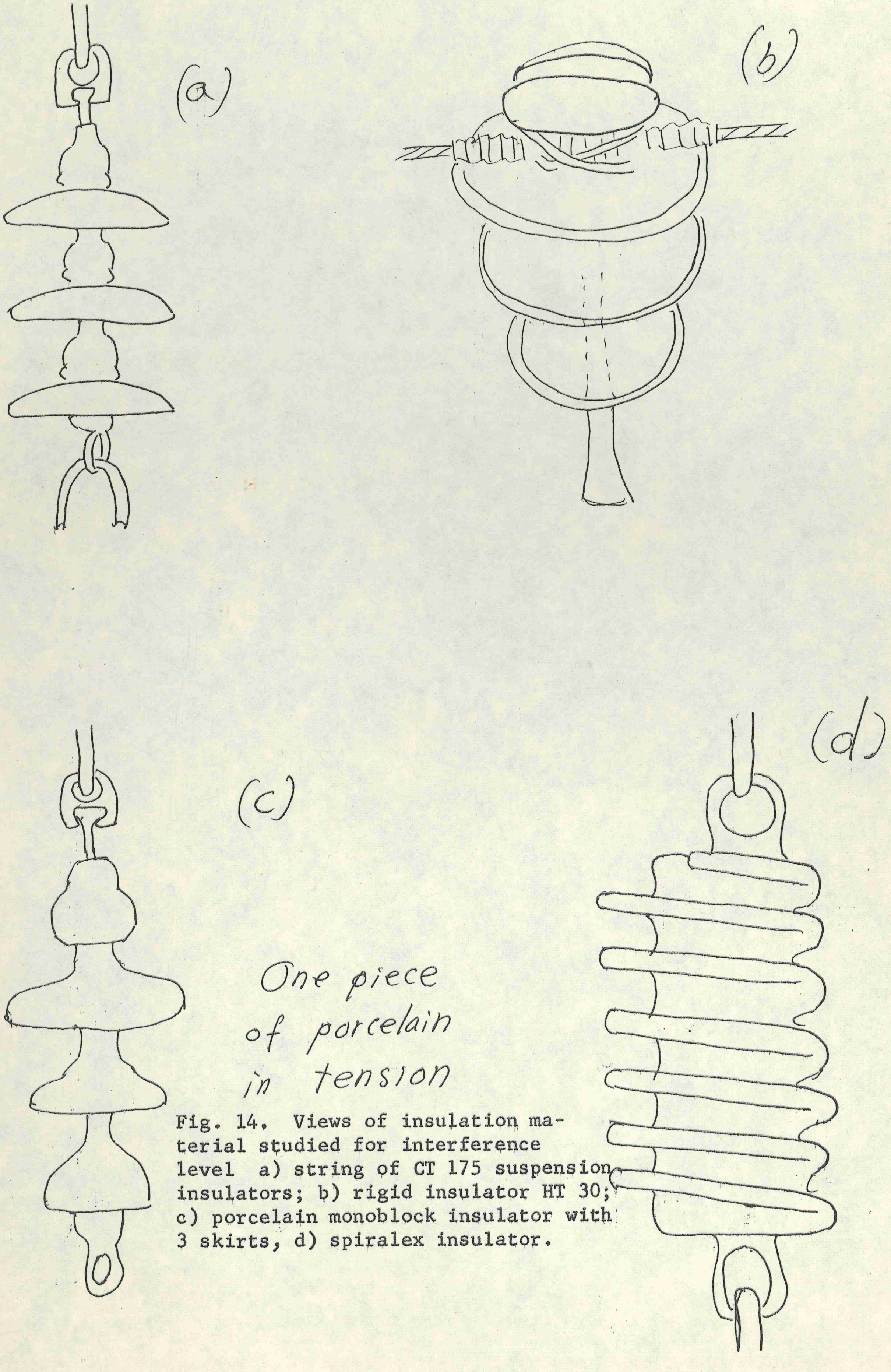

One piece
of porcelain
in tension

Fig. 14. Views of insulation material studied for interference level a) string of CT 175 suspension insulators; b) rigid insulator HT 30; c) porcelain monoblock insulator with 3 skirts, d) spiralex insulator.

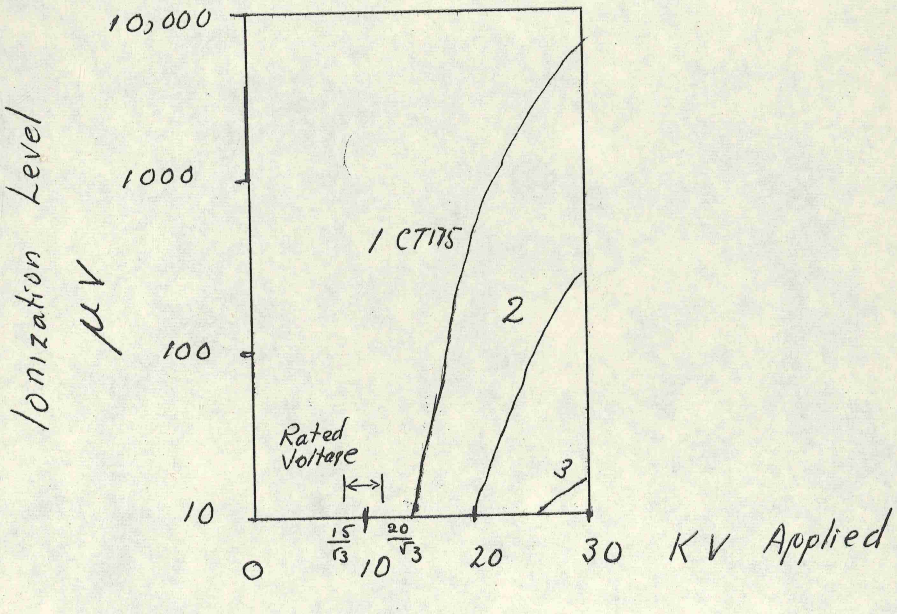

Fig. 15. Curves of disturbance level as a function of voltage for strings of 1, 2, or 3 CT 175 insulators.

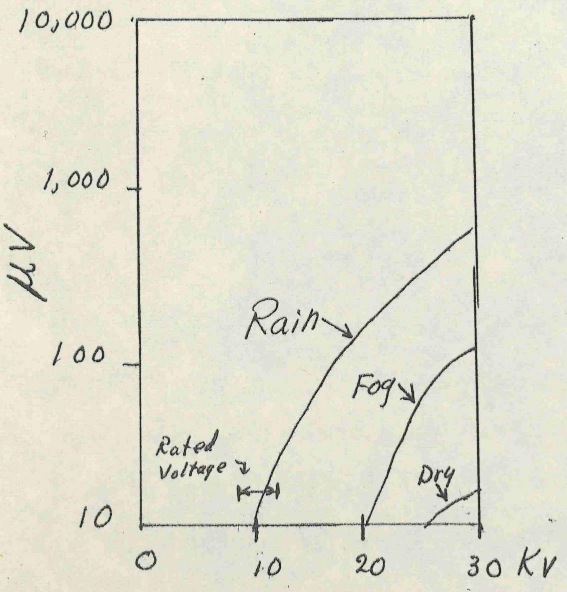

Fig. 16. Curves of disturbance level as a function of voltage for a string of 3 CT 175 insulators for different climactic conditions.

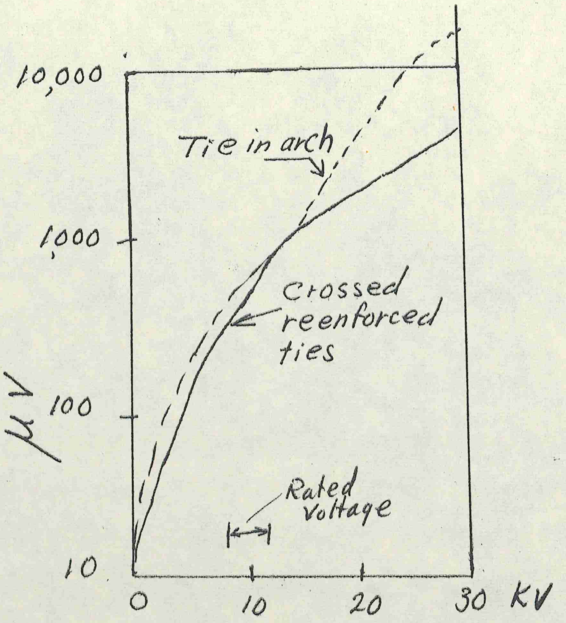

Fig. 18. Curves of the ionization level as a function of voltage, showing the influence of the method of tying on the disturbance level for HT 30 rigid insulators.

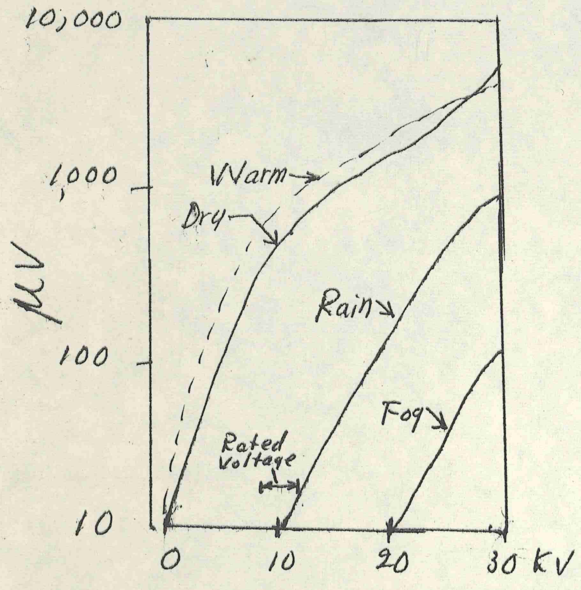

Fig. 17. Curves of disturbance level as a function of voltage for an HT 30 rigid insulator for different climactic conditions.

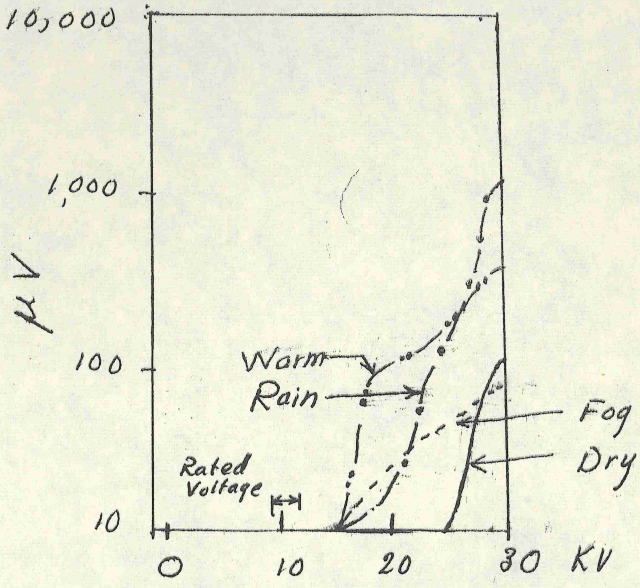

Fig. 19. Curves of the disturbance level as a function of voltage for an Isobloc insulator with 3 skirts for different climactic conditions.

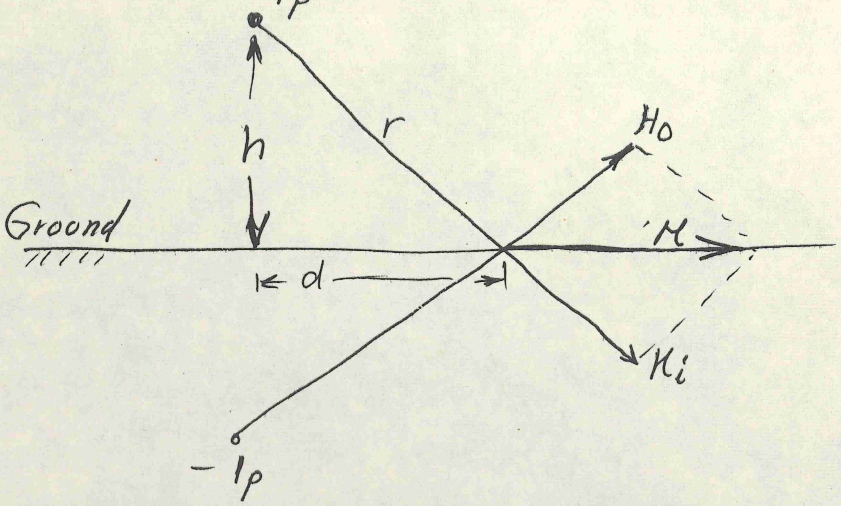

Fig. 20. Calculation of the homopolar disturbance field of a medium voltage line.

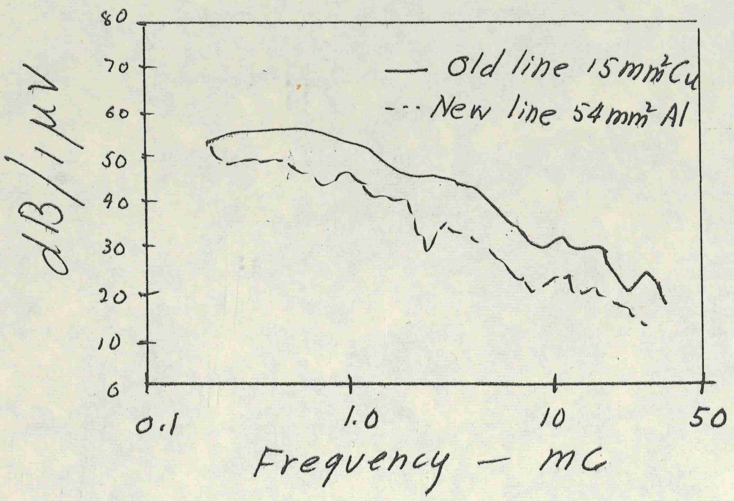

Fig. 21. Spectra of the magnetic component of the disturbance field taken beneath two lines with rigid insulators at 15 kv.

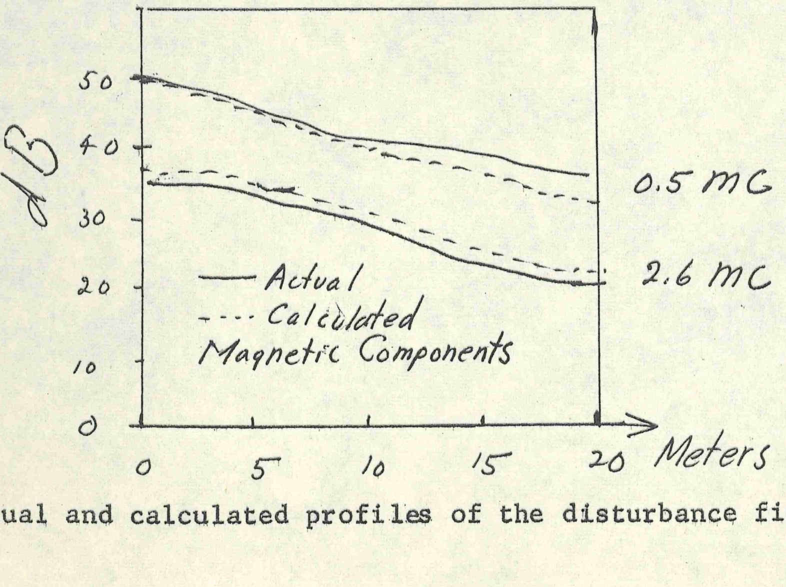

Fig. 22. Actual and calculated profiles of the disturbance field of a 15-kv line.

Research Laboratory
P. O. Box 1088
Schenectady, New York

Conférence Internationale des Grands Réseaux Électriques à Haute Tension
112, Boulevard Haussmann, Paris
Session 1964 — 1er-10 juin

411. — CORONA LOSS AND RADIO INTERFERENCE MEASUREMENTS AT HIGH VOLTAGE A.C. ON TEST LINES IN SWEDEN

by **N. KNUDSEN**,

Chalmers University of Technology
(Sweden)

SUMMARY

On a test plant erected by the Swedish State Power Board in connection with the Chalmers University of Technology in Gothenburg comprehensive corona tests have been carried out during the last years. Beside the general intention to broaden the theoretical and practical knowledge about the corona phenomenon there has been a special purpose namely to compare the behaviour of double and triple conductors of the types used in Sweden which contain cables witch a diameter of 3,2 cm and a spacing of 45 cm.

The results of the experiment indicate that by use of triple conductors instead of double conductors the yearly losses, apart from ice losses, are reduced from about 1,4 kW/km to about 0,4 kW/km and the radio interference level is reduced by about 8 dB in fair weather, and probably somewhat more in bad weather. Expressed in another way the triple conductor has given approximately the same losses and radio disturbances at 460 kV as the double conductor at 400 kV.

Variations between 40 and 95 % in the humidity in the air did not seem to affect the losses nameworthly but a slight decrease in radio interference with increasing humidity was observed. Bad weather has given increasing losses in the following order: fog, dry snow, rain, wet snow, hoar frost.

A method for calculating fair weather losses is proposed and future work is outlined.

REPORT

INTRODUCTION

The first 400 kV lines built in Sweden are equipped witch double conductors consisting of two 593 mm² A.C.S.R. cables at a distance of 45 cm. Before the choice of the conductor type, experiments regarding corona losses and radio interference had been carried out on a test line at the Institute of High-Tension Research of Uppsala [1]. Later on, when the lines had been in operation for some time, field tests were undertaken, the results of which were substantially in agreement with the experiments [2].

In 1956 it was decided through an agreement between the Swedish State Power Board and the Chalmers University of Technology that a new test plant should be built in connection with the high voltage laboratory belonging to the university in order to carry out further investigations and thereby broaden the theoretical and practical knowledge about the corona phenomenon [3]. One of the main reasons for this decision was that it was foreseen that in the future several 400 kV lines in this country should be equipped with conductors with three cables per phase and that it was of great importance to compare the behaviour of double and triple conductors with respect to corona.

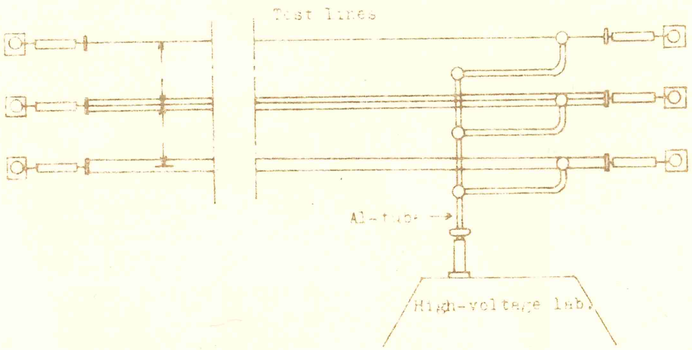

FIG. 1.—Test plant lay-out.

Even single conductors have been tested but mainly with regard to D.C. performance. These tests have been described elsewhere [4] and are not delt with in this paper.

TEST PLANT AND MEASURING EQUIPMENT

The original lay-out, which comprises the lines used for A.C. (and partly also for D.C.) tests is shown in *figure* 1 and a view of the plant in *figure* 2. The lines have a length of 300 m and a mean height above ground of 13 m. The double and triple conductor contain Curlew cables (593 mm², $r = 1{,}6$ cm) with a spacing of 45 cm, used in the 400 kV lines in this country.

The various lines can be connected to a bus formed by an aluminium tube of 12 cm diameter mounted at 10 m height on stack insulators. Ordinarily only one conductor is connected at a time, the other being free or earthed. For the connections between the bus and the lines and between the bus and the wall bushing leading into the high voltage laboratory flexible aluminium tubes are used. The system is fed from a high voltage single phase transformer rated 750 kV, 1 A.

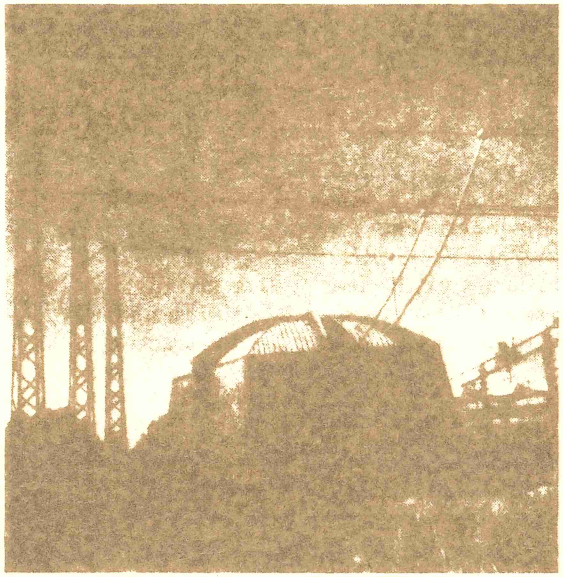

FIG. 2.—View of the test plant.

As may be seen, the whole outdoor equipment is of a rather simple construction and as a consequence the total cost has been relatively low. As a cause of the short line length the insulator and bus bar losses may at circumstances be relatively high and special precaution must be taken in order to eliminate them from the measuring results.

For measuring corona losses two different high-voltage bridges have been used. The one, which was first used, was of a special design constructed for the purpose (*fig.* 3). A part of the voltage drop caused by the load current in the resistor R is transferred to the low voltage branches through two equal pressure-gas capacitors rated 500 kV, 50 pF.

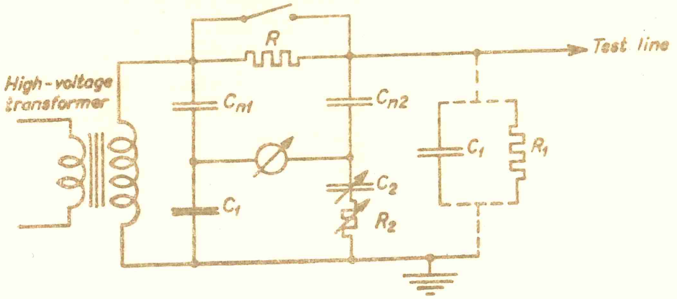

Fig. 3.—The first bridge used for corona loss measurements.

The total losses of the test system are divided into line losses and bus losses. By measuring total losses and bus losses in turn the line losses are calculated as the difference

$$P_{\text{line}} = P_{\text{total}} - P_{\text{bus}}.$$

At the same time as the total losses are measured the line insulator losses which should be subtracted from the line losses are obtained by means of the arrangement shown in *figure* 4. The last element in the insulator chain, i. e. the element connected to ground, is shunted by a resistor R_{is}, which forms a branch in the measuring bridge. If the voltage drop in this resistor caused by the capacitive current in the insulator is compensated, the remaining voltage drop caused by the active current can be measured. This gives the active current, which multiplied with the line voltage, gives the insulator loss.

In spite of the fact that the bridge shown in *figure* 3 is quite adequate, the whole procedure is rather complicated and time-consuming. This is a disadvantage especially in wet weather, when the losses are altering every minute. For this reason another bridge method has been tried which directly gives the line corona losses without correction (*fig.* 5).

This bridge is in principle an ordinary Schering-bridge and the only special feature is that instead of using the total return current through earth, which would not be correct owing to stray capacitances in the transformer, only a part of the return current picked up by an antenna is fed to the one low voltage branch. As antenne is used one of the free parallel test lines. This seems to justify the assumption that the antenna current is in phase with the sum of the capacitive current and the corona loss current flowing into the line. The loss factor measured by the bridge should then be equal to the loss factor of the conductor at test.

Because in this way the results obtained by use of the Schering-bridge are based upon a physical assumption, which may involve an approximation, is has been necessary to check the results against those obtained by the first bridge. For this purpose a series of fair-weather tests were undertaken. On each of 11 days

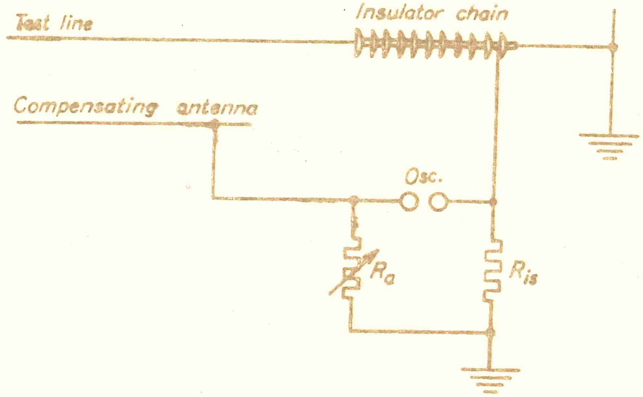

Fig. 4.—Arrangement for measuring of insulator losses.

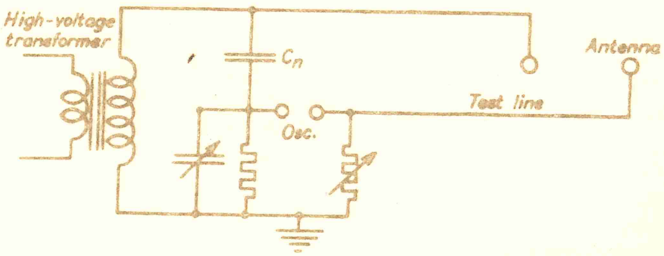

Fig. 5.—Schering-bridge for corona loss measurements.

the double conductor was tested at 300 kV by means of both bridges, the time interval between two comparative tests being at most a few hours. The result is given in *figure* 6.

If the two methods had given each day the same result—but of course somewhat different results from one day to the other—the eleven points in the figure would have been located on a straight line through origo with a slope of 45°. Instead the points are scattered around a line inclined 0,85 : 1 in relation to the abscissa. This means that the Schering-bridge has given in average 15 % lower values than the first bridge. The fact that the scattering in the direction of the mean line is greater than the scattering in the direction perpendicular to the line indicates that the variation is for the most part due to varying weather and test line conditions and only to a less degree due to inaccuracy in the setting of the bridge.

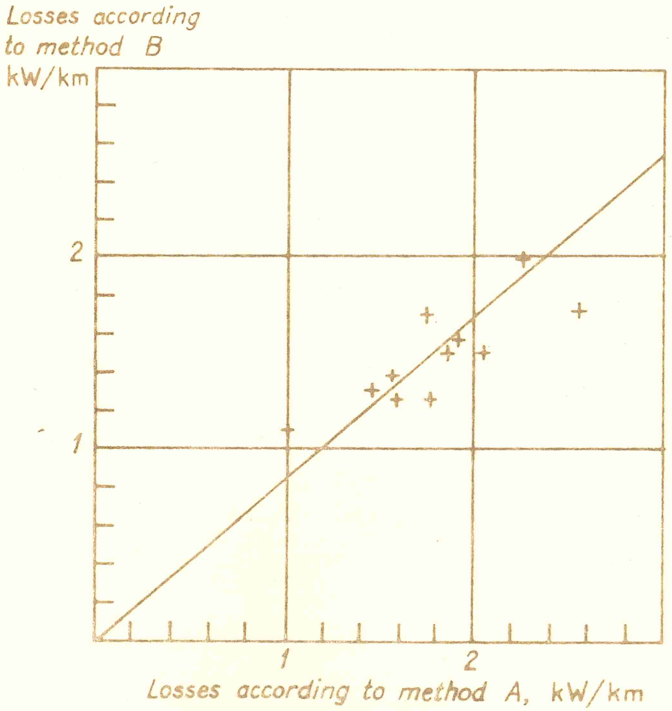

FIG. 6.—Comparison between results of corona loss measurements obtained by the two different methods. A. Method according to *figure* 3. B. Method according to *figure* 5.

The fact that the Schering-bridge here gives loss values which the variation in the coupling between the test line and the antenna seem to be somewhat too low, may partly be explained through in the middle of the span, where the losses are maximum on account of the lower height, the coupling is minimum. In this way at least 5 % of the 15 % deviation may be explained.

In judging the result shown in *figure* 6 it must be remembered that corona, such as it appears on high voltage lines, in practice is

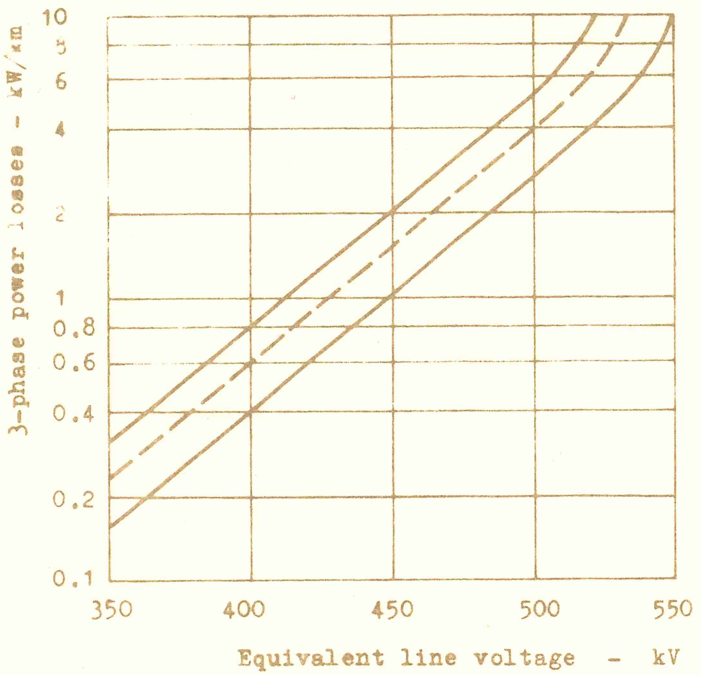

FIG. 7.—Boundary loss curves and mean loss curve from 15 voltage run tests in fair weather. Double conductor was used and temperature was between 6 °C and 26 °C. Tests carried out on various days from March 17, 1959 to July 8, 1959.

to a certain degree a statistical phenomenon. This is true as well with regard to the subcritical fair-weather corona as with regard to the more heavy corona caused by wet and icy conductors. Experience shows that fair-weather losses measured on a certain line may vary within a range of 1 : 2 or more. Further the relation between bad-weather and fair-weather losses of the same line and the same voltage may vary within a range of about

100 : 1 or in other words with 10 000 %. With these facts in mind the above result seems to be quite tolerable.

The measurements of radio interference have been made by means of a standard apparatus, the STMG 3800 constructed by Siemens which complies with the demands of C.I.S.P.R. The apparatus is placed under the midpoint of the conductor which is insulated with regard to high frequency voltages and currents from the bus by means of a choke coil. By this arrangement the variation of the noise with frequency shows a very pronounced but well defined pattern of peaks and valleys as a cause of the reflections of the waves at the line ends.

RESULTS OF LOSS MEASUREMENTS

Typical results from test series in fair weather and in rain are given in *figures* 7 to 10. In fair weather the voltage was varied in relatively small steps as it showed that the losses for each voltage level could be determined practically instantly and independent of the preceding voltage level. When the losses were plotted in a logaritmic scale as a function of voltage the curves from the various test series were nearly straight-lined apart from the region, where the critical voltage was approached (only in *fig.* 7).

The voltage values in these figures are not the actual test voltages but such equivalent line voltages, which on a Swedish 400 kV line of the normal flat configuration would give the same nominal voltage gradient on the cable surface. This means that

$$V_{\text{line}} = \sqrt{3}\, V_{\text{phase}}$$

and

$$V_{\text{phase}} \times c_{\text{phase}} = V_{\text{test}} \times c_{\text{test}} = E\,\frac{nr}{18}$$

where *c* denotes capacitance in μF/km, E voltage gradient in kV/cm, *n* number of cables in the conductor and *r* radius of the cable in cm.

For the double conductor we have

$$c_{\text{phase}} = 0{,}00115\ \mu\text{F/km},$$

and for the triple conductor

$$c_{\text{phase}} = 0{,}00129\ \mu\text{F/km}.$$

Corresponding to the normal line voltage 400 kV the voltage gradient is found to be

$$E = 15\ \text{kV/cm}$$

and

$$E = 11{,}2\ \text{kV/cm}$$

for the double and the triple conductor respectively, which values may be used, when comparing the results related here with results from other tests.

The following comments could be applied to *figures* 7 and 8.

1. The maximum deviation from the mean line is of order ± 30 %. About half of this seems to be due to variations in the air density, which was made evident by shifting the voltage scale in relation to this quantity.

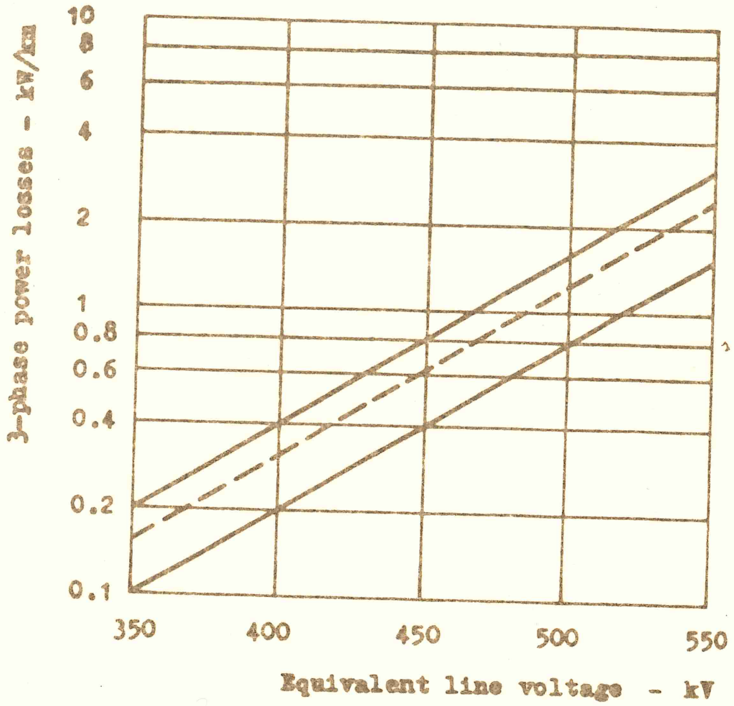

FIG. 8.—Boundary loss curves and mean loss curve from 15 voltage run tests in fair weather. Triple conductor was used and temperature was between 6 °C and 26 °C.

2. Well below the critical voltage the power losses are doubled when the voltage is increased by 40 kV in the case of the double conductor and by 50 kV in the case of the triple conductor. Expressed in a more general way this means that the losses are doubled when the voltage is increased by 10 % of that line voltage which

correspond to a nominal field gradient of 15 kV/cm. This rule may perhaps be used for precalculation of corona losses in fair weather as will be shown in the following.

3. The loss per cable in the triple conductor equals the loss per cable in the double conductor at a 20 % higher voltage on the triple conductor. That a still better result is not obtained by use of triple conductor shows that the loss per cable is not only defined by the voltage gradient but also to a certain extent by the voltage itself. It may also be that there are other explanations, for instance that the triple conductor as a cause of the low gradient was less "trained" than the double conductor.

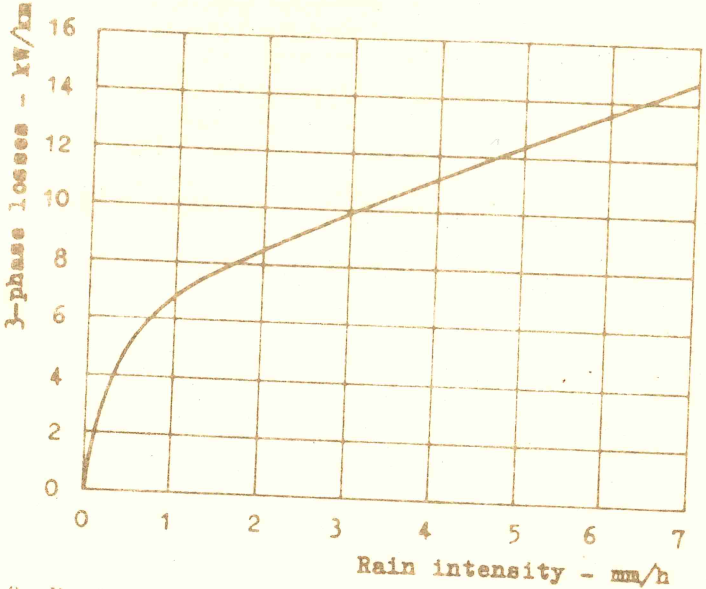

Fig. 9.—Result of rain test with double conductor exposed to a voltage corresponding to 400 kV.

4. The relative humidity did not seem to have any influence at all on the losses. This was made evident by means of a special test series including 20 tests on various days with the relative humidity varying between 40 % and 95 %.

Regarding the result of the measurements in rain the following may be said.

The typical saturation knee in the curve in *figure* 9 and in the two upper curves in *figure* 10 is probably due to space charges. This phenomenon is not observed in the lower curve in *figure* 10, which relates to 400 kV on a line with triple conductors. The explanation may perhaps be that in this case because of the low voltage gradient heavy discharges only occur on water drops, when they strike on or leave the conductor and not on hanging drops. The improvement by use of a triple conductor instead of a double conductor is here very remarkable.

Among other results of bad weather conditions it may be mentioned that fog and dry snow gave rise to losses about three times as great as in fair weather and that wet snow and hoar frost gave very heavy losses of about 40 to 60 kW/km at normal voltage on the double conductor.

CALCULATION OF ALL-WEATHER LOSSES

The yearly corona losses on a line can be estimated with more or less accuracy. The most simple way is to apply an empirical factor to the fair weather losses. However, this figure will depend not only on the climatic conditions but also on the line data,

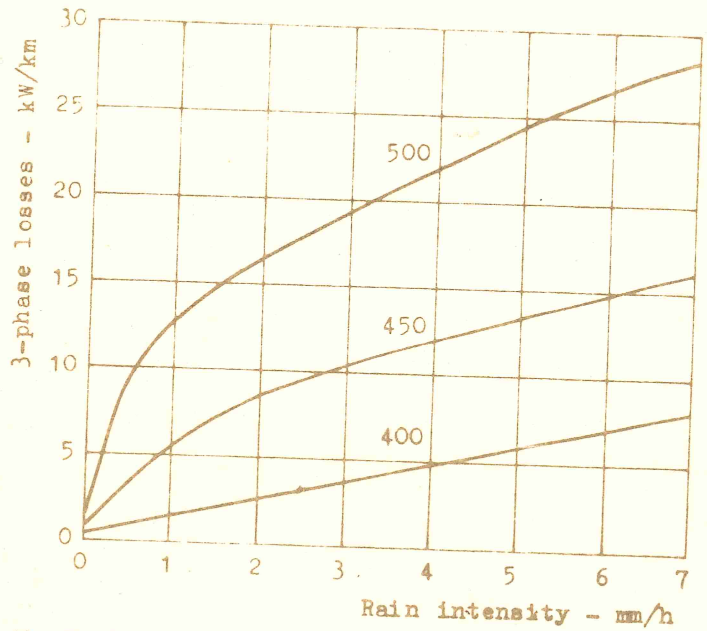

Fig. 10.—Results of rain tests with triple conductor at three voltage levels corresponding to 400, 450 and 500 kV line voltage.

which may be seen from [5], where values between 1,66 and 5 are found. Even higher and lower values are found in the literature.

A generally used method is to calculate the mean loss during a year by means of an expression of the following kind

$$P_{\text{mean}} = t_1 P_{\text{fair}} + t_2 P_{\text{fog}} + t_3 P_{\text{rain}} + t_4 P_{\text{snow}} + t_5 P_{\text{ice}}$$

where t_1, t_2, etc., denote the relative durations of the various weather types.

Amongst the above terms the last one is probably the one, which is determined with the least accuracy. With regard to the lines in the northern parts of Sweden this may introduce a special uncertainty in the calculation.

For the southern parts of Sweden the term can probably be neglected.

As dry snow gives lower losses and wet snow higher losses than rain, it seems reasonable to put

$$P_{\text{snow}} = P_{\text{rain}}$$

and add t_4 to t_3.

Let us—mainly as an example—assume that we for the climate in the middle and southern parts of this country can calculate with

$$\begin{aligned} t_1 &= 0{,}80 \\ t_2 &= 0{,}05 \\ t_3 + t_4 &= 0{,}15 \\ t_5 &= 0. \end{aligned}$$

The number of rain and snow hours per year should be about 1 300. The yearly precipitation is of order 600-700 mm in mean. Accordingly the mean rate of rainfall (snowfall) is about 0,5 mm/h. If we now assume that the corresponding loss figures taken from *figures* 9 and 10 can be regarded as representative, which is most sure in the case of the triple conductor because the 400 kV curve in *figure* 10 is practically straight-line shaped we find

$P_{\text{rain}} = 5{,}2$ for the double conductor,
$P_{\text{rain}} = 0{,}9$ for the triple conductor.

Now there only remains to fix the fog losses. Let us assume that they are three times as great as the fair weather losses. We then have for the double conductor

$$P_{\text{mean}} = 0{,}80 \times 0{,}6 + 0{,}05 \times 1{,}8 + 0{,}15 \times 5{,}2 = 1{,}35 \text{ kW/km}$$

and for the triple conductor

$$P_{\text{mean}} = 0{,}80 \times 0{,}3 + 0{,}05 \times 0{,}9 + 0{,}15 \times 0{,}9 = 0{,}42.$$

The relation between mean losses and fair weather losses should then be

$P_{\text{mean}}/P_{\text{fair}} = 2{,}3$ for the double conductor,
$P_{\text{mean}}/P_{\text{fair}} = 1{,}4$ for the triple conductor.

The gain in form of reduced losses by use of triple conductors instead of double conductors is mainly obtained during bad weather conditions. While the losses in fair weather are reduced in proportion 2 to 1 they are at light rain reduced in proportion 6 to 1.

RADIO INTERFERENCE MEASUREMENTS

In order to obtain a well defined frequency spectrum the field intensity meter was placed directly beneath the middle point of the test line, which was shielded from the bus bar by an inductive coil. By measuring over a wide frequency range curves like the one shown in *figure* 11 could be drawn, which curves were essentially of the same shape for various tests. With the well-known

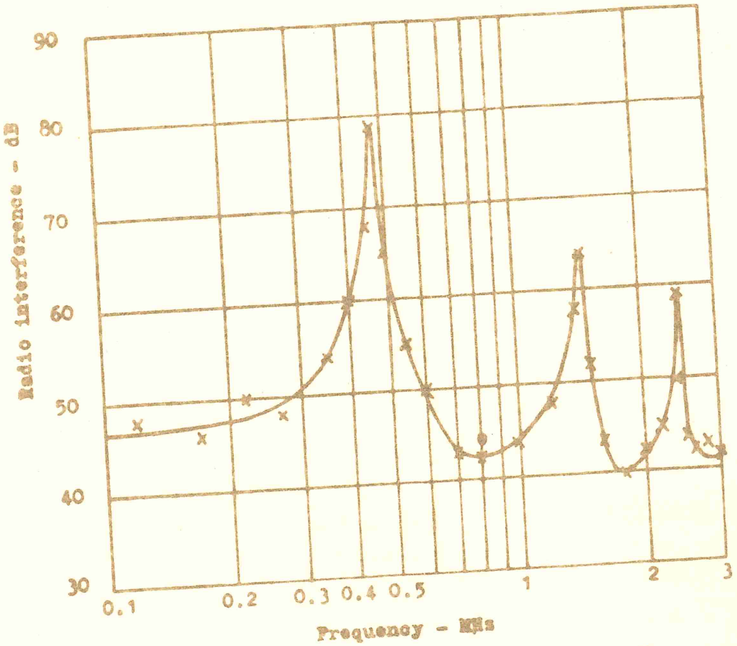

FIG. 11.—Typical frequency spectrum of 300 m test line.

fact in mind that the interference from an infinite line can be represented by a mean curve it was later on possible to restrict the measurements to one or a few frequencies and apply the appropriate corrections taken from representative wide range tests.

Typical results from measurements in fair weather are shown in *figure* 12. Each point in the figure is the mean value from 24 different tests on various days. The 24 individual values were originally plotted against the relative humidity, whereby it was found that although the scattering was rather great there was a clear tendency, that the interference level decreased with increasing humidity. Thus when the humidity varied within the range 45-95 % the disturbance level decreased about 2 or 3 dB.

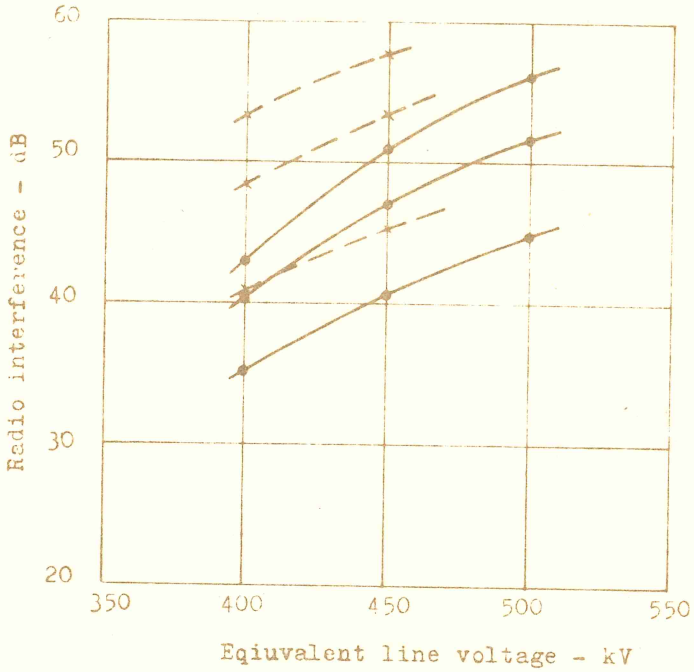

FIG. 12.—The three dotted curves give in downward direction the radio interference level for the double conductor at 0,2, 1 and 3 MHz. The full curves give correspondingly the losses of the triple conductor.

It may be noted that the greatest improvement by use of triple conductor instead of double conductor occur at the lower frequency 0,2 MHz at 400 kV and is about 10 dB. At 3 MHz the improvement is 6 dB. The triple conductor shows the same level at 460 kV as the double conductor at 400 kV.

Only a few measurements in rain have hitherto been made. They have indicated an increase in noise level about 5 to 10 dB. The increase is higher for the double conductor than for the triple conductor.

DISCUSSION OF FAIR WEATHER LOSSES. FUTURE WORK

It is often thought that the fair-weater corona is a phenomenon of a pronounced random nature being caused by irregularities along the conductor surface. Whatever this is true or not it may be said, that our general impression from numerous loss measurement during more years is that the constancy and reproductivity of the fair weather losses has not been bad. Moreover, the shape and the slope of the curves shown in *figure* 1 and 2 is in good agreement with the mean curve from a great number of investigations carried out in seven countries [6].

A special study [7] has shown that a precalculation of fair-weather losses may be carried out as follows:

1. Estimate the corona losses at normal air density and at the nominal surface gradient 15 kV/cm by means of the rule

$$P_{15} = n^2 r^2 P_{15u}$$

where P_{15u} is the value of P_{15} for unit values of n and r i. e. for a single conductor with a radius of 1 cm. According to tests in various parts of Sweden P_{15u} is of order 0,06 kW/km or perhaps about 0,08 if corrections are made with regard to air density. According to the above mentioned tests in other countries it is of order 0,12 kW/km. Select one of these values or an intermediate value. If reliable tests have been carried out under conditions which are somewhat similar to the actual case select a value, which used in the following calculations gives a result in accordance with such tests.

2. Calculate by means of the expression

$$V = \sqrt{3}\, E \frac{nr}{18c}.$$

where c is the line capacitance in μF/km either the voltage V_{15} which corresponds to the nominal surface gradient 15 kV/cm or the gradient E which corresponds to the actual voltage V and thereafter the radio

$$v = \frac{V}{V_{15}} = \frac{E}{15}.$$

3. Calculate the line losses at normal air density by means of the formula

$$P = P_{15} 2^{10 \cdot v - 1}.$$

This may be carried out arithmetically or graphically. In the latter case one may take advantage of the following approximation

$$\log 2 = 0{,}3010 \simeq 0{,}3$$

which implies that at E = 20 and correspondingly

$$v = \frac{20}{15} = \frac{4}{3}$$

we have

$$\frac{P_{20}}{P_{15}} = 2^{\frac{10}{3}} \simeq 10$$

Using the voltage gradient for the abscissa a logarithmic graph is very simple and easily made as shown in *figure* 13.

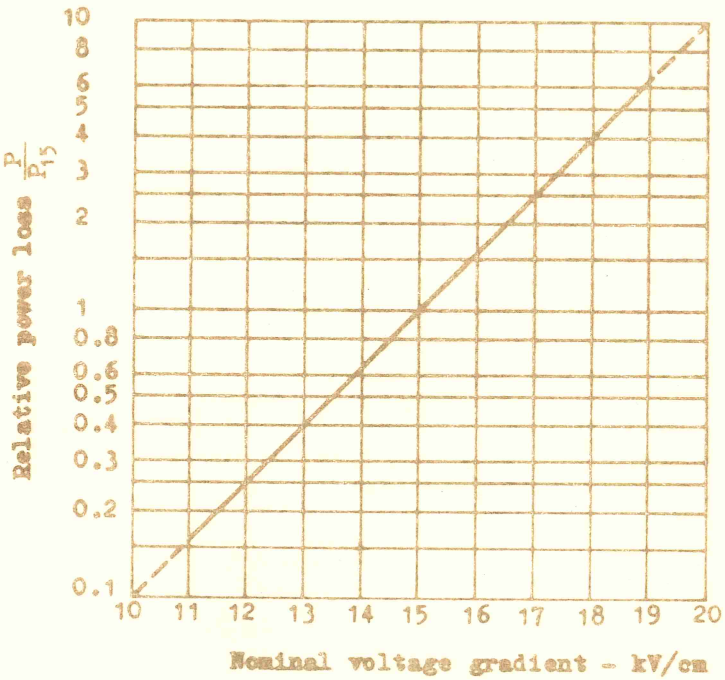

FIG. 13.—The relative power loss P/P_{15} as a function of the nominal voltage gradient. Note that the linear (or in fact exponential) relationship is considered to be most close within the range 11-19 kV/cm.

4. If a correction for air density is needed the relative air density δ should in a first approximation enter in the above expression for P in the following way

$$P = P_{15} 2^{10 \left(\frac{v}{\delta} - 1\right)}$$

which implies a scale shift in voltage. If δ is increased from 1 to 1,01 i. e. with 1 %, the result will be a decrease of P with 7 %.

With regard to future work it may be mentioned that during August 1963 three new conductors have been installed. It is the intention to study in first hand:

1. Influence of drawing and ageing of cables.
2. Reproductivity of fair weather losses and radio interference.
3. Influence of bad weather in order to get more information about losses as well as radio interference.
4. Behaviour of single and double conductors at D.C. voltage.

REFERENCES.

[1] HENNING B., SKAGERLIND S., Measurements of Corona Losses and Radio Disturbances. C.I.G.R.E., Report 412, 1948, Appendix A.

[2] HOLMGREN B., GROOP S., Corona Losses, Radio and Telephone Interference. Chapter 6 in the book "The Swedish 380 kV System".

[3] KNUDSEN N., TEDESTAL G., Corona Test Equipment at Chalmers University of Technology. *Elteknik,* vol. 5, No. 5, 1962.

[4] WITT H., Insulation Levels and Corona Phenomena on H.V.D.C. Transmission Lines. Dissertation. Gothenburg 1961.

[5] BARTENSTEIN R., LESCH G., Measurements of Corona Losses and Interference Levels at the 400 kV Research Station in Mannheim-Rheinau (Germany) with Special Reference to Bundle Conductors. C.I.G.R.E., Report 402, 1956.

[6] BURGSDORF V.V., EGODORA L.V., EMELJANOV N.P., TIHODEEV N.N., Corona Investigations on Extra-High-Voltage Overhead Lines. C.I.G.R.E., Report 413, 1960.

[7] KNUDSEN N., Corona Power Losses on Bundle Conductors, *Elteknik,* vol. 6, No. 4, 1963.

Extrait de la *Conférence Internationale des Grands Réseaux Electriques.* Session 1964.

CHAIX-PARIS - ST-OUEN. — 2104-9-63. — Imprimé en France.

March 10, 1964

To Chairman and Members
of R. N. Sub-Committee:

Enclosed is a revised version of our working group report finally reviewed by the group listed below at the Winter Meeting in New York.

If you have any further comments, please send them to Mr. Rorder directly with a copy to me. Thank you.

RECEIVED
MAR 17 1964
ENG. DEPT.

Very truly yours,

T. W. Liao

T. W. Liao, Chairman
Working Group No. 4
"Line & Station Components"

F. Reed Dallye
Aluminum Company of America
536 Alcoa Bldg.
Pittsburg 19, Pennsylvania

F. A. Denbrock
Commonwealth Associates
209 E. Washington Avenue
Jackson, Michigan

C. D. Fiero
Mechanical Engineer
Lapp Insulator Company
LeRoy, New York

O. Nigol (J. R. Leslie)
Research Division
Hydro-Electro Power
Commission of Ontario
620 University Avenue
Toronto 2, Ontario, Canada

T. W. Liao (Chairman)
Engineering Research
General Electric Company
6901 Elmwood Avenue
Philadelphia 42, Pennsylvania
SA.4-1500, Ext. 8221

C. J. Miller
Research Engineer
Ohio Brass Company
Barberton, Ohio

H. H. Newell
Worcester Polytechnic Institute
Worcester,
Massachusetts

P. D. Tuttle
Aluminum Company of America
Massena,
New York

F. W. Warburton
New England Power Service Company
939 Southbridge Street
Worcester 10, Massachusetts

SECTION ON "LINE AND STATION COMPONENTS"

FOR

RADIO NOISE SUBCOMMITTEE REPORT

CONTENTS

1. GENERAL DISCUSSION
2. RIV VERSUS RI
3. PROPOSED RIV LIMITS
4. CONDUCTOR ACCESSORIES AND LINE HARDWARE
5. FLOATING GAPS AND UHF NOISE
6. MYSTICS OF TRANSMISSION LINE NOISE
7. BIBLIOGRAPH
8. FIGURES 1 AND 2
9. MEMBERSHIP OF WORKING GROUP ON "LINE AND STATION COMPONENTS"

1. GENERAL DISCUSSION

In addition to the radio noise from the line conductors, there are other components in the power transmission system that also produce radio noise under normal operating conditions. Such components as insulators,conductor accessories, lightning arresters,switchgear and transformers, etc., are referred to herein as line and station components. The radio noise generated from these components may be different from the conductor noise, both in noise level and in frequency band.

For instance, insulators and accessories of EHV lines are placed at intervals several hundred feet apart and their noise generation is, therefore, scattered as contrasted to the numerous corona sources that might occur along the surface of the conductors. Consequently, the contribution of the former is expected to be smaller, unless the conductor noise is kept unusually low by a special design, such as over-sized conductors. This condition is often true for lower voltage lines, especially of 69 KV and below. When sparking is found in insulators or from hardware, much higher frequency components than the conductor noise will be expected.

Station components are all located within a station, which may be many miles from another station. Therefore, the centers of their noise generation are scattered at even greater distances. Furthermore, since the noise generation is localized in individual stations, their effect on the RI level at a distance from the station will be smaller, because the noise attenuates along the line. In addition, the station components, in general, have high capacitance to ground which offer low impedance to radio frequency noise. Therefore, it is even conceivable that when a low noise component is put in a station, it could lower the over-all noise level of the station, because the noise reduction due to its low impedance may be greater than the noise contributed by the component.

Where several lines are terminated at a sub-station, radio noise from one line may be coupled to another line by induction or through power transformers. Experiences show that the inductive coupling between adjacent lines may be considerable. Special considerations must be given to the case when one of them is a low voltage line, which may carry the noise to residential area. Radio noise voltages that are transmitted from one side of a sub-station to the other side through transformers and other station equipment are found to be relatively small because of the low impedance of the sub-station, particularly for large sub-stations.

2. RI VERSUS RIV

The nominal radio influence (RI) level of a transmission line is determined in fair weather with a radio noise meter having a vertical antenna at some designated distance laterally from the outer line conductor. It is expressed in terms of microvolt per meter. For instance, the RI level of a 230 kv line might be 50 μv/m (Using a quasi-peak meter with 6 KC bandwidth at 1 Mc) at 100 feet from the line. On the other band, the radio influence voltage (RIV) of an insulator string or a station equipment is to be measured according to a standard NEMA-107 method(1), in which the meter is coupled capacitatively to the apparatus under test and is expressed in terms of microvolts. For instance, the RIV of a 230 KV disconnect switch might be 1000 to 2000 µv.

In the NEMA circuit the noise is measured at 1 Mc conductively with a noise meter with little, or no, attenuation between the equipment and the meter. But when the component is placed on a transmission line, its noise propagates along the line, producing electromagnetic waves around the line conductors. If a radio noise meter is placed in the vicinity of the line, a voltage will be induced at its antenna. The magnitude of the induced voltage is inversely proportional to approximately the square of the distances between the meter and the line up to $1/2\ \pi f$, where f is the tuned frequency of the meter. Thus, if a noisy component is far away from the location of the meter, the noise suffers two types of attenuation; first, it attenuates longitudinally along the line and, then, laterally from the line to the meter. Both types of attenuation have been determined analytically(2) and experimentally(3).

The rate of noise attenuation differs for different line configurations, The longitudinal attenuation of the principle mode of propagation is as much as 6 db per mile and laterally an RIV to RI ratio(4) is between 200 to 300 at 100 feet from the line. Thus, if a noisy insulator string having a RIV of 2000µv is located over a mile from the meter which is placed 100 ft. laterally from the transmission line, then the meter would register less than (2000/2 x 200) or 5 µv/m, as illustrated by the top sketch of Figure 1. However, if the same insulator string is placed in a station with the same distance from the meter, the meter would read even less than 0.5 µv/m, as illustrated by the bottom sketch of Figure 1. The reason lies in the fact that a radio noise source produces a given noise current independent of the impedance of the circuit in which it is measured. Since the impedance of a station is, in general, less than a tenth of the NEMA-107 circuit, the same insulator string would produce less than 200 µv in the station.

It is recognized that a complete description of the RI versus RIV problem would entail the use of a model three-phase system. Not only does radio noise propagate by means of a line-to-ground component (as described above), but also by line-to-line modes without any current flowing through ground. Because of that, the line-to-line model attenuation rates are significantly lower than the line-to-ground rate, and thus the effects of the line-to-line modes are more pronounced as the distance becomes farther away from the source. At present, work on a complete model analysis for the "discrete source" situation (as described above) is in progress.* In general, one might expect that the noise level at 100 ft. from a three-phase line may be twice of the single phase case described above, although the estimate is very rough and is depending on many factors of the line in question.

* Mr. LaForest plans to submit an IEEE paper on this subject. If he has a Paper No. before submission of our paper, a reference may be made of his paper.

3. PROPOSED RIV LIMITS

The NEMA-107 method of measuring radio noise voltages was documented in 1940. However, the measuring techniques and instruments have improved over the years. Consequently, a revision of the existing NEMA-107 Method and the new ASA Specification C63.2 for Radio Noise and Field Strength Meters are being discussed and will be officially issued soon.* However, the RIV limits for the line and station components of the various voltage classes have not been seriously reviewed and no proposals of such limits for the EHV components have been suggested.

It is the opinion of the working group (see membership list) that the existing NEMA RIV Limits are conservative and that the limits for EHV station equipments may be raised proportionally according to the system voltages because of the fact that the distances between substations are farther apart.

Another reason which is not so obvious, is that station equipment of EHV classes are in general larger in physical dimensions and consequently have higher capacitances to ground. As mentioned previously, higher capacitance of the station equipment means lower impedance for the substation, resulting in an overall lower RI level for the transmission system. However, considerations should be given to suppressing station equipment RIV that can be cheaply achieved, because conductor noise may be suppressed in the future to a point that station noise becomes dominant.

---

* See Attachment No 1

A proposed RIV Limits ** for insulators and hardware assemblies of the various voltage classes at a test voltage 110% of nominal line-to-ground voltage is shown in Figure 2. If the insulators are used in a station, the limits can be raised perhaps by a factor of several because of the low station impedance effect mentioned previously.

The RIV limit of other station equipment can also be raised above that shown in Figure 1 by a similar factor. In fact, the RIV values for some station equipments are kept low, not because of their radio influence but, because of the fact that high RIV often indicates internal corona which may lead to ultimate failure of the equipment. For instance, the RIV value of a power transformer is much lower than its NEMA RIV Limit when it is free of internal corona. On the other hand, RIV values of other types of station equipments, such as disconnect switches, are entirely due to external corona which does not affect the quality of the equipment. Extremely low RIV limit on such type of components would increase the cost of the equipments without upgrading their performance. Therefore, it is important that the NAME RIV Limits should be reviewed so that the cost and performance of the EHV equipments may be kept in balance.

** See Attachment No. 2

4. CONDUCTOR ACCESSORIES AND LINE HARDWARE

Along with insulators and insulator strings, the conductor accessories (such as joints, deadends, dampers, armor rods, spacers) and line hardware (such as suspension clamps, grading rings, yoke plates) are considered as possible radio noise sources on a transmission line. However, unlike the situation with insulators, there have been no existing or proposed RIV limits for the various voltage classes of conductor accessories and line hardware. Reliance has been placed on the manufacturers of these items to provide designs that give satisfactory corona and RIV performance on the lines to which they are applied. The criterion of "no visible corona" from accessories and hardware at the voltage at which the conductor itself develops corona has been adopted by many as satisfactory because when there is no visible corona there is no RIV and because there are no hidden regions where corona could not be seen, as there are in the case of insulators. The standard NEMA RIV circuit is used to read RIV over a voltage range from well below working voltage to such values that corona does occur and thw RIV meter indications provide a sure check on the presence of any corona that might escape visible notice. As with RIV limits, there are no standard test conditions and procedures for use in "visible corona" testing of accessories and hardware although the factors influencing the test results are, in general, well recognized and the results themselves have been satisfactory as evidenced by lines in service.

One factor is the surface voltage gradient. In the controlled but more confined environment of the indoor laboratory, this gradient is higher than it is for the same voltage on the operating line. The gradients of the conductor on the line and in the laboratory may be calculated and test voltages chosen to develop the same gradient as the working value. Or the gradient may be measured by means of simple devices to be the same in both instances. Again, because it is necessary to use the appropriate conductor as a part of the set-up when some accessories (eg. joints) are to be tested, it is convenient to use the conductor as a reference for all accessories and hardware associated with it. In effect, the conductor becomes a gradient reference that automatically corrects for the differences in configuration between the line and the laboratory. In brief, the corona voltage under working conditions and the corona voltage under test conditions indicate the same surface gradient.

Surface condition is another factor sometimes taken into account. Conductor, accessories and hardware are subject to weathering and contamination in service. Weathering refers to that hard, close-grained, adherent coating that develops on energized parts and which cannot be wiped or washed off. It cannot be simulated with confidence but invariably improves the RI performance of a working line. Contamination refers to temporary deposits of dust, pollen, insect parts, and other air-borne particles that are not fused into becoming part of the weathered coating but which can be wiped off or washed off. Such contamination is adverse in the production of RI but varies so widely in type, amount, and influence, a simulation of the condition is difficult to agree upon. Therefore, the standard to be used as the reference for test is logically clean, new conductor.

In summary then, a suitable and adequate criterion for judging the RI characteristics of conductor accessories and line hardware may be expressed thus:

> "Conductor accessories and line hardware shall be tested while fitted to the conductor with which they are to be used. The test items and conductor shall be in the new, clean, and dry condition. The visual corona voltage of the items under test shall be equal to or better than the visual corona voltage of the conductor to which they are attached."

5. FLOATING GAPS* AND ULTRA-HIGH FREQUENCY NOISE

One of the powerful tools in attenuation experiments is the so-called "Floating Gap" such as those developed by Prof. L. N. Stone and Prof. H. H. Newell. A floating gap is essentially a spark gap with a relatively large capacitance which can be hung on a line conductor. The radio noise produced by such a gap can over-ride any existing noise of an energized transmission line over a wide frequency range, thus attenuation and similar measurements can be made without interrupting power transmission.

Valuable data have been obtained by the use of such gaps, not only on rates of noise attenuation, mentioned previously, but also the determination of station impedances, noise coupling factors between circuits and the like. Photographs of two such gaps are shown in Figure 3. New gaps of improved characteristics are still being developed.

It is well known that the line conductor noise falls off rapidly beyond 10 megacycles. However, the noise produced by line or station components can have frequency components beyond hundreds of megacycles. For instance, sparking has been observed at string insulators with light mechanical loads on them and sparking between hardware could cause television or radar interference over 100 megacycles within a circular area of several miles in radius. However, such high frequency noises attenuate rapidly as they travel along the transmission line. Thus, their effect is largely localized as a point source of radiation. In general, they can be detected and pin-pointed rather easily by means of directional antennas with, or without the method of triangulation.

---

* See Attachment No. 3

The ultra-high frequency noises are very objectionable to commercial and military communications and guidance systems. Especially with the advent of extra-sensitive radio telescopes, such noises are intolerable even with a magnitude of a few microvolts. Some unattended recording devices were developed to monitor UHF and VHF noises.(5) It appears that UHF noise influence is an area that the radio noise conscious groups of the power industry may have to pay more attention to in the future.

6. MYSTICS OF TRANSMISSION LINE NOISE

Conductor sizes or diameters for transmission lines below 230 KV are often determined by their current carrying capacities rather than the criterion of radio noise. In most cases, the calculated surface gradients of these conductors are much lower than that required to produce corona or radio noise. Laboratory tests on such samples at their operating voltages also confirm that they are either free of corona or with intermittent corona of extremely low magnitude. However, when the same conductors were used on the line, RI Levels of concernable magnitudes were measured in fair weather; thus the mystics of transmission line noise.

One of the theories was postulated by Newell and Warburton(6). They believe that conductor noise can be produced by the foreign materials such as vegetation and insects that come in contact with and then adhere on the conductor surface.

Tests (7,8,9) made in the laboratories have indicated that not only the type of insulating materials but also their sizes have a profound influence in the magnitude of corona or level of radio noise as well as the inception of such phenomena. Tests also showed that corona discharges emanating from insulating points are during the positive half cycle of the 60 cycle voltage. Field measurements(10) have shown that it is this so-called "positive corona" that is responsible for most of the RI on high voltage lines.

Mr. Warburton has made numerous observations* in the field, primarily at night, on 230 KV lines in New England

* See Attachment No. 4

and framentary confirming data have also been obtained from 345, 500 and 700 KV circuits. Portions of insects and other dielectric particles of about 1/32" in length were actually removed from the conductors by means of a special "Duxseal" covered roller with a hot stick where, and while, the visible plume discharges were emanating. Accumulated data have given convincing evidence that the critical length and conductance of the few foreign particles in each span are responsible for producing significant level of noise to affect the RI level of transmission lines in fair weather. Since this thesis of explaining the mystics is supported by both laboratory and field tests, it appears that the next challenging step is to find a means to suppress such plume discharges through an intensive theoretical and experimental study of the phenomenon.

BIBLIOGRAPHY AND ATTACHMENTS

1. "Method of Measuring Radio Noise", Report of the Joint Coordination Committee on Radio Receiption of EEI, NEMA and RMA -- See NEMA Publication 107, New York 1940

2. "The Calculation of Attenuation Constants for Radio Noise Analysis of Overhead Lines," G.E. Adams, L.O. Barthold, AIEE Transactions, Vol. 78, Pt. III, Pp. 975-81 (Dec. 1960)

3. "Radio Noise Propagation and Attenuation Tests on Bonneville Power Administration McNary-Ross 345-KV Line," G. E. Adams, T.W. Liao, M.G. Poland, F.J. Trebby, AIEE Transactions, Vol. 78, Pt. III, Pp. 380-88 (June, 1959)

4. "Radio Noise from High Voltage Transmission Lines," AIEE Radio Noise Subcommittee Report, Table I

5. "Unattended Recording of VHF Receiver Site Noise," R. E. Bloor, AIEE Conference Paper No. 57-1045 (Oct, 1957 - Fall General Meeting)

6. "Variations in Radio and Television Interference from Transmission Lines", H. H. Newell, F. W. Warburton, AIEE Transactions, Vol. 75, Pt. III, Pp. 420-29 (June, 1956)

7. "Effect of Atmospheric Contamination on Generated Radio Influence Voltage", by C. J. Miller, Jr., AIEE Conference Paper No. 56-1046

8. "Relationship between Corona and Radio Influence on Transmission Lines, Laboratory Studies, I-Point and Conductor Corona," T. W. Liao, W.A. Keen, Jr., D. R. Powell, AIEE Transactions, Vol. 76, Pt. III, Pp. 530-40 (Aug. 1957)

9. "Radio Influence Voltages Caused by Surface Imperfections on Single and Bundle Conductors," T. W. Liao, AIEE Transactions, Vol. 78, Pt. III, Pp. 1038-46 (Dec. 1959)

10. "Corona Tests on Hardware for EHV Transmission Lines," O. Nigol and J. Reichman, Ontario Hydro Research News, Vol. 14, No. 3, Pp. 1-7 (1962)

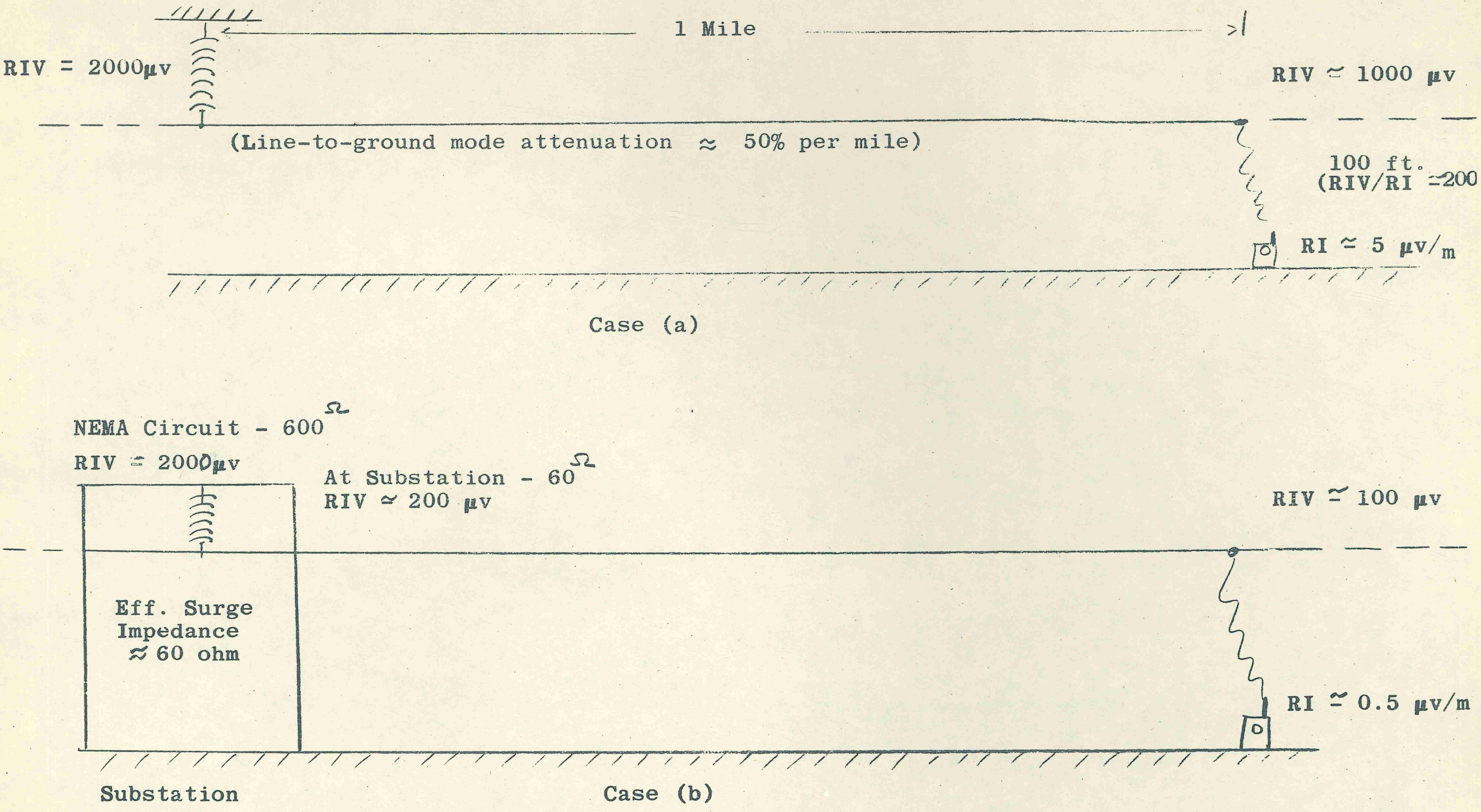
1 Mile
RIV = 2000µv
RIV ≃ 1000 µv
(Line-to-ground mode attenuation ≈ 50% per mile)
100 ft.
(RIV/RI ≃200
RI ≃ 5 µv/m
Case (a)
NEMA Circuit - 600Ω
RIV ≃ 2000µv
At Substation - 60Ω
RIV ≃ 200 µv
RIV ≃ 100 µv
Eff. Surge
Impedance
≈ 60 ohm
RI ≃ 0.5 µv/m
Substation
Case (b)

FIGURE 1 - SCHEMATIC DIAGRAM ILLUSTRATING ATTENUATION OF RADIO NOISE FROM A NOISY INSULATOR STRING
(a) INSULATOR STRING ON A TRANSMISSION LINE
(b) INSULATOR STRING IN A SUBSTATION

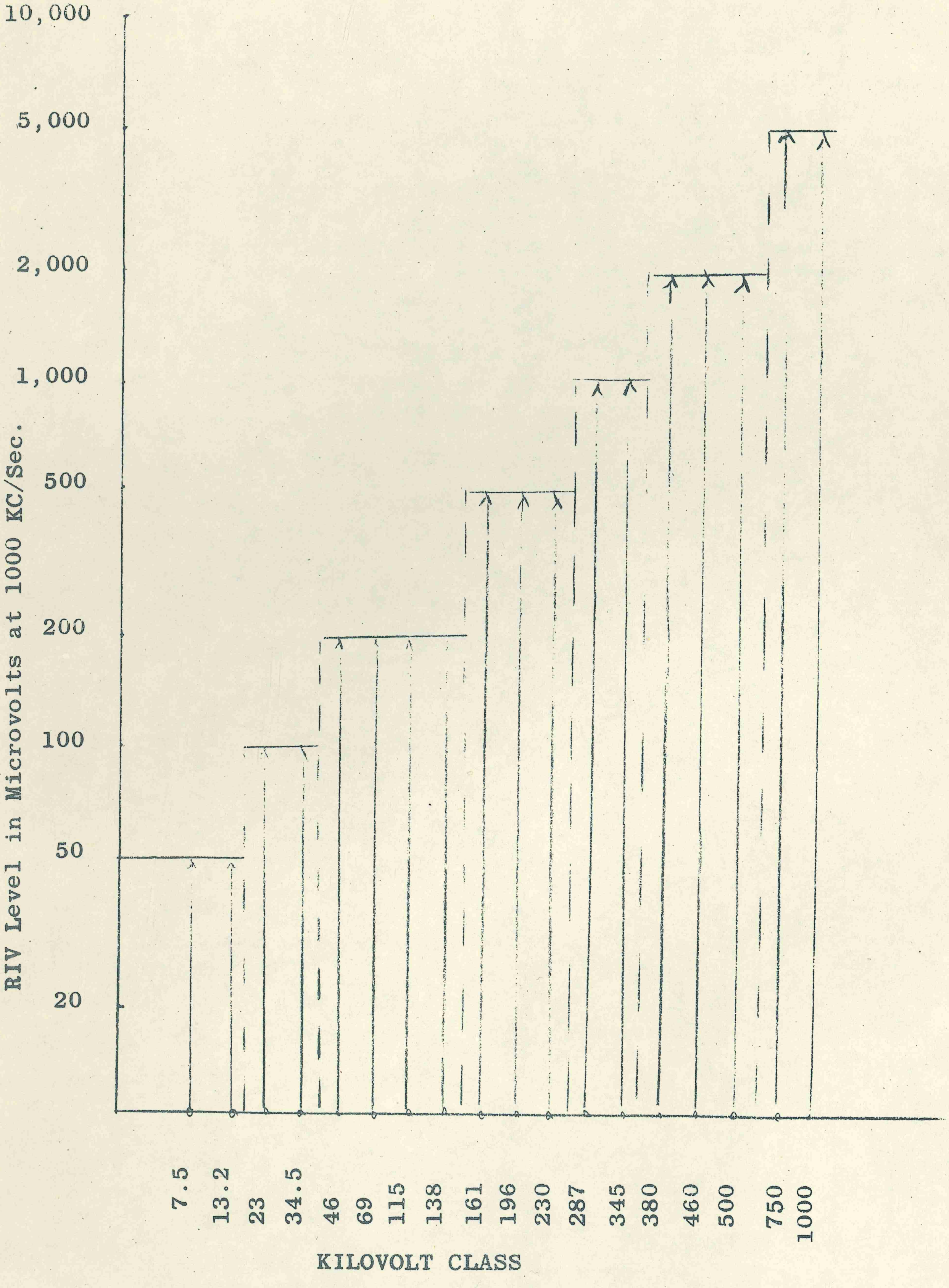

FIGURE 2 - NEMA CIRCUIT RIV LEVELS FOR INSULATORS AND HARDWARE ASSEMBLIES FOR VARIOUS VOLTAGE CLASSES AT A TEST VOLTAGE 110% OF NOMINAL LINE-TO-GROUND VOLTAGE

MEMBERSHIP - WORKING GROUP on "LINE AND STATION COMPONENTS" OF RADIO NOISE SUBCOMMITTEE

P. L. Bellaschi
Consulting Engineer
7417 S. E. Yamhill Street
Portland 16, Oregon

H. H. Brustle
General Electric Company
Bldg. 9
Pittsfield, Massachusetts

F. Reed Dallye
Aluminum Company of America
536 Alcoa Bldg.
Pittsburg 19, Pennsylvania

F. A. Denbrock
Commonwealth Associates
209 East Washington Avenue
Jackson, Michigan

C. D. Fiero
Mechanical Engineer
Lapp Insulator Company
LeRoy, New York

J. Kaminski, Jr.
Insulator Division
General Electric Company
P. O. Box 57
Baltimore 3, Maryland

J. R. Leslie
Research Division
Hydro-Electro Power
Commission of Ontario
620 University Avenue
Toronto 2, Ontario, Canada

T. W. Liao (Chairman)
Engineering Research
General Electric Company
6901 Elmwood Avenue
Philadelphia, Penna. 19142
SA.4-1500, Ext. 3221

C. J. Miller
Research Engineer
Ohio Brass Company
Barberton, Ohio

A. C.Neaderland
Project Engineering Section
Burndy Corporation
Norwalk, Connecticut

H. H. Newell
Worcester Polytechnic Institute
Worcester
Massachusetts

W. E. Pakala
Westinghouse Research laboratory
Beulah Road, Churchill Borough
Pittsburg 35, Pennsylvania

B. M. Pickens
Engineering Department
Anaconda Wire and Cable Company
Hastings-on-Hudson, New York

L. N. Stone, Dept. Head
Electrical Engineering
Oregon State College
Corvallis, Oregon

P. D. Tuttle
Aluminum Company of America
Massena
New York

F. W. Warburton
New England Power Service Company
939 Southbridge Street
Worcester 10, Massachusetts

#117

Transactions Paper

(Reviewed and Accepted for Publication)

Discussion in Duplicate Due February 21, 1964.

RADIO NOISE STUDIES ON POWER LINES WITH THE CORONAPHONE

J. R. Leslie
Senior Member IEEE

H. O'Beirne
Member IEEE

Both of:
The Hydro-Elec. Pwr. Com. of Ontario
Toronto, Ont., Canada

A paper recommended by the IEEE Transmission and Distribution Committee and approved by the IEEE Technical Operations Committee for presentation at the IEEE Winter Power Meeting, New York, N. Y., February 2-7, 1964. Manuscript submitted November 1, 1963; made available for printing December 4, 1963.

Price: $ .60 To Members
$1.00 To Nonmembers

(10¢ per copy additional if
first class mailing desired)

(Minimum Mail Order $1.00)

All Rights Reserved by
The Institute of Electrical and Electronics Engineers,
Inc.,

P. O. Box A,
Lenox Hill Station,
New York 21, N. Y.

Litho in USA

Paper No.

64-52

RADIO NOISE STUDIES ON POWER LINES WITH THE CORONAPHONE

J.R. Leslie H. O'Beirne

The exact location of radio interference sources on a power line has been a problem of long standing in the utility field. The difficulties have been such that even today opinions differ as to the source of radio noise on many common types of lines. One of the reasons for this is that corona currents generated at the point of an electrical discharge travel in both directions along the conductor for considerable distances. A radio noise meter responds to these currents for large distances along the line by picking up the induction and radiation fields around the conductors. Thus, localization of the source by this means has been difficult.

This problem is now believed to be solved by the use of the coronaphone described here and shown in Figure 1. The coronaphone operates by detecting the audible sound produced by the corona discharge. The audible sound does not travel along the conductor, but is confined to the immediate area of the source; hence, it may be used to locate the noise source.

This paper reviews the development of the coronaphone; it shows that a correlation between acoustic noise and the radio influence voltage exists. Finally the application to the study of power line corona sources on high-voltage lines is discussed. One observation is important; on operating lines up to 230 kv in voltage, conductor corona has not been found to be a major contributor to the radio noise field either in dry or wet weather. Hardware noise on the contrary is believed to predominate.

A technical description of the coronaphone is given in the Appendix.

DESCRIPTION OF INSTRUMENT

Briefly the coronaphone consists of an assembly of a high-frequency microphone, a parabolic reflector, and an amplifying and metering system The microphone and reflector are designed to have a highly directional characteristic by responding only to sound waves between 10 and 20 kilocycles in frequency. The design is such that the instrument can separate corona sources less than three feet apart at a distance of 100 feet.

The amplifier and detector circuits are designed to operate on the quasi-peak value of the signal, as early studies in 1959 showed that the noise produced was impulsive in character and the quasi-peak detector would give increased sensitivity compared to an average reading detector. Furthermore, this detector corresponds to that used by RI meters.

COMPARISON OF ACOUSTIC AND CORONA PULSES

Initial field tests on the coronaphone in 1959 had shown that as a location device for corona noise, its sensitivity and directivity was

adequate. But to be of greatest value in studying noise sources on high-voltage lines, a correlation with the radio influence voltage (riv) should exist. Could such a correlation be found? The experiments described below were made in order to explore this question.

A few typical corona sources were set up in the laboratory using a NEMA riv circuit and comparisons were made between the radio noise meter and acoustic signals, the latter at a standard distance from the source. Waveforms of the acoustic and electric (riv) pulses were displayed on an oscilloscope.

A close similarity between the two types of signals was found, each corona burst producing a corresponding acoustic pulse. Figure 2 compares waveforms from the noise meter, trace 2, and the coronaphone, trace 3, for a conductor having artificially applied contamination. The conductor used was a short piece of 1/4-inch-diameter aluminum tie-wire with some dirt that had been removed from an aged ACSR conductor adhering to it. The applied voltage was 21.9 kv and the coronaphone was approximately 15 feet from the conductor. The photograph shows corona to be present only on the positive polarity of the exciting voltage. The time scales have been adjusted horizontally to compensate roughly for the travel time of the sound pulse in the air.

The corona and acoustic pulses from a single suspension insulator at 18.9 kv are shown in traces 4 and 5 of the same figure. The riv level was 2000 uv quasi-peak. Both polarities now contribute to the noise (a fact easily noted in field testing because of the change of the sound). Traces 6 and 7 again compare the pulses, but with a 20 per cent increase in voltage across the insulator, with an riv level of 17,000 uv.

The riv pulses were taken using the field intensity position on the noise meter.

The mechanism of noise generation with the insulator unit is different from that on the conductor. A visual observation in the dark shows that the noise is being generated by two rings of small sparks, one jumping vertically across the small air-gap that exists between the top metal cap and the porcelain, and the second jumping radially from the bottom pin to the porcelain. The equivalent electrical circuit of a single insulator unit is therefore almost symmetrical; it does not matter which end of the unit is positive--there is always a metal-to-porcelain air-gap on one side and a porcelain-to-metal air-gap on the other. Hence, as Figure No. 2 shows, both radio and acoustic noise are generated in both half cycles. Furthermore, since the discharge appears as a number of small sparks all round the insulator, many more acoustic pulses occur in each half cycle; this can be seen in trace No. 5 of Figure 2.

The close correspondence which has been demonstrated between the two types of signals has led to a search for a theory relating the two. The technical literature revealed no useful references. The authors would propose that two mechanisms exist which can cause movement of the air molecules. First of all, the air will contain some ionized molecules; being in an electrostatic field, these ions will move. When the discharge takes place, the electrostatic field will suddenly change and the ions will violently change their direction of movement. From this change, an acoustic pressure wave will be propagated in the air, and will be heard as sound.

The second mechanism is caused by the heating effect of the spark discharge. A small column of air along the path of the discharge will be suddenly heated to a very high temperature; it will expand rapidly, thus generating a positive step pressure wave. As soon as the discharge is over, the air will cool again, contract, and generate a negative pressure wave.

From a theoretical analysis of the dynamical properties of a gas a "time of relaxation" can be derived, a measure of the rate at which a gas approaches steady-state conditions after being disturbed. For air at normal ambient conditions, this "time of relaxation" is 0.17 nanosecond. In other words, disturbances in the air movement caused by electrostatic forces or heating can generate acoustic pulses with rise times faster than one nanosecond. As mentioned above, the riv pulses show similar time constants; it seems reasonable to assume that each corona spark discharge will produce simultaneously an acoustic pulse and an riv pulse, both with similar time constants.

Both riv and acoustic pulses are measured with narrow band meters having time constants less than the original pulse time constants. In this respect both types of meters are bandwidth limited. Their quasi-peak responses should be similar.

However, variations in the riv/acoustic ratio may be caused by acoustic shielding and reflection effects due to the proximity of the hardware surfaces which are producing the corona discharges.

CORRELATION OF RIV AND CORONAPHONE READINGS

As noted above, preliminary tests had indicated that a qualitative relationship exists between quasi-peak measurements of riv and quasi-peak measurements of acoustic noise. In a series of tests to investigate this relationship further, a number of paired readings of riv and acoustic noise were taken on a wide variety of hardware items. Thus insulators from a number of manufacturers were tested, including suspension units and pin-type units of various voltage ratings. Wet and dry tests were made, and on the pin-type units, a number of different ties and clamps were investigated. Finally experimental arrangements to simulate noisy conductors and hardware were tested.

The highest voltage that could be used in the laboratory on the test arrangement was 26 kv, which with higher voltage insulators did not generate sufficient noise to make a correlation possible. For the same reason, it was not possible to test a complete suspension insulator string with clamp, though tests were made on individual suspension insulator units. However, the relationship between acoustic noise and riv appeared to be sufficiently constant that application to field surveys seem justified.

Standard statistical techniques of linear regression analysis were used to establish the correlation and also to measure the significance of the differences between correlations for the various types of insulators and hardware.

This relationship varies only slightly for various items of hardware; for a suspension insulator unit, for example it is

$$\text{Riv} = 31 + 0.87C \qquad S = 1.5 \text{ db}$$

Where riv is the noise meter reading, db above 1 microvolt

C is the coronaphone reading, arbitrary units, db.

S is the standard deviation at 100 feet.

Similar equations were developed for the other corona sources, using in all cases the arbitrary coronaphone units.

The regression equation for all items tested fell within the band shown in Figure 3. Thus it would appear that the riv level for any item of hardware may be estimated from acoustic measurements without regard for the type of source, to an accuracy of ±5 db, provided that some precautions are taken with regard to the viewing of the source (Table V).

SURVEYS OF OPERATING LINES

The question of prime interest in the field was that of locating the major sources of radio influence on high-voltage lines. Some of the first tests showed that line conductors, except where noticeably damaged, did not give any response on the coronaphone, throughout the length of the several spans tested. These were 230-kv circuits of standard 795 MCM construction. Each support point did however give readings detectable several hundred feet from the towers and the individual hardware items could in most cases be separated. On the 500-kv Coldwater experimental line on the contrary, the suspension points were quiet whereas the conductors all showed a number of specific corona sources along their length. The number was possibly a dozen or so per phase, in a 1/2-mile section. The suspension hardware in these tests was either well shielded, or of the self-shielded type.

With this early experience at hand, an extensive survey of transmission line hardware was undertaken. The average of the readings from each item of hardware at a number of tower locations was obtained. The noise levels were normalized to a standard 100-foot distance from each source, using a simple inverse distance law.

All the riv estimates were then converted by using the regression line represented by the upper edge of the band in Figure 3. This line was obtained from a test arrangement in which an aluminum spike was generating noise, probably a reasonably close approximation to the actual noise mechanisms on a transmission line. The aluminum spike gave higher riv generation for a given acoustic noise than any of the other arrangements; if the average riv figures quoted in the tables are in error, they will probably all err on the high side.

The results of a survey on a 12-year-old 230-kv line are given in Table I. The conductors are 795 MCM ACSR. Some of the measurements were taken on a section with single-circuit steel towers, and some with double-circuit steel towers; the data for both have been combined. The loop support clamp, suspension clamp and dampers appear to be the large noise source. Line voltage was 240 kv. The conductor noise was everywhere below background, and the weather during the tests was fair. The Table lists the mean value, m, and the standard deviation, s. Table II summarizes the field results on the four classes of operating lines which were examined, all tests being in fair weather. Column A repeats the results in Table I.

Column B refers to a new section of 230-kv double-circuit line. This line uses a design of tower with close-circuit spacing, conductors 1843 MCM ACSR, single-bolt torsional dampers. When these measurements were taken, the line had been in service for only one month. The suspension clamps and loop clamps are again the predominant noise sources.

Column C summarizes measurements of a 5-year-old section of single-circuit wood pole line hybrid construction, operating at about 250 kv. The centre conductor is 1192 MCM ACSR with double U-bolt torsional dampers, the outer conductors, 795 MCM ACSR with single-bolt torsional dampers. Phase spacing is 18 feet. A large proportion of the readings were at the background noise level, so statistical techniques for a truncated normal distribution were used.

Some of the data for single-circuit towers are analyzed to find if there is any significant difference between the noise generated on the centre and the outer phases. The centre conductor of this line operates at a 5 per cent higher voltage gradient than the outer conductors. Using the rule-of-thumb that a 10 per cent increase in voltage gradient doubles the radio interference, we would expect about 40 per cent more riv on the centre phase. Of course, these gradients are calculated for the conductors at mid-span, whereas most noise sources will be on hardware close to the tower. Nevertheless, as can be seen in Table III, coronaphone readings clearly showed higher noise generation. These figures indicate that the acoustic noise on the centre phase averages 3.6 db higher than that on the outer phase. This figure converted to riv represents 50 per cent higher radio noise generation on the centre-phase hardware. This agrees remarkably well with the rule-of-thumb.

Some comparisons were made between the noise generated in dry weather and in wet weather on 230-kv hardware. The conductor, which in dry weather is quiet unless damaged, is found to generate considerable noise in rain. The average increase in acoustic noise, as measured with the coronaphone, is given in Table IV. The suspension clamp is still 11 db (i.e. almost four times) noisier than the adjacent section of conductor.

It is difficult to estimate from the acoustic noise the riv generated, because no longer do we have a single-point noise source; the coronaphone measures the quasi-peak value of the noise generated by a number of independent sources on a length of conductor of about three feet.

Laboratory tests were, in fact, made to show the nature of the response. The reading changed by a negligible amount as the number of sources on a short length of conductor was increased from one to four.

Provided the quasi-peak relationship truly holds, the hardware should thus predominate over the conductor in foul weather. This conclusion is borne out by recent foul-weather ri tests wherein the quasi-peak-to-average ratio on the Stoddart meter does not change from fair to foul weather, on a given line. If the origin of the predominant noise does in fact change in rain from a relatively small number of hardware sources to numerous conductor discharges, one would expect this ratio to change. The argument has great practical value because, if this conclusion is valid, a reduction in the foul-weather ri can be achieved at relatively small cost, by minor changes to suspension hardware designs. Additional study and tests are required, however, before the source of radio noise during precipitation can be determined without question.

The actual ri values estimated from the field tests are close to the values to be expected from under the line ri measurements. Taking the ratio of on-line to under-line noise at 200/1 for a measurement 100 feet out, the ri would be of the order of 50 to 75 microvolts per meter. Actual values are close to this.

115-KV DATA

Readings have been made on 115-kv circuits of various types. A total of 42 samples of suspension insulators with clamps and 54 samples of dampers gave only one reading above background, and that on a damaged insulator. However, the background was unusually high at this time, caused by birds and insects. It can be said that the riv level for each noise source was below 1000 uv.

Some results (Column D, Table II) were obtained at a later date, using the technique of truncated normal distribution. They gave a mean of 31 db (estimated riv = 2800 uv) for 18 samples of suspension insulators with clamps, but noise on 42 samples of dampers was all below background. These results agree with radio interference measurements on the right-of-way where the levels are found to be negligible.

EFFECT OF VIEWING ANGLE

Because some corona discharges might be shielded in the field from direct view with the instrument, tests were made of this effect. Readings were taken on a 230-kv line from eight equally spaced 45-degree points on the circumference of the circle centered on each sample. In Table V, each line represents one sample, the maximum and minimum readings are given.

Two interesting points may be noted. First, the acoustic range is smaller for the suspension insulator with clamp and double U-bolt damper (where the noise source was visible from all angles) than for the other three types of hardware (where the noise source was hidden when viewed from certain positions). Second, it took about 10 minutes to make the eight readings on each item: there is a possibility that the corona discharges fluctuated during this time, adding to the range.

REPEATED READINGS

During the measurements on a 230-kv double-circuit line, readings were repeated on some items six days later under similar voltage and weather conditions, and an analysis made of the differences between the first and second sets of readings. The results obtained are shown in Table VI.

A statistical t-test shows that these differences can be taken as zero, with less than a 5 per cent risk of error in all but the last case. The possibility exists that the line voltage changed between the two sets of readings.

TESTS ON ONTARIO HYDRO'S EHV LINE AT COLDWATER

The first tests of the coronaphone on Ontario Hydro's 600-kv test line were conducted to demonstrate that the coronaphone was a practical device for locating noise sources from a distance, and second to determine which of two microphones was more suitable. In making these tests, the locations of a number of noise sources were accurately recorded and their intensities measured.

Some three months later these same points were checked, again one week later, and again one day later. It was found that of the dozen or so noise sources recorded on each day, many could not be detected on the next survey; however, new noise sources of approximately the same number had appeared at different locations. The explanation was taken to be that noise was caused by insects or by particles of dirt adhering to the conductor, particularly at small scratches or at areas of mechanical damage, and that between observations, these contaminants had either been washed off by rain or burned off.

Some stationary corona sources proved to be due to areas of conductor damage, which were subsequently examined with the line unenergized. In every instance, signs of mechanical damage were found wherever strong noise sources existed on the conductors.

In another test, the acoustic noise generated by a number of artificial corona sources at a series of line voltages was measured with the coronaphone, and a correlation attempted between these readings and the corresponding ri measurements. The results were not conclusive, possibly because the ehv test line is so short that a pronounced standing wave pattern of riv is set up, and hence the level of the ri measured depends greatly on the position of the noise source along the line.

NOISE LOCATION TESTS

One interesting investigation concerned the location of a noisy insulator in a distribution station bus. The insulator was one of a group situated close to a noisy transformer, and although the buzzing from the insulator was easily discernible by ear from the ground, it was difficult to pin-point the source exactly. The coronaphone easily picked out the insulator, identifying it accurately and quickly from its neighbours.

Sources of television interference cannot be detected with the coronaphone, possibly because of the frequency response limitations in the microphone.

CONCLUSIONS

A new method of locating radio interference sources on high-voltage lines and apparatus, by the use of an acoustical detector, has been demonstrated. A reasonable correlation between the riv level and the acoustical signal radiated from a single corona source has been found.

The principal noise source on high-voltage lines operating in the 230-kv class has been found to be hardware; the conductors are relatively quiet. On ehv lines where gradients are closer to the maximum corona-starting values, the conductor may be the predominant source.

The coronaphone should prove particularly useful in the study and field testing of new hardware and conductor designs, in determining their corona properties.

APPENDIX

In the coronaphone, shown in Figure 1, the parabolic reflector is constructed from a 24-inch-diameter radar antenna, with a focal length of 9.75 inches. This reflector is mounted on a tripod through geared pan and tilt controls. A polarized ring sight is mounted at the edge of the reflector to help the operator locate or identify noise sources. The microphone is mounted near the focal point on a bracket rigidly attached to the reflector.

The three microphone characteristics considered most important for coronaphone application are, adequate sensitivity, appropriate frequency response, and low internal-noise level. A condenser microphone measures up well to all these requirements, and was chosen in spite of the fact that a unit of this type requires a polarizing battery and a cathode follower. The model selected has a threshold sensitivity of 4.3 nanobars, a frequency upper limit of 20 kilocycles, and is so insensitive to external fields that its performance is not impaired even directly under a 600-kv test line.

Tests after assembly showed that this microphone-reflector combination gives adequate directionality, the 6-db beamwidth at 10 kc being 4.2 degrees. This directionality is sufficient to enable a skilled operator to locate a noise source 100 feet away with an accuracy of about one foot and to separate sources which are 3 feet apart. The sound absorption by the atmosphere is negligible at these frequencies, in a 100-foot path.

The coronaphone amplifier, filter and meter circuits together with the necessary batteries are housed in the box shown in Figure 1. Transistors are used throughout the amplifier in order to reduce battery requirements, thereby increasing portability. Between the microphone and the first stage of the amplifier is a high-pass filter for the attenuation of the relatively large noise energies of low harmonics of 60-cycle and voice frequencies. The maximum voltage gain of the amplifier is 100,000. The effective frequency response is 10 db down at 1500 and 20,000 cycles. The quasi-peak detector has time constants of 1-m-sec rise time and 600-m-sec delay. An audible output is provided.

The arbitrary units quoted are based on 0 db = 2×10^{-4} microbar, when the band-pass filters and reflector have been removed from the system.

TABLE I. CORONAPHONE SURVEY ON 230-KV CIRCUIT

	No. Samples	Acoustic Level in db m	Acoustic Level in db s	Calculated riv uv
Conductor, 759 MCM	-	Background		1,500
Clamps - suspension with insulators	295	47	4.1	12,000
- loop support with insulators	28	50	5.0	15,000
- dead end with insulators	56	39	6.0	5,700
Dampers - double U-bolt torsional	531	47	4.3	12,000
- stock bridge	12	40	4.9	6,400
Joints - compression	92	31	10.0	2,900
- repair sleeve	5	26	3.0	1,800

m = mean, s = standard deviation

TABLE II. CORONAPHONE FIELD SURVEYS SUMMARIZED

	A	B	C	D
Tower Type	Steel	Narrow Steel	Wood	Steel
Conductor size MCM	795	1843	1192/759	
Nominal line voltage	230 kv	230 kv	250 kv	115 kv
Corona Source	riv (uv)	riv (uv)	riv (uv)	riv (uv)
Conductors	*	*	*	*
Clamps - suspension with insulators	12000	9300	14000	2800
- loop support with insulators	15000	11000	12000	
- dead-end with insulators	5700	7900	3300	
Dampers - double U-bolt torsional	12000	-	7500	*
- stockbridge	6400	-	-	
- single-bolt damper	-	*	1500	
Joints - compression	2900		17000	
- repair sleeve	1800	-	-	

*Samples of these items were measured, but the acoustic noise was below background. The level of riv generated must therefore be below about 1000 uv.

TABLE III. COMPARISON OF RIV ON CENTRE AND OUTER PHASES

	Number of Samples	East	Centre	West
Suspension clamp with insulator	29	45.47	49.49	45.97
Damper, double U-bolt torsional	58	46.73	50.19	46.66
Averages	-	46.10	49.84	46.31

TABLE IV. INCREASE IN ACOUSTIC NOISE IN WET WEATHER

	Number of Samples	Dry Weather db	Wet Weather db	Increase db
Conductor	12	Background	52.3	Over 17.8
Damper double U-bolt torsional	6	45.2	55.6	10.4
Suspension clamp with insulator	5	48.9	63.0	14.1

TABLE V. EFFECT OF VIEWING ANGLE

	Range Max & Min (db)
Suspension insulator with clamp	51.1 to 49.1
	48.1 to 40.6
	49.1 to 46.5
Double U-bolt damper	55.9 to 48.6
	53.0 to 48.1
	50.6 to 41.6
	50.6 to 45.6
Compression joint	61.0 to 44.0
	37.8 to 33.1
	54.2 to 30.0
Dead-end insulator with clamp	53.4 to 35.3
	45.8 to 38.3
	51.8 to 39.9

TABLE VI. REPEATABILITY OF READINGS

	Number of Samples	Difference Between Paired Readings (db) m	s
Dampers	36	-1.2	4.9
Suspension insulators with clamps	30	-1.3	3.8
Compression joints	6	+3.6	12.9
Dead-end insulators with clamps	4	-8.0	5.2
Loop support insulators with clamps	6	-6.0	2.5

m = mean, s = standard deviation

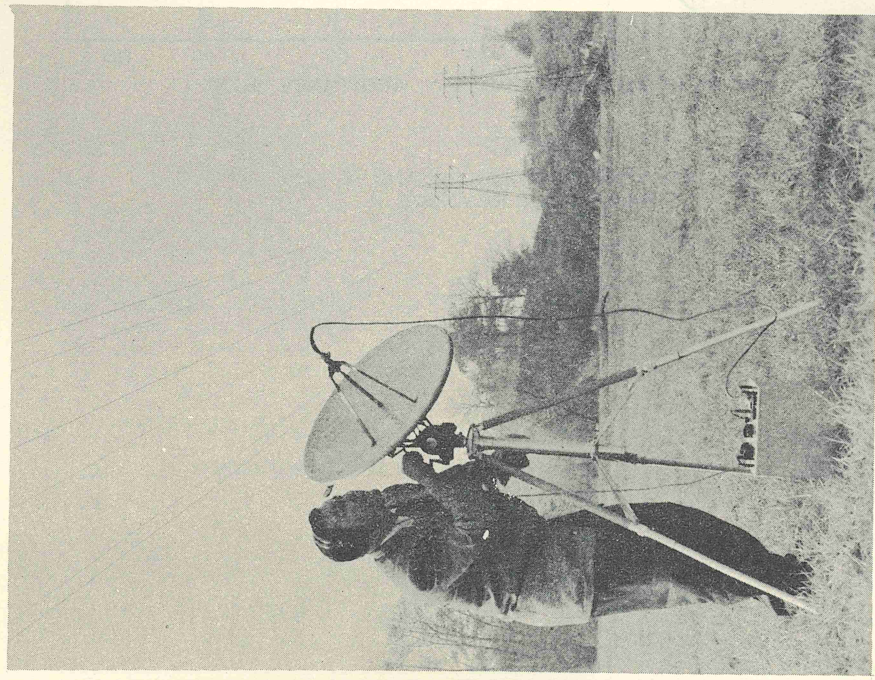

Figure 1. Photograph of the Coronaphone, Showing Parabolic Microphone Assembly and Box Containing Electronic Circuitry and Batteries.

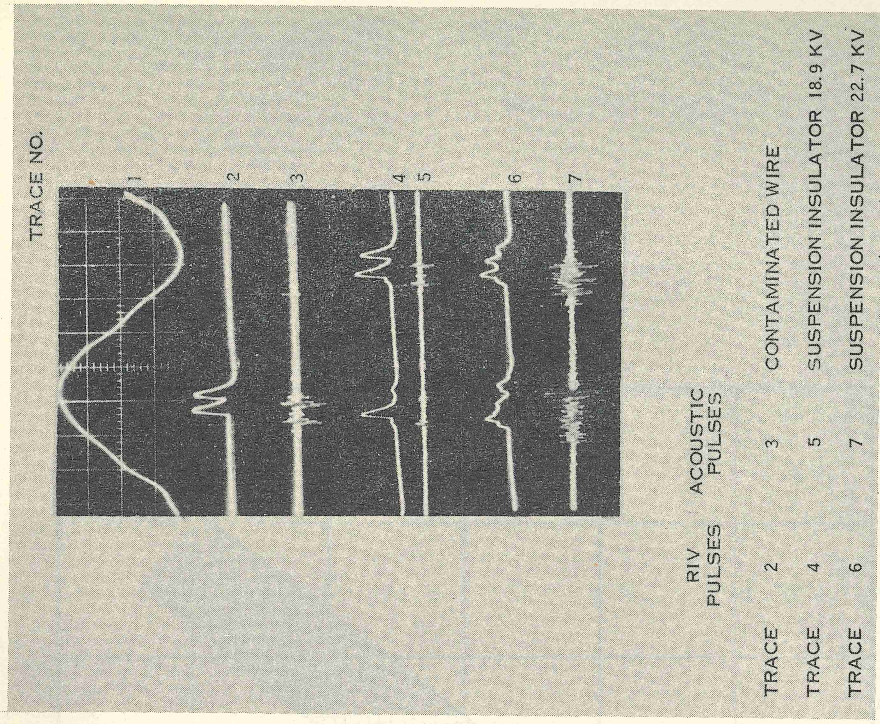

Figure 2. Comparison of Electric and Acoustic Corona Pulses.

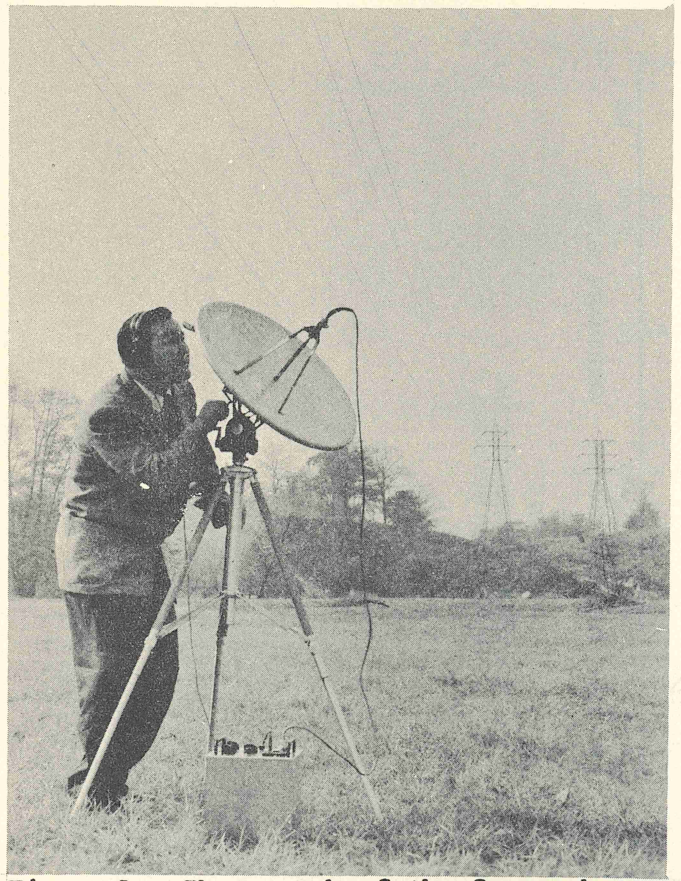

Figure 1. Photograph of the Coronaphone, Showing Parabolic Microphone Assembly and Box Containing Electronic Circuitry and Batteries.

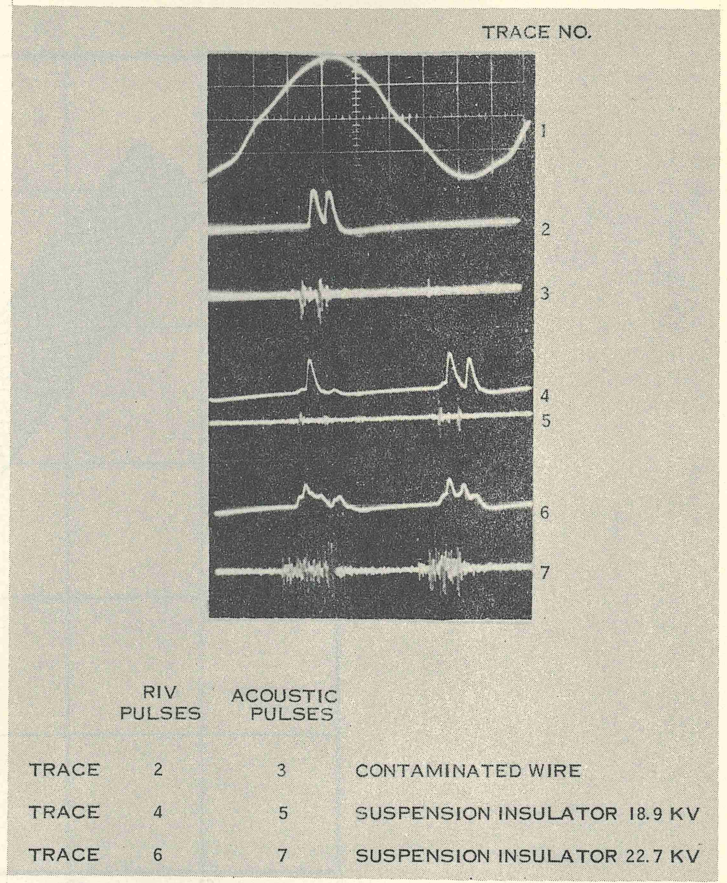

Figure 2. Comparison of Electric and Acoustic Corona Pulses.

FOR USE OF G-E EMPLOYEES ONLY

GENERAL ELECTRIC

TECHNICAL INFORMATION SERIES

Title Page

AUTHOR JJ LA FOREST	SUBJECT CLASSIFICATION IV File 6-J	NO. DF-63-AD-51 DATE 12-23-63

TITLE

THE EFFECT OF INSULATOR NOISE CURRENTS ON THE RADIO NOISE LEVEL OF A TRANSMISSION LINE

ABSTRACT An analysis is made to show what the lateral radio noise profile would be for a 3-phase transmission line as a result of noise currents generated solely by the insulator strings. Typical cases for 345-, 500-, and 700-kv lines are examined. At distances generally used to evaluate the RI field from a transmission line, the effect of insulator noise currents is seen to be low.

G.E. CLASS IV GOV. CLASS.	REPRODUCIBLE COPY FILED AT Pittsfield Works Project EHV	NO. PAGES 19

CONCLUSIONS

The use of modal analysis has enabled the computation of the effect of insulator noise on the radio noise performance of a transmission line. The computation is facilitated by using eigen roots, field factors, and attenuation values obtainable from the General Electric Radio Noise Program. Values of insulator noise currents are obtained from laboratory tests. This analysis can also be used to determine the effect on line radio noise performance of point sources other than insulator strings such as station equipments.

By cutting out this rectangle and folding on the center line, the above information can be fitted into a standard card file.

For list of contents—drawings, photos, etc. and for distribution see next page (FN-610-2).

INFORMATION PREPARED FOR POWER SYSTEMS ENGINEERING OPERATION

TESTS MADE BY

COUNTERSIGNED DIV.

DIVISIONS LOCATION Pittsfield, Massachusetts

FN-610-1 (1-49) new

GENERAL ELECTRIC COMPANY
TECHNICAL INFORMATION SERIES
CONTENTS PAGE

CONTENTS OF REPORT

NO. PAGES TEXT	16 (including 2 Tables)
NO. CHARTS	4 Figures
DRAWING NOS.	
PHOTO NOS.	

DISTRIBUTION

JG Anderson - 9-205 - Pittsfield
LO Barthold - 2-612 - Schenectady
HH Brustle - 9-314 - Pittsfield
HA Frey - Insulator Dept. - Baltimore
MH Hesse - 2-628 - Schenectady
EM Hunter - 2-616 - Schenectady
JJ LaForest - 9-205 - Pittsfield
TW Liao - 21-4 HV Sw. G. - Philadelphia
DD MacCarthy 9-202 - Pittsfield
F Olsen - 9-205 - Pittsfield
RJ Pileggi - 2-605 - Schenectady
TA Cramer - Communication Products Dept. - Lynchburg, Va.
RB Kaufman - 16-309 - Pittsfield
JR Meador - 9-204 - Pittsfield
ME Scoville - Capacitor - Hudson Falls

THE EFFECT OF INSULATOR NOISE CURRENTS ON THE RADIO NOISE LEVEL OF A TRANSMISSION LINE

INTRODUCTION

There are two main sources of radio noise currents on an ehv transmission line. One source, which has been treated extensively,[1,2,3] results from corona discharges on the line. The second source is the insulator strings. The purpose of this memorandum is to find out what the lateral radio noise profile would be for a transmission line as a result of noise solely from the insulator strings. Measured laboratory RIV values for a typical insulator string, using a standard NEMA test circuit, are assumed to be available.

The analysis will be done on a modal basis using line currents and line-to-ground voltages. Also, a spectral density argument will be used, especially to tie in uncorrelated values of current and voltage. Voltages and currents within a mode, at a specific point on the transmission line, are assumed to be correlated and these quantities between different modes are assumed to be uncorrelated.

ANALYSIS AND DISCUSSION

Laboratory Tests

Figure 1 shows the results of a typical laboratory test on a string of insulators where RIV values as measured in a standard test setup are given versus applied 60-cycle potential. The RIV values in this chart are those measured with a Stoddart quasi-peak RI meter. From this test setup it is assumed that a ratio, $\emptyset$, can be found, by measurement, that will relate a Stoddart noise meter reading to one that would be obtained with an RMS meter. The spectral density, $SD[i]$, of the measured noise current would be:

$$SD[i] = \frac{(RIV_{(STOD.)})^2}{\emptyset_1{}^2 (Z_T)^2 \Delta f} \text{ amperes}^2\text{-sec.} \tag{1}$$

where $RIV_{(STOD.)}$ = voltage as measured by a Stoddart meter in volts

$\emptyset_1$ = ratio in $\dfrac{\text{Volts (Stoddart)}}{\text{Volts (RMS meter)}}$

Z_T = Total test circuit impedance in ohms.

Δf = bandwidth in sec^{-1}

Hence, from laboratory tests and equation (1), values of SD$[i]$ can be found for a variety of 60-cycle line-to-ground voltages.

Propagation Characteristics

A section of a transmission line including one set of insulator strings is shown in Figure 2. It is assumed that the insulator strings act as constant current generators (large internal impedance). As stated before, a modal treatment of the propagation phenomenon is desired, therefore each of the line currents that will affect the observer is broken up into its modal components. The following matrix equations apply:

$$\begin{bmatrix} i_A^{(1)} \\ i_A^{(2)} \\ i_A^{(3)} \end{bmatrix} = 2\pi \begin{bmatrix} \lambda^{(1)}\left(A^{(1)}\right)^2 & \lambda^{(1)}A^{(1)}B^{(1)} & \lambda^{(1)}A^{(1)}C^{(1)} \\ \lambda^{(2)}\left(A^{(2)}\right)^2 & \lambda^{(2)}A^{(2)}B^{(2)} & \lambda^{(2)}A^{(2)}C^{(2)} \\ \lambda^{(3)}\left(A^{(3)}\right)^2 & \lambda^{(3)}A^{(3)}B^{(3)} & \lambda^{(3)}A^{(3)}C^{(3)} \end{bmatrix} \bullet \begin{bmatrix} \frac{i_A}{2} \\ \frac{i_B}{2} \\ \frac{i_C}{2} \end{bmatrix} \qquad (2)$$

and

$$\begin{bmatrix} i_B^{(1)} \\ i_B^{(2)} \\ i_B^{(3)} \end{bmatrix} = 2\pi \begin{bmatrix} \lambda^{(1)}\left(B^{(1)}\right)^2 & \lambda^{(1)}B^{(1)}C^{(1)} & \lambda^{(1)}B^{(1)}A^{(1)} \\ \lambda^{(2)}\left(B^{(2)}\right)^2 & \lambda^{(2)}B^{(2)}C^{(2)} & \lambda^{(2)}B^{(2)}A^{(2)} \\ \lambda^{(3)}\left(B^{(3)}\right)^2 & \lambda^{(3)}B^{(3)}C^{(3)} & \lambda^{(3)}B^{(3)}A^{(3)} \end{bmatrix} \bullet \begin{bmatrix} \frac{i_B}{2} \\ \frac{i_C}{2} \\ \frac{i_A}{2} \end{bmatrix} \qquad (3)$$

and

$$\begin{bmatrix} i_C^{(1)} \\ i_C^{(2)} \\ i_C^{(3)} \end{bmatrix} = 2\pi \begin{bmatrix} \lambda^{(1)}\left(C^{(1)}\right)^2 & \lambda^{(1)}C^{(1)}A^{(1)} & \lambda^{(1)}C^{(1)}B^{(1)} \\ \lambda^{(2)}\left(C^{(2)}\right)^2 & \lambda^{(2)}C^{(2)}A^{(2)} & \lambda^{(2)}C^{(2)}B^{(2)} \\ \lambda^{(3)}\left(C^{(3)}\right)^2 & \lambda^{(3)}C^{(3)}A^{(3)} & \lambda^{(3)}C^{(3)}B^{(3)} \end{bmatrix} \bullet \begin{bmatrix} \frac{i_C}{2} \\ \frac{i_A}{2} \\ \frac{i_B}{2} \end{bmatrix} \tag{4}$$

where $\lambda^{(n)}$ = eigen root for mode n

$N^{(n)}$ = eigen vector for mode n and phase N

$\frac{i_N}{2}$ = injected insulator current in phase N flowing to the observer

$i_N^{(n)}$ = line current for mode n in phase N

$\lambda^{(n)}$ and $N^{(n)}$ are obtained from the present General Electric Radio Noise Program. A typical set for an ehv line where the modes are numbered in order of increasing value of eigen root and therefore impedance is shown below.

TABLE I

	Mode 1	Mode 2	Mode 3
A	+ .0758	- .11074	+ .0729
B	- .1270	0	+ .0868
C	+ .0758	+ .11074	+ .0729
λ	5.75	6.49	8.76

With the above equations, each of the injected insulator currents flowing toward the observer can be obtained. Assuming independent current generators, the method is as follows:

Modal currents due to current only from the insulator string in phase A

Let $i_B = i_C = 0$

From equations (2), (3), and (4)

$$
\begin{aligned}
i_A{}^{(1)} &= 2\pi\lambda^{(1)}\left(A^{(1)}\right)^2\left(\frac{i_A}{2}\right)\\
i_A{}^{(2)} &= 2\pi\lambda^{(2)}\left(A^{(2)}\right)^2\left(\frac{i_A}{2}\right)\\
i_A{}^{(3)} &= 2\pi\lambda^{(3)}\left(A^{(3)}\right)^2\left(\frac{i_A}{2}\right)\\
i_B{}^{(1)} &= 2\pi\lambda^{(1)}B^{(1)}A^{(1)}\left(\frac{i_A}{2}\right)\\
i_B{}^{(2)} &= 2\pi\lambda^{(2)}B^{(2)}A^{(2)}\left(\frac{i_A}{2}\right)\\
i_B{}^{(3)} &= 2\pi\lambda^{(3)}B^{(3)}A^{(3)}\left(\frac{i_A}{2}\right)\\
i_C{}^{(1)} &= 2\pi\lambda^{(1)}C^{(1)}A^{(1)}\left(\frac{i_A}{2}\right)\\
i_C{}^{(2)} &= 2\pi\lambda^{(2)}C^{(2)}A^{(2)}\left(\frac{i_A}{2}\right)\\
i_C{}^{(3)} &= 2\pi\lambda^{(3)}C^{(3)}A^{(3)}\left(\frac{i_A}{2}\right)
\end{aligned}
\tag{5}
$$

Modal currents due to current only from the insulator string in phase B

Let $i_A = i_C = 0$

$$\begin{aligned}
i_A^{(1)} &= 2\pi\lambda^{(1)} A^{(1)} B^{(1)} \left(\frac{i_B}{2}\right) \\
i_A^{(2)} &= 2\pi\lambda^{(2)} A^{(2)} B^{(2)} \left(\frac{i_B}{2}\right) \\
i_A^{(3)} &= 2\pi\lambda^{(3)} A^{(3)} B^{(3)} \left(\frac{i_B}{2}\right) \\
i_B^{(1)} &= 2\pi\lambda^{(1)} \left(B^{(1)}\right)^2 \left(\frac{i_B}{2}\right) \\
i_B^{(2)} &= 2\pi\lambda^{(2)} \left(B^{(2)}\right)^2 \left(\frac{i_B}{2}\right) \\
i_B^{(3)} &= 2\pi\lambda^{(3)} \left(B^{(3)}\right)^2 \left(\frac{i_B}{2}\right) \\
i_C^{(1)} &= 2\pi\lambda^{(1)} C^{(1)} B^{(1)} \left(\frac{i_B}{2}\right) \\
i_C^{(2)} &= 2\pi\lambda^{(2)} C^{(2)} B^{(2)} \left(\frac{i_B}{2}\right) \\
i_C^{(3)} &= 2\pi\lambda^{(3)} C^{(3)} B^{(3)} \left(\frac{i_B}{2}\right)
\end{aligned} \tag{6}$$

Modal currents due to current only from the insulator string in phase C

Let $i_A = i_B = 0$

$$\begin{aligned}
i_A^{(1)} &= 2\pi \lambda^{(1)} A^{(1)} C^{(1)} \left(\frac{i_C}{2}\right) \\
i_A^{(2)} &= 2\pi \lambda^{(2)} A^{(2)} C^{(2)} \left(\frac{i_C}{2}\right) \\
i_A^{(3)} &= 2\pi \lambda^{(3)} A^{(3)} C^{(3)} \left(\frac{i_C}{2}\right) \\
i_B^{(1)} &= 2\pi \lambda^{(1)} B^{(1)} C^{(1)} \left(\frac{i_C}{2}\right) \\
i_B^{(2)} &= 2\pi \lambda^{(2)} B^{(2)} C^{(2)} \left(\frac{i_C}{2}\right) \\
i_B^{(3)} &= 2\pi \lambda^{(3)} B^{(3)} C^{(3)} \left(\frac{i_C}{2}\right) \\
i_C^{(1)} &= 2\pi \lambda^{(1)} \left(C^{(1)}\right)^2 \left(\frac{i_C}{2}\right) \\
i_C^{(2)} &= 2\pi \lambda^{(2)} \left(C^{(2)}\right)^2 \left(\frac{i_C}{2}\right) \\
i_C^{(3)} &= 2\pi \lambda^{(3)} \left(C^{(3)}\right)^2 \left(\frac{i_C}{2}\right)
\end{aligned} \tag{7}$$

The sets shown in equations (5), (6), and (7) are given to show that in phase N there are 3 components of modal current (n); each component a result of injected current from each of the 3 insulator strings. The components in each phase must be added in some manner. Since the three current generators in each phase which represent generation in the insulator strings can be considered uncorrelated, a spectral density argument can be used.

Thus from (5), (6), and (7)

$$\begin{aligned}
SD\left[i_A{}^{(1)}\right] &= \pi^2\left(\lambda^{(1)}\right)^2\left[\left(A^{(1)}\right)^4 SD\left[i_A\right] + \left(A^{(1)}B^{(1)}\right)^2 SD\left[i_B\right] + \left(A^{(1)}C^{(1)}\right)^2 SD\left[i_C\right]\right] \\
SD\left[i_B{}^{(1)}\right] &= \pi^2\left(\lambda^{(1)}\right)^2\left[\left(B^{(1)}A^{(1)}\right)^2 SD\left[i_A\right] + \left(B^{(1)}\right)^4 SD\left[i_B\right] + \left(B^{(1)}C^{(1)}\right)^2 SD\left[i_C\right]\right] \qquad (8) \\
SD\left[i_C{}^{(1)}\right] &= \pi^2\left(\lambda^{(1)}\right)^2\left[\left(C^{(1)}A^{(1)}\right)^2 SD\left[i_A\right] + \left(C^{(1)}B^{(1)}\right)^2 SD\left[i_B\right] + \left(C^{(1)}\right)^4 SD\left[i_C\right]\right]
\end{aligned}$$

Equation (8) in matrix form would be:

$$\begin{bmatrix} SD\left[i_A{}^{(1)}\right] \\ SD\left[i_B{}^{(1)}\right] \\ SD\left[i_C{}^{(1)}\right] \end{bmatrix} = \pi^2\left(\lambda^{(1)}\right)^2 \begin{bmatrix} \left(A^{(1)}\right)^4 & \left(A^{(1)}B^{(1)}\right)^2 & \left(A^{(1)}C^{(1)}\right)^2 \\ \left(B^{(1)}A^{(1)}\right)^2 & \left(B^{(1)}\right)^4 & \left(B^{(1)}C^{(1)}\right)^2 \\ \left(C^{(1)}A^{(1)}\right)^2 & \left(C^{(1)}B^{(1)}\right)^2 & \left(C^{(1)}\right)^4 \end{bmatrix} \bullet \begin{bmatrix} SD\left[i_A\right] \\ SD\left[i_B\right] \\ SD\left[i_C\right] \end{bmatrix} \qquad (9)$$

Matrices for modes 2 and 3 are the same as (9), except for a change in mode designation.

At this point it is seen that the insulator noise currents are divided by (9) into modal currents on a spectral density basis. Now the original set of eigen vectors were signed quantities and, as can be seen by equation (9), the spectral density argument eliminates information as to the relation, positive or negative, of the current quantities in a particular mode. This is a normal consequence of using the spectral density argument; however, it is recognized that a portion of the current in phase A is correlatable to portions of current in phases B and C for a particular mode. This can be seen from equations (5), (6), or (7).

It is interesting to note that while the spectral density argument eliminates the signed relationship of the modal quantities, the |ratio| of the intermodal currents remains the same. As an example, from equation set (8):

$$\frac{SD\left[i_A{}^{(1)}\right]}{SD\left[i_B{}^{(1)}\right]} = \frac{\pi^2\left(\lambda^{(1)}\right)^2\left[\left(A^{(1)}\right)^4 SD\left[i_A\right] + \left(A^{(1)}B^{(1)}\right)^2 SD\left[i_B\right] + \left(A^{(1)}C^{(1)}\right)^2 SD\left[i_C\right]\right]}{\pi^2\left(\lambda^{(1)}\right)^2\left[\left(B^{(1)}A^{(1)}\right)^2 SD\left[i_A\right] + \left(B^{(1)}\right)^4 SD\left[i_B\right] + \left(B^{(1)}C^{(1)}\right)^2 SD\left[i_C\right]\right]} \qquad (10)$$

$$\therefore \quad \frac{SD\left[i_A{}^{(1)}\right]}{SD\left[i_B{}^{(1)}\right]} = \left(\frac{A^{(1)}}{B^{(1)}}\right)^2$$

$$\therefore \left(\frac{SD\ i_A{}^{(1)}}{SD\ i_B{}^{(1)}}\right)^{1/2} = \left|\frac{A_1}{B_1}\right|$$

With the above in mind, it is intended in this discussion to continue using the spectral density argument for quantities within a modal system; however, the final summation of the electric fields for a particular mode as a result of charges on individual phase conductors will take into account signed modal ratios of the eigen vectors. This will be developed later.

The correlation argument for quantities in different modal systems is somewhat different. It is very probable that propagation velocity differences exist between the three modal systems which detracts from correlation considerations between modal systems. This analysis will therefore treat these as completely uncorrelated.

Going back to equations (8), it is recognized that from a measurements consideration that:

$$SD\left[i_A\right] = SD\left[i_B\right] = SD\left[i_C\right]$$

and from theory that:

$$\left(A^{(n)}\right)^2 + \left(B^{(n)}\right)^2 + \left(C^{(n)}\right)^2 = \frac{1}{2\pi\lambda^{(n)}}$$

Therefore

$$SD\left[i_A{}^{(1)}\right] = \frac{\pi}{2}\lambda^{(1)}\left(A^{(1)}\right)^2 SD\left[i_A\right]$$

$$SD\left[i_B{}^{(1)}\right] = \frac{\pi}{2}\lambda^{(1)}\left(B^{(1)}\right)^2 SD\left[i_A\right] \tag{11}$$

$$SD\left[i_C{}^{(1)}\right] = \frac{\pi}{2}\lambda^{(1)}\left(C^{(1)}\right)^2 SD\left[i_A\right]$$

Equations for modes 2 and 3 are the same as (11), except for a change in mode designation.

now $SD\left[i_A{}^{(1)}\right] = \dfrac{SD\left[v_A{}^{(1)}\right]}{Z^{(n)}{}^2}$ (12)

and for the modal system

$$Z^{(n)} = \frac{Z_0}{2\pi}\lambda^{(n)} \tag{13}$$

$$\therefore\ SD\left[v_A{}^{(1)}\right] = \left[\frac{Z_0}{2\pi}\lambda^{(1)}\right]^2 \frac{\pi}{2}\lambda^{(1)}\ A^{(1)}{}^2 SD\left[i_A\right] \tag{14}$$

simplifying (14) and for all phases,

$$\therefore\ SD\left[v_A{}^{(1)}\right] = \frac{Z_0{}^2}{8\pi}\left(\lambda^{(1)}\right)^3\left(A^{(1)}\right)^2 SD\left[i_A\right]$$

$$SD\left[v_B{}^{(1)}\right] = \frac{Z_0{}^2}{8\pi}\left(\lambda^{(1)}\right)^3\left(B^{(1)}\right)^2 SD\left[i_A\right] \tag{15}$$

$$SD\left[v_C{}^{(1)}\right] = \frac{Z_0{}^2}{8\pi}\left(\lambda^{(1)}\right)^3\left(C^{(1)}\right)^2 SD\left[i_A\right]$$

and expressions similar to (15) are had for modes 2 and 3.

Up to this point, only a single set of three insulator strings has been considered. The effect of a large number of sets of strings to the right and to the left of an observer will be considered. Figure 3 shows an observer located at the center of a span receiving contributions of $SD\left[v_N^{(n)}\right]$ from sets of insulator strings to the right and to the left.

Therefore the total value of $SD\left[v_N^{(n)}\right]$ at the point of observation is:

$$SD\left[v_N^{(n)}\right]_{TOTAL} = 2 \bullet \frac{Z_0^{\,2}}{8\pi}\left(\lambda^{(n)}\right)^3\left(N^{(n)}\right)^2 SD\left[i_A\right] \bullet T \tag{16}$$

$$\text{where } T = \left[e^{-1(\frac{s}{2})2\alpha^{(n)}} + e^{-3(\frac{s}{2})2\alpha^{(n)}} --- e^{-(2m+1)s\alpha^{(n)}}\right]$$

$$\text{or } T = \sum_{m=0}^{\infty}\left(e^{-(2m+1)s\alpha^{(n)}}\right) \tag{17}$$

where $\alpha^{(n)}$ = modal attenuation$^{(4)}$ in nepers/foot

s = tower span in feet

The sum of the exponential series in equation (17) is:

$$T = \frac{1}{2\sinh\left(s\alpha^{(n)}\right)} \tag{18}$$

A range of the factor $\sinh(s\alpha^{(n)})$ found in practice allows the approximation

$$s\alpha^{(n)} \cong \sinh\left(s\alpha^{(n)}\right) \tag{19}$$

$$\therefore\; T = \frac{1}{2s\alpha^{(n)}} \tag{20}$$

Substituting (20) into (16) yields for the general case:

$$SD\left[v_N^{(n)}\right] = \frac{(Z_0)^2}{8\pi s\alpha^{(n)}} \left(\lambda^{(n)}\right)^3 \left(N^{(n)}\right)^2 SD\left[i_A\right] \tag{21}$$

Equation (21) will yield all line-to-ground components of the spectral density of voltage (nine in all) at the point of observation. The next step is to obtain the electric field intensities.

Restating the correlation argument, the mode n components in phases A, B, and C are expressed as spectral density quantities, whereas the modal argument implies signed values. As stated before, the elements of current in phase A for a particular mode at the point of observation are completely uncorrelated but each element has correlatable companions in phases B and C. It would thus appear reasonable to consider that normal mode correlation between phase conductors exists. Noncorrelation between different modes is still assumed.

To see how, for a single mode, electric field values are obtained, consider the example in Figure 4. Now, normally, if the electric field at ⓧ is desired, the following steps are made:

$$[v] = [A][Q] \tag{22}$$

where v = line voltage

A = potential coefficients

Q = lineal charge densities

$$\text{and } [Q] = [A]^{-1}[v] \tag{23}$$

Once the charge density for each phase conductor is known, then the contribution to $\vec{E}_x$ can be obtained and summed to get the total field.

Thus $$\overset{\geq}{E}_x = \frac{Q_A \; 2h_A}{2\pi\epsilon_0 \; (h_A^2 + (x-\ell_A)^2)} + \frac{Q_B \; 2h_B}{2\pi\epsilon_0 \; (h_B^2 + (x-\ell_B)^2)} + \frac{Q_C \; 2h_C}{2\pi\epsilon_0 \; (h_C^2 + (x-\ell_C)^2)} \qquad (24)$$

Now if v_A, v_B, and v_C are modal quantities then:

$$\overset{\geq}{E}_x{}^{(n)} = \frac{1}{\lambda^{(n)}}\left[\frac{v_A{}^{(n)} \; 2h_A}{h_A{}^2 + (x-\ell_A)^2} + \frac{v_B{}^{(n)} \; 2h_B}{h_B{}^2 + (x-\ell_B)^2} + \frac{v_C{}^{(n)} \; 2h_C}{h_C{}^2 + (x-\ell_C)^2}\right] \qquad (25)$$

Now if $v_A{}^{(n)}$ is known,

then $$v_B{}^{(n)} = v_A{}^{(n)} \frac{B^{(n)}}{A^{(n)}}$$

$$(26)$$

and $$v_C{}^{(n)} = v_A{}^{(n)} \frac{C^{(n)}}{A^{(n)}}$$

substituting (26) into (25) and rearranging

$$\overset{\geq}{E}_x{}^{(n)} = \frac{v_A{}^{(n)}}{A^{(n)}\lambda^{(n)}}\left[\frac{A^{(n)} \; 2h_A}{(h_A{}^2 + (x-\ell_A)^2)} + \frac{B^{(n)} \; 2h_B}{(h_B{}^2 + (x-\ell_B)^2)} + \frac{C^{(n)} \; 2h_C}{(h_C{}^2 + (x-\ell_C)^2)}\right] \qquad (27)$$

Thus for a pure modal system, only the modal voltage on phase A is required to determine the total field produced by single mode charges on all three conductors.

Now equation (27) on a spectral density basis would be

$$SD\left[E_x{}^{(n)}\right] = \frac{SD\left[v_A{}^{(n)}\right]}{(A^{(n)})^2 \, (\lambda^{(n)})^2} \, (\gamma_x{}^{(n)})^2$$

$$(28)$$

where $$\gamma_x{}^{(n)} = \left[\frac{A^{(n)} \; 2h_A}{(h_A{}^2 + (x-\ell_A)^2)} + \frac{B^{(n)} \; 2h_B}{(h_B{}^2 + (x-\ell_B)^2)} + \frac{C^{(n)} \; 2h_C}{(h_C{}^2 + (x-\ell_C)^2)}\right]$$

It is now seen that using the field factor $\gamma_x^{(n)}$ as defined above introduces the needed degree of correlation between modal quantities for the same mode on different phases.

Now from equation (21)

$$SD\left[v_A^{(n)}\right] = \frac{(Z_0)^2 (\lambda^{(n)})^3 (A^{(n)})^2 SD\left[i_A\right]}{8\pi s \alpha^{(n)}} \qquad (29)$$

Substituting (29) into (28) yields

$$SD\left[E_x^{(n)}\right] = \frac{(Z_0)^2 \lambda^{(n)} (\gamma_x^{(n)})^2 SD\left[i_A\right]}{8\pi s \alpha^{(n)}} \qquad (30)$$

Since the modal systems are assumed to be uncorrelated, the sum of the modal fields at point x is:

$$SD\left[E_x\right]_{TOTAL} = SD\left[E_x^{(1)}\right] + SD\left[E_x^{(2)}\right] + SD\left[E_x^{(3)}\right] \qquad (31)$$

and from (30)

$$SD\left[E_x\right]_{TOTAL} = \frac{(Z_0)^2 SD\left[i_A\right]}{8\pi} \left[\frac{\lambda^{(1)} (\gamma_x^{(1)})^2}{s\alpha^{(1)}} + \frac{\lambda^{(2)} (\gamma_x^{(2)})^2}{s\alpha^{(2)}} + \frac{\lambda^{(3)} (\gamma_x^{(3)})^2}{s\alpha^{(3)}} \right] \qquad (32)$$

assume now that, similar to ϕ_1 in equation (1),

ϕ_2 exists such that:

$$\left[RI_{(STOD.)}\right]^2 = \phi_2^{\,2} \Delta f SD\left[E_x\right]_{TOTAL} \qquad (33)$$

Substituting (32) into (33) and taking the square root yields:

$$RI_{(STOD.)} = \frac{Z_0 \phi_2 (\Delta f)^{1/2}}{\sqrt{8\pi}} (SD[i_A])^{1/2} \left[\frac{\lambda^{(1)} (\gamma_x^{(1)})^2}{s\alpha^{(1)}} + \frac{\lambda^{(2)} (\gamma_x^{(2)})^2}{s\alpha^{(2)}} + \frac{\lambda^{(3)} (\gamma_x^{(3)})^2}{s\alpha^{(3)}} \right]^{1/2} \qquad (34)$$

From (1)

$$(SD[i_A])^{1/2} = \frac{RIV_{(STOD.)}}{\phi_1 Z_T (\Delta f)^{1/2}} \qquad (35)$$

Substituting (35) into (34) yields:

$$RI_{(STOD.)} = RIV_{(STOD.)} \frac{1}{2\sqrt{2\pi}} \left(\frac{\phi_2}{\phi_1}\right) \left(\frac{Z_0}{Z_T}\right) \left[\frac{\lambda^{(1)} (\gamma_x^{(1)})^2}{s\alpha^{(1)}} + \frac{\lambda^{(2)} (\gamma_x^{(2)})^2}{s\alpha^{(2)}} + \frac{\lambda^{(3)} (\gamma_x^{(3)})^2}{s\alpha^{(3)}} \right]^{1/2} \qquad (36)$$

Equation (36) relates the RI field at any lateral point x to a value of RIV measured on a single insulator string in the laboratory at operating line-to-ground voltage. Eigen roots ($\lambda^{(n)}$), field factors ($\gamma_x^{(n)}$), and attenuation values ($\alpha^{(n)}$) are obtainable from the General Electric Radio Noise Program.

Table II illustrates typical values of $\frac{RI_{(STOD.)}}{RIV_{(STOD.)}}$ for 345-, 500-, and 700-kv transmission lines. It is assumed that:

$s = 1200$ feet

$\phi_2 = \phi_1$

$Z_T = 150$ ohms

with $Z_0 = 377$ ohms

TABLE II

Computer Case	Nominal Line Voltage (KV)	Cond. Per Bundle	Cond. Dia. (In.)	Cond. Ht. (Ft.)	Phase Spacing (Ft.)	RI/RIV (Meters^{-1}) Distance From Ctr. of R/W		
						100 Ft.	150 Ft.	200 Ft.
NP01	345	1	1.750	41	28	3.14×10^{-2}	1.17×10^{-2}	0.585×10^{-2}
PG01	500	2	1.600	39	42	3.61×10^{-2}	1.28×10^{-2}	0.626×10^{-2}
HQ-20	700	4	1.382	59	56	5.85×10^{-2}	2.41×10^{-2}	1.14×10^{-2}

As an example of the use of the above table, assume that an extra-high-voltage line is had corresponding to case PG01 (500 KV). Assume that a laboratory NEMA RIV test on a representative single insulator string with normal line-end hardware resulted in a measured RIV value of 2,000 μv at a test voltage of $500/\sqrt{3} = 288$ KV.

The radio noise level from this 500 KV line at 150 feet from the center of the right-of-way resulting from insulator noise alone would be:

$$RI = (1.28 \times 10^{-2} \text{ meters}^{-1})(2{,}000\ \mu v)$$

$$\therefore RI = 25.6\ \mu v/\text{meter}$$

The above computation shows that a fairly high laboratory RIV test voltage of 2,000 μvolts gives rise to a fairly small RI value of 25.6 μv/meter at 150 feet from the center of the right-of-way. With a phase spacing of 42 feet and a conductor height of 59 feet, this would be 115 feet from the nearest conductor.

James J. LaForest
J. J. LaForest
Development Engineer - Corona and Radio Noise
Project EHV
POWER SYSTEMS ENGINEERING OPERATION
December 23, 1963

ed

REFERENCES

1. The Calculation of the Radio Interference Level of Transmission Lines, G. E. Adams. AIEE Transactions, vol. 75, pt. III, 1956, pp. 411-19.

2. Radio Interference From High Voltage Transmission Lines as Influenced by the Line Design, G. E. Adams. AIEE Transactions, vol. 77, pt. III, 1958, pp. 54-63.

3. Radio-Frequency Propagation and Attenuation on the American Electric Power Dequine-Olive 345-KV Line, L. O. Barthold, J. J. LaForest, R. H. Schloman, F. J. Trebby. AIEE Transactions, vol. 79, pt. III, 1960, pp. 303-09.

4. The Calculation of Attenuation Constants for Radio Noise Analysis of Overhead Lines, G. E. Adams, L. O. Barthold. AIEE Transactions, vol. 79, pt. III, 1960, pp. 975-81.

5. Digital Calculation of Radio Noise Levels, A. K. Abboushi, L. O. Barthold. AIEE Transactions, vol. 80, pt. III, pp. 841-47.

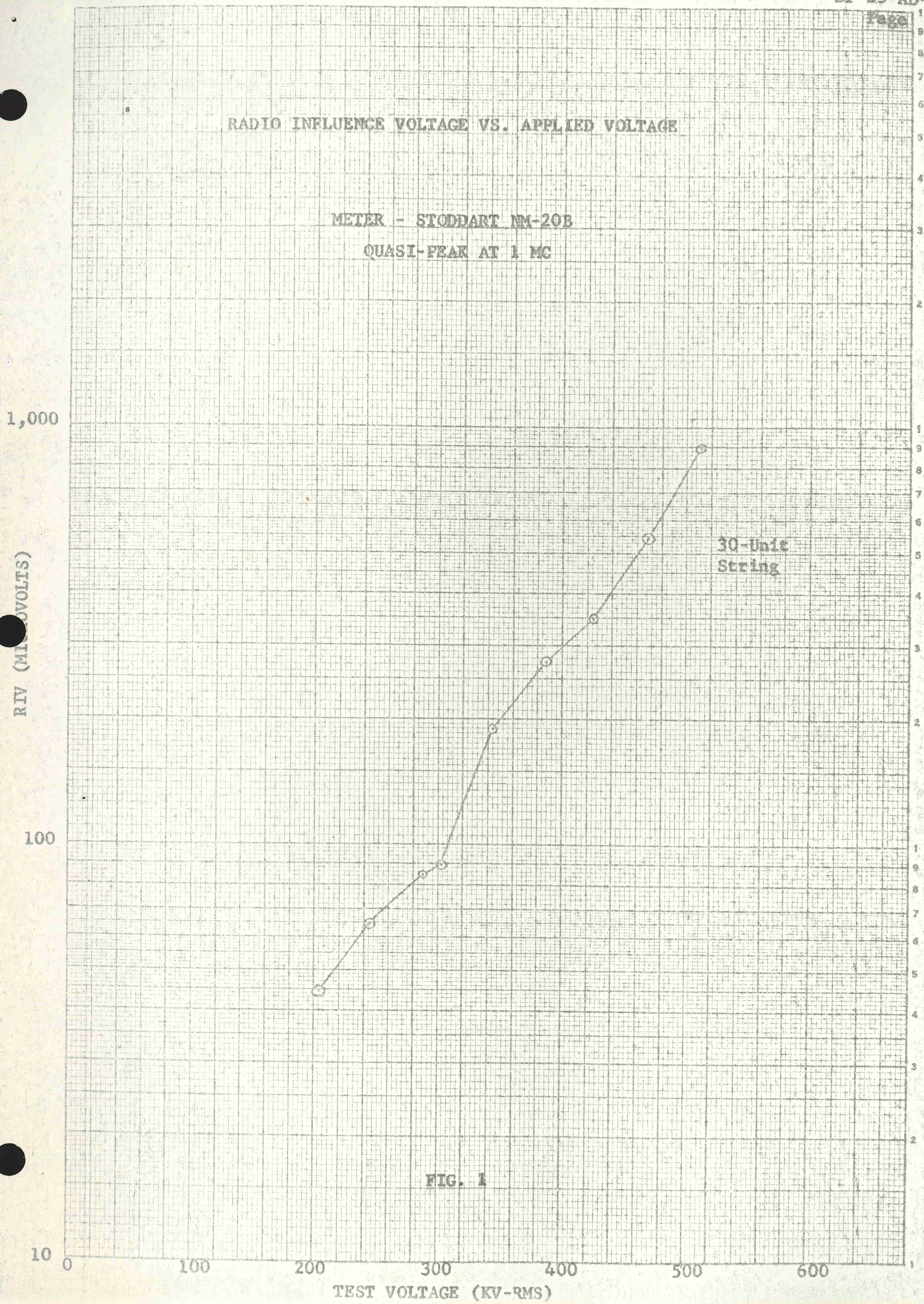

RADIO INFLUENCE VOLTAGE VS. APPLIED VOLTAGE

METER - STODDART NM-20B
QUASI-PEAK AT 1 MC

FIG. 1

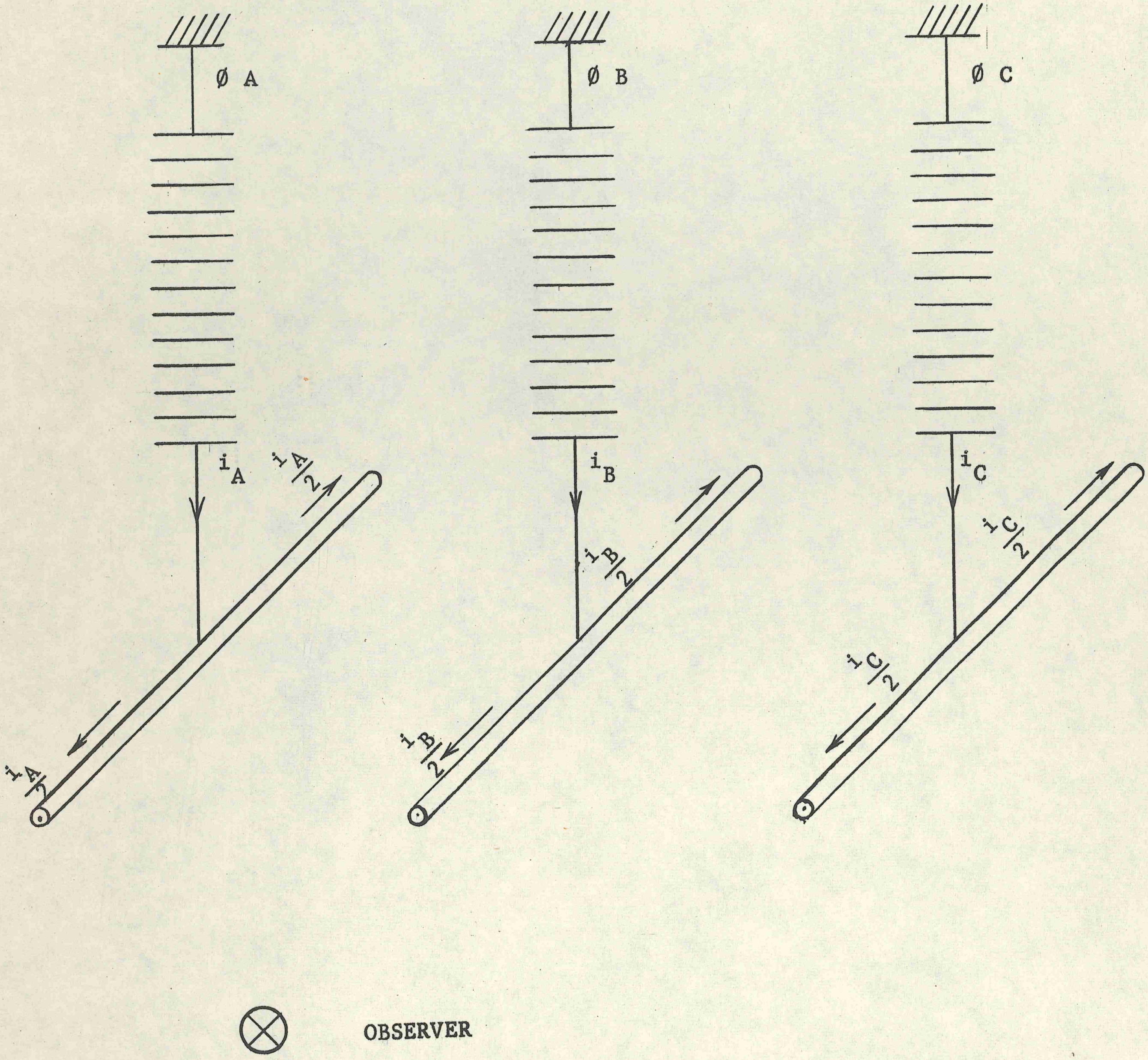
Ø A
Ø B
Ø C
i_A
i_B
i_C
$i_A/2$
$i_B/2$
$i_C/2$
OBSERVER

FIG. 2

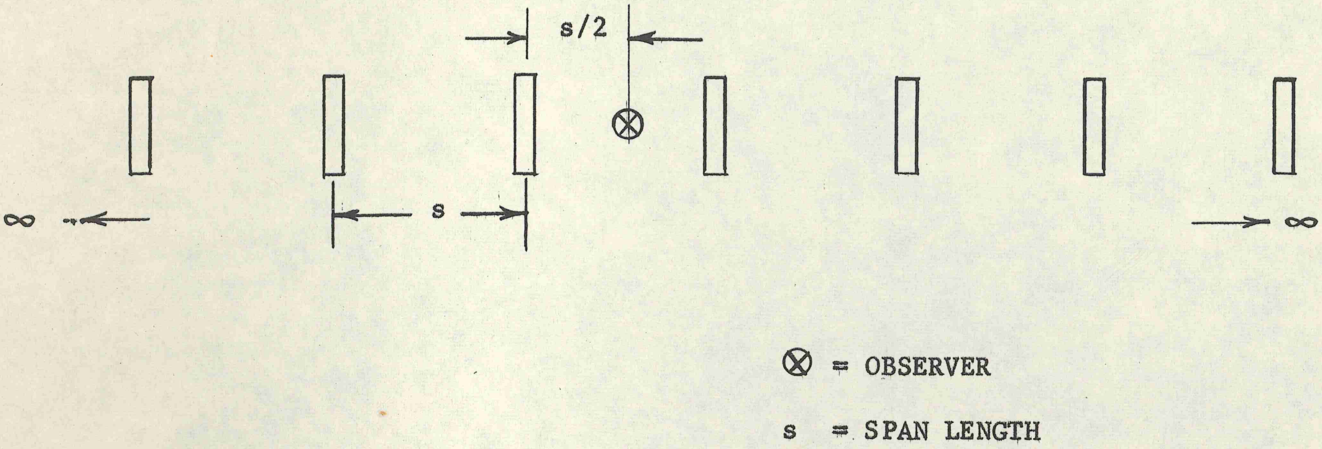
s/2
s
∞
∞
⊗ = OBSERVER
s = SPAN LENGTH

FIG. 3

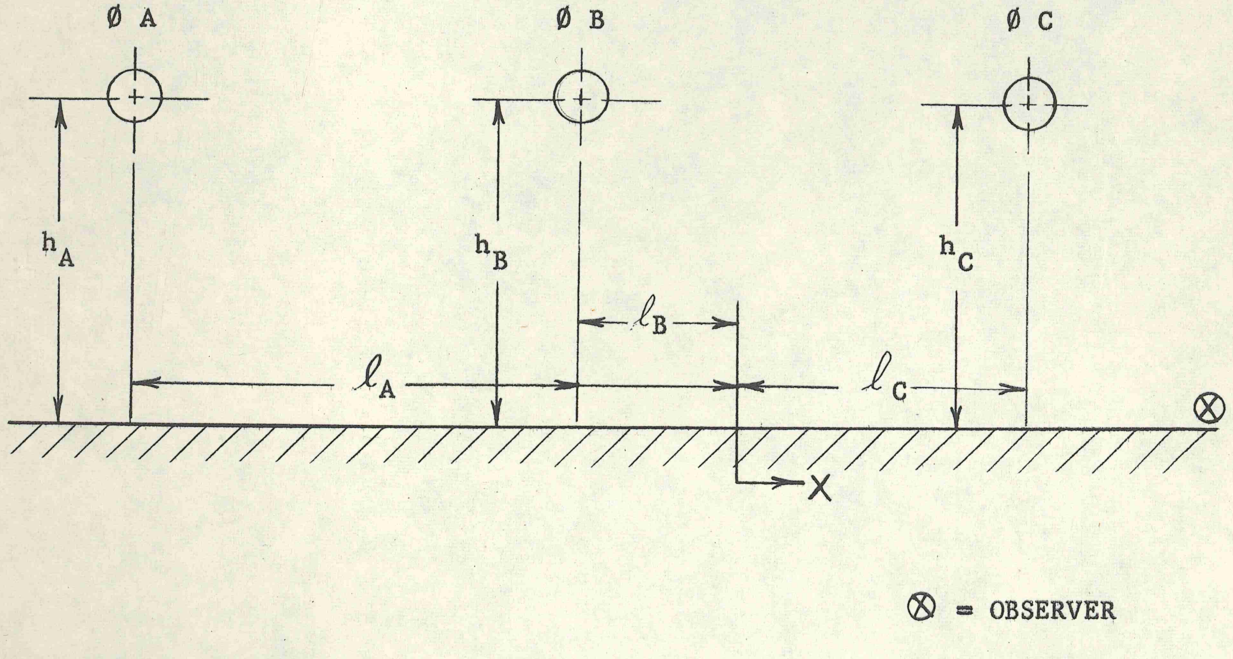
Ø A
Ø B
Ø C
h_A
h_B
h_C
ℓ_A
ℓ_B
ℓ_C
X
⊗ = OBSERVER

FIG. 4

Mr Joseph Kaminski, Jr
Insulator Dept.
Baltimore

Transactions Paper

(Reviewed and Accepted for Publication)

Discussion in Duplicate Due February 19, 1965.

THE EFFECT OF STATION RADIO NOISE SOURCES ON TRANSMISSION LINE NOISE LEVELS

J. J. LaForest
Senior Member IEEE
General Electric Company
Schenectady, N. Y.

RECEIVED
JAN - 6 1965
ENG. DEPT.

A paper recommended by the IEEE Transmission and Distribution Committee of the IEEE Power Group for presentation at the IEEE Winter Power Meeting, New York, N. Y., January 31-February 5, 1965. Manuscript submitted November 2, 1964; made available for printing December 8, 1964.

Price: $1.00
(75¢ at meeting)

(15¢ per copy additional if first class mailing desired)

(25¢ per copy additional if air mail is desired)

All Rights Reserved by

The Institute of Electrical and Electronics Engineers, Inc.
345 East 47th Street
New York, N. Y. 10017

Litho in USA

Paper No.

31 TP 65-134

THE EFFECT OF STATION RADIO NOISE SOURCES ON TRANSMISSION LINE NOISE LEVELS

J. J. LaForest,* Senior Member IEEE

INTRODUCTION

During the past 15 years, much attention has been given to the determination of transmission-line radio-noise (RI) levels resulting from conductor corona. Excellent results have been obtained using a theoretical approach based on radio-noise power analysis and modal propagation arguments.[1,2,3,4] It is now appropriate to examine the effect of bus-and-station-equipment corona on transmission-line radio-noise levels. Many of the arguments and techniques used in describing the effects of conductor corona on RI levels can be used directly for the case of corona generated in a station. Examination of the question of whether or not station noise is important to line noise levels is particularly timely now because of the large amount of ehv station apparatus being designed and built, and the interest in uprating stations to higher voltage levels than those for which they were designed. Situations where the radio-noise performance of equipment is used as a quality-control index are not considered in this discussion.

This paper will first describe a procedure for calculating line RI levels where the corona effects originate from station equipment and then apply this procedure to two cases with comments on the results thereof.

ANALYSIS AND DISCUSSION

Station Considerations

The initial analysis considers a single noise source on one phase of a typical three-phase station-and-line arrangement. Later, procedures for combining multiple sources, either on the same phase or on all phases, will be discussed. Figure 1 shows a block diagram of the station-and-line impedances with radio-noise generation from a piece of equipment being represented as a constant-current noise generator. The noise current, represented as a spectral-density function,[1] divides into a portion entering the line and a portion entering the station.

Evaluation of Noise Current From an Item of Station Apparatus

The total noise current from an item of energized equipment is determined by means of a single-phase laboratory test. The 60-cycle test-voltage and facility arrangement should be such that the electric field conditions found in the energized 3-phase station for the equipment in question are essentially duplicated in the laboratory test.

The value of the noise current on a spectral-density basis can be determined by using a radio-noise meter with a root-mean-square (rms) detector. Since this type of instrument is not in widespread use, the total noise current will be evaluated by a standard NEMA[5] Radio Influence Voltage (RIV) laboratory test on the equipment in question, using the standard quasi-peak instrument. This evaluation assumes that a ratio k_1 exists, which can be found by measurement, that will relate a quasi-peak noise-meter reading obtained from a NEMA test to one that would be obtained with an rms meter having the same bandwidth. The same problem of relating rms to quasi-peak values will also be encountered at the end of this analysis since quasi-peak instruments are commonly used both for RIV and RI field measurements. At that point in the analysis, a constant k_2 will be introduced which enables the results to be given on a quasi-peak basis and the two constants k_1 and k_2 will be assumed to be the same.

---

*General Electric Company, Pittsfield, Massachusetts.

The spectral density of the total noise current entering phase A, in Fig. 1, will be:

$$SD\left[i_t\right] = \frac{(RIV)^2}{k_1^{\,2}\, Z_{tc}^{\,2}\, \Delta f} \tag{1}$$

The impedance of the laboratory-test circuit, Z_{tc} would normally be equal to 150 ohms. Nomenclature is given after Appendix I.

Modal Current Distribution

A value of the spectral density of the noise current feeding into one phase of the 3-phase line has been determined. The next step in the analysis is to take this current and apportion it into the three natural propagation modes of the 3-phase (conductor) system, there being n modes for an n conductor system. The procedure for doing this has been outlined in a previous paper.[6] The details of this apportionment are given in Appendix I. The following developments are also included in Appendix I:

1. Determination of modal conductor voltages at the station.
2. Finding these voltages at a desired point of observation down the line.
3. At this longitudinal point of observation, determining the resultant electric field at a desired lateral point from the line, point X in Fig. 2.

Correlation Considerations

An important consideration of the analysis in Appendix I and other developments in this paper is the question of correlation between noise voltages, or currents, within modes, from different modes, and from different sources of generation. Generally, correlation between voltages implies that a knowable phase-relation exists between them. Noncorrelation would imply that the phase-relation is not knowable and this situation would arise when comparing voltages from two or more different sources of noise. Noncorrelation also arises in some degree when comparing voltages from different modes after propagation down a line has taken place. These correlation considerations have been discussed in a previous paper.[7] The analysis in this paper will assume the following:

1. Correlation within a mode exists for a single-source problem.
2. Correlation is lost between modes as pulses travel away from the station.
3. Noise voltages or currents from different sources are uncorrelated.

Radio Noise Level

From Appendix I, the following equation applies to the modal electric field at a point s down the line from the station and a lateral point x from the line:

$$SD\left[E_x^{(n)}\right] = \frac{\epsilon^{-2s\alpha^{(n)}}\left(\left|\zeta^{(n)}\right|\right)^2\left(\gamma_x^{(n)}\right)^2 SD\left[i_t\right]}{\left(N_a^{(n)}\right)^2\left(\lambda^{(n)}\right)^2} \qquad (2)$$

With noncorrelation between modes, the total electric field at point x (location of observer) would be

$$SD\left[E_x\right] = \sum_{n=1}^{3} SD\left[E_x^{(n)}\right] \qquad (3)$$

Assume, as discussed previously, that k_2 exists such that

$$(RI)^2 = k_2^2\,\Delta f\,SD\left[E_x\right] \qquad (4)$$

and also that $k_1 = k_2$ (5)

Combining equations 1, 2, 3, 4, and 5, and taking the square root yields the following for the 3-conductor case:

$$RI = (RIV)\left(\frac{1}{Z_{tc}}\right)\left(\frac{\epsilon^{-2s\alpha^{(1)}}\left(\left|\zeta^{(1)}\right|\right)^2\left(\gamma_x^{(1)}\right)^2}{\left(N_a^{(1)}\right)^2\left(\lambda^{(1)}\right)^2} + \frac{\epsilon^{-2s\alpha^{(2)}}\left(\left|\zeta^{(2)}\right|\right)^2\left(\gamma_x^{(2)}\right)^2}{\left(N_a^{(2)}\right)^2\left(\lambda^{(2)}\right)^2} + \frac{\epsilon^{-2s\alpha^{(3)}}\left(\left|\zeta^{(3)}\right|\right)^2\left(\gamma_x^{(3)}\right)^2}{\left(N_a^{(3)}\right)^2\left(\lambda^{(3)}\right)^2}\right)^{1/2} \qquad (6)$$

With equation 6 and line and station constants, the RI value at a distance x laterally from the line and a distance S from the station can be found if the RIV test value of the equipment is known.

Multiple Sources

The preceding analysis was made on the basis of a single source of corona. The addition of other sources, either on the same phase or on other phases, is made on an uncorrelated basis and, thus, their contributions to the total electric field at the point of observation are calculated separately and simply added as in equation 3. This would imply, for example, that two identical sources, both on the same outside phase, or one on each outside phase, would give a resultant RI field which would be 3 decibels (db) higher than the case of one source on one of the outside phases.

Illustrative Examples

A. One Source on One Outside Phase.

As an illustration of the use of equation 6, consider the following data for a horizontal, single conductor per phase, 3-phase, long line and station. For this example, the coupling between phases in the station was assumed to be negligible and wave traps were not present.

f = 1 megacycle

Z_{tc} = 150 ohms

$$\boxed{Z_s} = \boxed{\begin{matrix} -j79.6 & 0 & 0 \\ 0 & -j79.6 & 0 \\ 0 & 0 & -j79.6 \end{matrix}} \text{ ohms}$$

h = 46 feet

x = 139 feet from line center

r = 1.25 inches

s = 0.1 miles to 7 miles

phase spacing = 39 feet

and from the Project EHV computer program

$$\boxed{N} = \begin{array}{ccc} (1) & (2) & (3) \\ \hline +.458 & +.707 & +.538 \\ -.763 & 0 & +.647 \\ +.458 & +.707 & +.538 \end{array}$$

and

$\alpha^{(1)}$ = .03025 nepers/mile

$\alpha^{(2)}$ = .1642 nepers/mile

$\alpha^{(3)}$ = .735 nepers/mile

and

$$\left.\begin{aligned}\lambda^{(1)}&=5.653\\ \lambda^{(2)}&=6.348\\ \lambda^{(3)}&=8.350\end{aligned}\right\}\quad \text{Modes are numbered in order of increasing eigenroot.}$$

All of the above data was combined with the development in Appendix I and equation 6 to yield the lower curve in Fig. 3, which gives the ratio of RI/RIV for distances along the line up to 7 miles. As an example of the use of this curve, assume that the corona-producing device on an outside phase in the station has an RIV test voltage of 2,000 microvolts (μv). The RI level at a distance of 1 mile from the station and at the 139-foot lateral point as a result of the station generation on the outside phase would be

From Fig. 3 (lower curve)

$$\text{RI/RIV} = 1.2 \times 10^{-3} \text{ meters}^{-1} \tag{7}$$

therefore

$$\text{RI} = (1.2 \times 10^{-3})(2000) = 2.4\ \mu\text{v/meter} \tag{8}$$

B. One Source on Each of Three Phases.

For this example, it was assumed that in the station three identical sources exist (one on each phase) with the same line data as for Example A. The calculation procedure here is to compute the value of $\text{SD}\left[E_x^{(n)}\right]$, n = 1, 2, and 3, for a noise generator on the center phase only. These values are added with twice those obtained from Example A, since the two outside phases are symmetrical. The procedure for calculating the RI/RIV ratio would then be the same as outlined in equations 1 through 6. The results of this calculation are given in the upper curve in Fig. 3.

It is interesting to note the per cent distribution of $\text{SD}\left[E_x^{(n)}\right]$ with respect to the total value as distance from the station is increased. This is plotted in Fig. 4, for Example B. These curves show that the line-to-ground mode predominates at the start for about one mile and declines rapidly. Mode 2 reaches a maximum at $s \approx 3$ miles and then declines. Mode 1 rises almost linearly, initially, and eventually predominates because of its low attenuation rate. These distribution curves are, of course, dependent on the lateral distance from the center of the line.

The illustrative examples given yield answers for the specific cases only. They are not intended as generalizations, but are intended to illustrate the calculation procedure. These results would be modified by changes in modal attenuation values, line geometry, station impedances (self and mutual), and other quantities treated in the analysis.

CONCLUSIONS

1. A method has been presented for calculating the effect of single or multiple sources of station radio-noise on the transmission-line noise level.
2. Two illustrative examples are given; to show the results of noise on one phase only, and on all three phases in a station.
3. For the example shown, the influence of mode 3 (line-to-ground) predominates close to the station, while at distances greater than approximately 1 mile the line-to-line modes predominate for the 139-foot lateral point.

4. The techniques presented are applicable to calculate the effects on transmission-line RI levels of corona from line hardware, regularly or irregularly spaced along the line.

APPENDIX I

Phase Voltages

As seen in Fig. 1, noise current is injected into one phase, and the resultant phase voltages are obtained from the following development. A phasor voltage and current argument is used since correlation is present.

$$\boxed{I_t} = \boxed{I_L} + \boxed{I_s} \tag{9}$$

and

$$\boxed{I_L} = \boxed{Z_L}^{-1}\boxed{V} \tag{10}$$

and

$$\boxed{I_s} = \boxed{Z_s}^{-1}\boxed{V} \tag{11}$$

therefore

$$\boxed{I_t} = \boxed{\boxed{Z_L}^{-1} + \boxed{Z_s}^{-1}}\,\boxed{V} \tag{12}$$

and

$$\boxed{V} = \boxed{\boxed{Z_L}^{-1} + \boxed{Z_s}^{-1}}^{-1}\boxed{I_t} \tag{13}$$

The elements of the line-impedance matrix $\boxed{Z_L}$ are

$$Z_{ii} = 60\,\ell n\left(\frac{2h}{r}\right)\quad i = 1, 2, 3 \tag{14}$$

$$Z_{ij} = 60\,\ell n\left(\frac{R_{ij}'}{R_{ij}}\right)\quad \begin{aligned} i &= 1, 2, 3\\ j &= 1, 2, 3\\ i &\neq j\end{aligned} \tag{15}$$

The elements of the station-impedance matrix $\boxed{Z_s}$ will, in general, contain both self and mutual terms.

The voltage and current matrices in equation 14, written out, would be

$$\boxed{V} = \begin{bmatrix} v_a \\ v_b \\ v_c \end{bmatrix} \tag{16}$$

$$\boxed{I_t} = \begin{bmatrix} i_t \\ 0 \\ 0 \end{bmatrix} \tag{17}$$

As indicated in the section on Multiple Sources, the analysis for sources on all three phases will always be carried out on a one-source-at-a-time basis; hence, the current column matrix will contain only one nonzero element.

Modal Voltages

The next step in the analysis is to transform the phase voltages into modal-phase voltages. The phasor argument is continued since correlation is present. It has been shown[6] that a transformation matrix $\boxed{M}$ exists such that modal voltages and phase voltages are related as follows:

$$\boxed{V^{(n)}} = \boxed{M}\,\boxed{V} \tag{18}$$

let us now define an $\boxed{N}$ matrix such that

$$\boxed{N} = \boxed{M}^{-1} \tag{19}$$

and therefore

$$\boxed{V} = \boxed{N}\,\boxed{V^{(n)}} \tag{20}$$

equation 20, written out, would be

$$\begin{bmatrix} v_a \\ v_b \\ v_c \end{bmatrix} = \begin{bmatrix} N_a^{(1)} & N_a^{(2)} & N_a^{(3)} \\ N_b^{(1)} & N_b^{(2)} & N_b^{(3)} \\ N_c^{(1)} & N_c^{(2)} & N_c^{(3)} \end{bmatrix} \begin{bmatrix} v_a^{(1)} \\ v_a^{(2)} \\ v_a^{(3)} \end{bmatrix} \tag{21}$$

The elements of the $\boxed{N}$ matrix are derived from an eigenvector analysis of the conductor system. Three properties of the set of $\boxed{N}$ matrix elements are

$$N_a^{(n)} = \Delta^{(n)} \frac{v_a^{(n)}}{v_c^{(n)}}$$

$$N_b^{(n)} = \Delta^{(n)} \frac{v_b^{(n)}}{v_c^{(n)}}$$

$$N_c^{(n)} = \Delta^{(n)} \tag{22}$$

and

$$1 = \left(N_a^{(n)}\right)^2 + \left(N_b^{(n)}\right)^2 + \left(N_c^{(n)}\right)^2 \tag{23}$$

and

$$\boxed{N} = \boxed{M}' \tag{24}$$

Computer programs are available for computing the elements of the $\boxed{N}$ matrix for 1- or 2-circuit, 3-phase lines with a maximum of 2 ground wires and 4 conductors per bundle.

Matrix equation 18 can be transformed by means of equations 19, 21, and 24 to

$$\begin{bmatrix} v_a^{(1)} \\ v_a^{(2)} \\ v_a^{(3)} \end{bmatrix} = \begin{bmatrix} N_a^{(1)} & N_b^{(1)} & N_c^{(1)} \\ N_a^{(2)} & N_b^{(2)} & N_c^{(2)} \\ N_a^{(3)} & N_b^{(3)} & N_c^{(3)} \end{bmatrix} \begin{bmatrix} v_a \\ v_b \\ v_c \end{bmatrix} \tag{25}$$

It is convenient from a notational standpoint to summarize the results of the development shown in equations 9 through 25 for obtaining modal voltages from injected current as follows:

$$v_a^{(n)} = \zeta^{(n)} \, i_t \qquad (26)$$

where $\zeta^{(n)}$ is a transfer function obtainable from equations 9 through 25 and dependent on line geometry, station impedance, and the phase where noise current is injected.

At this point, the phasor-voltage argument presented in equation 26 is transformed to a spectral-density argument with

$$\mathrm{SD}\left[v_a^{(n)}\right] = \left(\left|\zeta^{(n)}\right|\right)^2 \mathrm{SD}\left[i_t\right] \qquad (27)$$

At a distance s from the station, and with regard to attenuation, the modal voltage on phase A would be

$$\mathrm{SD}\left[v_a^{(n)}\right]_s = \epsilon^{-2s\alpha^{(n)}} \left(\left|\zeta^{(n)}\right|\right)^2 \mathrm{SD}\left[i_t\right] \qquad (28)$$

Electric Field Intensities

To see how, for a single mode, electric field values are obtained, consider Fig. 2. Now, if the electric field at point x is desired, the following steps are made

$$\boxed{V} = \boxed{A}\,\boxed{Q} \qquad (29)$$

and

$$\boxed{Q} = \boxed{A}^{-1}\,\boxed{V} \qquad (30)$$

Once the lineal charge density for each phase conductor is known, the contributions to E_x can be obtained and summed to get the total field

$$E_x = \frac{Q_a \, 2h_a}{2\pi\epsilon_o\left(h_a^2 + (x-\ell_a)^2\right)} + \frac{Q_b \, 2h_b}{2\pi\epsilon_o\left(h_b^2 + (x-\ell_b)^2\right)} + \frac{Q_c \, 2h_c}{2\pi\epsilon_o\left(h_c^2 + (x-\ell_c)^2\right)} \qquad (31)$$

Now, if v_a, v_b, and v_c are modal quantities, then

$$E_x^{(n)} = \frac{1}{\lambda^{(n)}}\left[\frac{v_a^{(n)} \, 2h_a}{h_a^2 + (x-\ell_a)^2} + \frac{v_b^{(n)} \, 2h_b}{h_b^2 + (x-\ell_b)^2} + \frac{v_c^{(n)} \, 2h_c}{h_c^2 + (x-\ell_c)^2}\right] \qquad (32)$$

and if $v_a^{(n)}$ is known

then $v_b^{(n)} = v_a^{(n)}\left(\frac{N_b^{(n)}}{N_a^{(n)}}\right)$ and $v_c^{(n)} = v_a^{(n)}\left(\frac{N_c^{(n)}}{N_a^{(n)}}\right)$ (33)

substituting 33 into 32, and rearranging

$$E_x^{(n)} = \frac{v_a^{(n)}}{N_a^{(n)}\lambda^{(n)}}\left[\frac{N_a^{(n)} \, 2h_a}{h_a^2 + (x-\ell_a)^2} + \frac{N_b^{(n)} \, 2h_b}{h_b^2 + (x-\ell_b)^2} + \frac{N_c^{(n)} \, 2h_c}{h_c^2 + (x-\ell_c)^2}\right] \qquad (34)$$

Thus, for a pure modal system, only the modal voltage on one phase is required to determine the total field produced by single-mode charges on all three conductors.

Equation 34 on a spectral-density basis would be

$$SD\left[E_x^{(n)}\right] = \frac{SD\left[v_a^{(n)}\right]\left(\gamma_x^{(n)}\right)^2}{\left(N_a^{(n)}\right)^2\left(\lambda^{(n)}\right)^2} \qquad (35)$$

where $\gamma_x^{(n)} = \left[\frac{N_a^{(n)}\,2h_a}{h_a^2 + (x-\ell_a)^2} + \frac{N_b^{(n)}\,2h_b}{h_b^2 + (x-\ell_b)^2} + \frac{N_c^{(n)}\,2h_c}{h_c^2 + (x-\ell_c)^2}\right]$

substituting equation 28 into 35 yields

$$SD\left[E_x^{(n)}\right] = \frac{e^{-2s\alpha^{(n)}}\left(\left|\zeta^{(n)}\right|\right)^2\left(\gamma_x^{(n)}\right)^2 SD\left[i_t\right]}{\left(N_a^{(n)}\right)^2\left(\lambda^{(n)}\right)^2} \qquad (36)$$

NOMENCLATURE

SD [ ] = spectral density of

k = empirical constant

Z_{tc} = laboratory-test circuit impedance

$\boxed{I}$ = phase-current matrix

$\boxed{Z}$ = impedance matrix

$\boxed{V}$ = phase-voltage matrix

$\boxed{V^{(n)}}$ = modal-voltage matrix

f = frequency

Δf = bandwidth

(n) = modal-number superscript

s = longitudinal distance from station to point of observation

x = lateral distance to point of observation

h = conductor height

R_{ij} = distance between conductor i and j

$R_{ij'}$ = distance between actual conductor i and image conductor j

r = conductor radius

ℓ = horizontal distance to axis

v = phasor voltage

i = phasor current

E = electric-field intensity

$\boxed{M}$ = modal-transformation matrix

$\boxed{N}$ = inverse of $\boxed{M}$

$\alpha^{(n)}$ = attenuation constant for mode n

$\gamma_x^{(n)}$ = normalized-field factor at point x for mode n

$\lambda^{(n)}$ = eigenroot for mode n

A = potential coefficient

Q = lineal-charge density

$\Delta^{(n)}$ = modal-normalizing constant

$\zeta^{(n)}$ = transfer function

REFERENCES

1. The Calculation of the Radio Interference Level of Transmission Lines Caused by Corona Discharges, G. E. Adams. AIEE Transactions, pt. III (Power Apparatus and Systems), vol. 75, June 1956, pp. 411-19.

2. Wave Propagation Along Unbalanced High-Voltage Transmission Lines, G. E. Adams. Ibid., pt. III-A, vol. 78, August 1959, pp. 639-47.

3. Radio-Frequency Propagation and Attenuation on the American Electric Power Dequine-Olive 345-Kv Line, L. O. Barthold, J. J. LaForest, R. H. Schlomann, F. J. Trebby. Ibid., vol. 79, June 1960, pp. 303-09.

4. The Calculation of Attenuation Constants for Radio Noise Analysis of Overhead Lines, G. E. Adams, L. O. Barthold. Ibid., pp. 975-81.

5. Radio Noise - Methods of Measuring. NEMA Standard 107 - 1964.

6. Radio Frequency Propagation on Polyphase Lines, L. O. Barthold. IEEE Transactions on Power Apparatus and Systems, July 1964, pp. 665-71.

7. Some Important Assumptions in the Calculation of Radio Noise Levels of EHV Lines, L. O. Barthold, W. S. Price, R. H. Schlomann. CIGRE Report No. 303, May 1962.

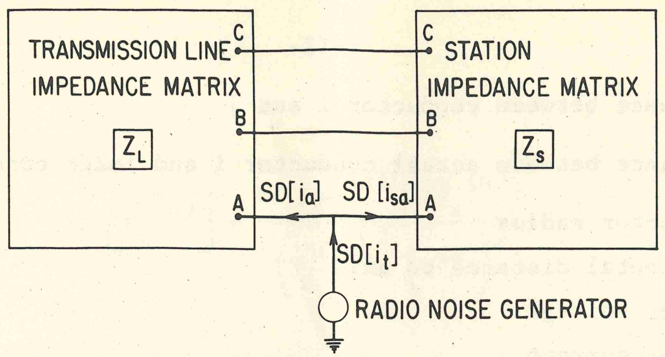
TRANSMISSION LINE IMPEDANCE MATRIX
Z_L
C
B
A
STATION IMPEDANCE MATRIX
Z_s
C
B
A
SD[i_a]
SD [i_{sa}]
SD[i_t]
RADIO NOISE GENERATOR

Fig. 1. Line and station impedance matrices and constant-current radio-noise generator.

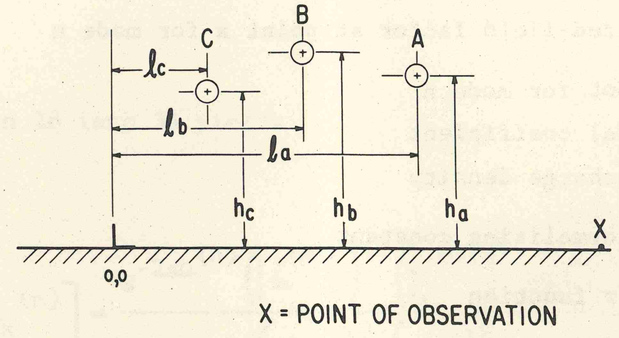
C
B
A
l_c
l_b
l_a
h_c
h_b
h_a
X
0,0
X = POINT OF OBSERVATION

Fig. 2. Three-phase line.

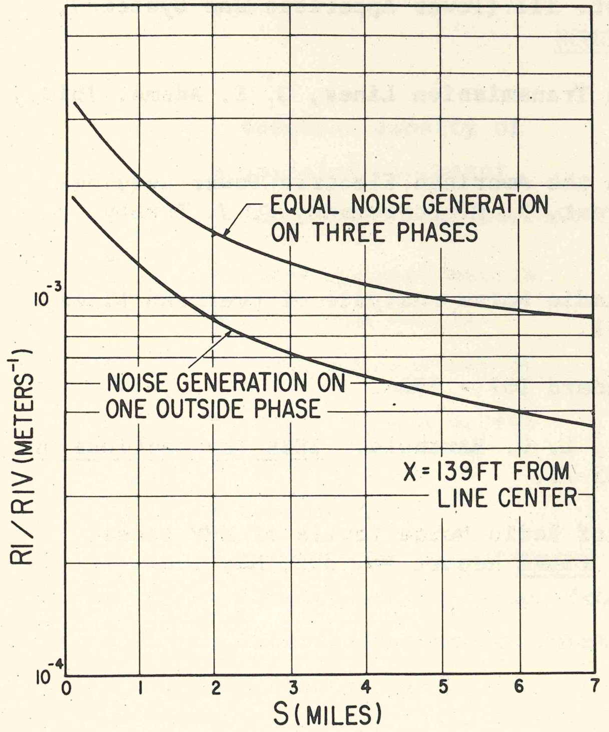

Fig. 3. RI/RIV ratios vs. distance from station.

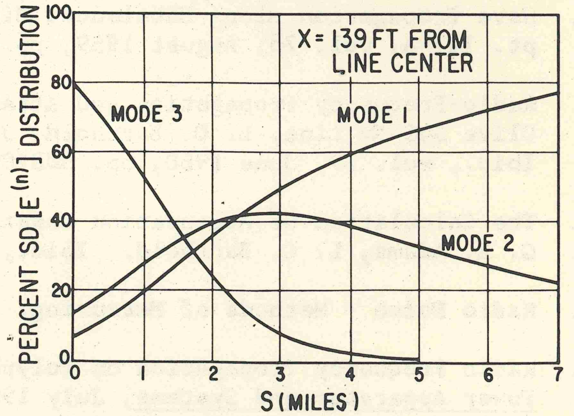

Fig. 4. Per cent modal distribution of SD $\left[E_x\right]$.